PALEOCLIMATE RECONSTRUCTION FROM VARVED SEDIMENTS IN KÖYCEĞİZ LAKE, SOUTHWEST ANATOLIA

A THESIS SUBMITTED TO
THE GRADUATE SCHOOL OF NATURAL AND APPLIED SCIENCES
OF
MIDDLE EAST TECHNICAL UNIVERSITY

BY

ÖZLEM KARADAŞ

IN PARTIAL FULFILLMENT OF THE REQUIREMENTS
FOR
THE DEGREE OF MASTER OF SCIENCE
IN
GEOLOGICAL ENGINEERING

AUGUST 2022

Approval of the thesis:

PALEOCLIMATE RECONSTRUCTION FROM VARVED SEDIMENTS IN KÖYCEĞİZ LAKE, SOUTHWEST ANATOLIA

submitted by **ÖZLEM KARADAŞ** in partial fulfillment of the requirements for the degree of **Master of Science** i**n Geological Engineering, Middle East Technical University** by,

Prof. Dr. Halil Kalıpçılar
Dean, Graduate School of **Natural and Applied Sciences** _____

Prof. Dr. Erdin Bozkurt
Head of the Department, **Geological Engineering** _____

Assoc. Prof. Dr. Ulaş Avşar
Supervisor, **Geological Engineering, METU** _____

Examining Committee Members:

Prof. Dr. İsmail Ömer Yılmaz
Department of Geological Eng., METU _____

Assoc. Prof. Dr. Ulaş Avşar
Department of Geological Eng., METU _____

Assoc. Prof. Dr. Fatma Toksoy Köksal
Department of Geological Eng., METU _____

Assoc. Prof. Dr. Mustafa Tuğrul Yılmaz
Department of Civil Eng., METU _____

Assist. Prof. Dr. Nazlı Olğun Kıyak
Eurasia Institute of Earth Sciences, ITU _____

Date: 10.08.2022

I hereby declare that all information in this document has been obtained and presented in accordance with academic rules and ethical conduct. I also declare that, as required by these rules and conduct, I have fully cited and referenced all material and results that are not original to this work.

Name Last name : Özlem Karadaş

Signature :

ABSTRACT

PALEOCLIMATE RECONSTRUCTION FROM VARVED SEDIMENTS IN KÖYCEĞİZ LAKE, SOUTHWEST ANATOLIA

Karadaş, Özlem
Master of Science, Geological Engineering
Supervisor: Assoc. Prof. Dr. Ulaş Avşar

August 2022, 88 pages

Understanding how the Earth's climate has changed in the past is vital to understand the current climate change and forecast the climate in the future. Thus, high resolution paleoclimate archives provide insight into the idea of how climate has changed over time far beyond instrumental records. Among many paleoclimate archives, annually laminated lake sediments "varves" provide the possibility to obtain highly resolved climate proxies as well as excellent chronological time control. The aim of this study is to obtain high resolution paleotemperature records from varved sediments of Köyceğiz Lake in southwest Turkey. Along a 124.95 cm-long gravity core, ITRAX micro-XRF core scanning was performed at a resolution of 0.2 mm. Varve counting in the light of visual inspections together with peaks along Ca/Ti ratio profile results in total of 609 years-long sedimentary record. By using only the ITRAX data at yellowish carbonaceous laminae, which are deposited in summer season, it was found that the ratios of Br, Cl and Zr to clastic elements (CA; Si, S, K, Ti, V, Cr, Mn, Fe, Ni and Rb) have high correlation with the summer (JJAS) temperatures measured at Muğla, Köyceğiz and Dalaman meteorological stations. Accordingly, the $AVE_{[Br\text{-}Cl\text{-}Zr]}$ / CA profile obtained from Köyceğiz sediments has strong correlation with the Global Average Temperature Change

(GATC) reconstruction curve (R^2 = 0.67). In order to achieve a quantitative paleotemperature reconstruction, multiple linear regression was applied to estimate regression equation between ITRAX micro-XRF and meteorological data. The obtained paleotemperature reconstruction (REC), which successfully illustrates the recent Global Warming, also achieves a strong correlation with the GATC (R^2 = 0.63). By using both $AVE_{[Br\text{-}Cl\text{-}Zr]}$ / CA and REC, compared to the GATC, two relatively warmer (ca. 1890-1860 CE and 1630-1600 CE) and one relatively colder (ca. 1770-1800 CE) periods were detected in Köyceğiz varve-based paleotemperature record.

Keywords: Paleoclimate, Paleotemperature Reconstruction, ITRAX micro-XRF Scanning, Principle Component Analysis, Multiple Regression Analysis

ÖZ

KÖYCEĞİZ GÖLÜ'NDEKİ (GÜNEYBATI ANADOLU) VARVLI SEDİMANLARDAN PALEOİKLİM ÇALIŞMASI

Karadaş, Özlem
Yüksek Lisans, Jeoloji Mühendisliği
Tez Yöneticisi: Doç. Dr. Ulaş Avşar

Ağustos 2022, 88 sayfa

Dünyanın ikliminin geçmişte nasıl değiştiğini anlamak, mevcut iklim değişikliğini anlamak ve gelecekteki iklimi tahmin etmek için hayati önem taşımaktadır. Bu nedenle, yüksek çözünürlüklü paleoiklim arşivleri iklimin zaman içinde nasıl değiştiğini araçsal kayıtların çok ötesinde anlamaya olanak verir. Pek çok paleoiklim arşivi arasında, yıllık olarak lamine edilmiş gölsel çökeltiler "varv", mükemmel kronolojik zaman kontrolünün yanı sıra, yüksek çözünürlüklü iklim vekilleri elde etme imkânı sağlar. Bu çalışmanın amacı, Türkiye'nin güneybatısındaki Köyceğiz Gölü'nün çökellerinden yüksek çözünürlüklü paleosıcaklık kayıtları elde etmektir. 124.95 cm uzunluğundaki gravite karotu boyunca, 0.2 mm çözünürlükte ITRAX mikro-XRF taraması yapıldı. Ca/Ti oranı profili boyunca ve görsel incelemeler ışığında varv sayımı, toplam 609 yıllık tortul kayıtla sonuçlanır. Yaz mevsiminde biriken sarımsı karbonatlı laminaların sadece ITRAX verileri kullanılarak Br, Cl ve Zr elementlerinin klastik elementlere (CA; Si, S, K, Ti, V, Cr, Mn, Fe, Ni ve Rb) oranının Muğla, Köyceğiz ve Dalaman meteoroloji istasyonlarında ölçülen yaz (JJAS) sıcaklıkları ile yüksek korelasyona sahip olduğunu gösterdi. Buna göre Köyceğiz çökellerinden elde edilen AVE[Br-Cl-Zr] / CA profili, Küresel Ortalama Sıcaklık Değişimi (GATC) yeniden yapılandırma eğrisi (R^2 = 0.67) ile önemli bir

korelasyona sahiptir. Nicel bir paleosıcaklık rekonstrüksiyonu elde etmek için, ITRAX mikro-XRF ve meteorolojik veriler arasındaki regresyon denklemini tahmin etmek için çoklu doğrusal regresyon uygulandı. Son Küresel Isınmayı başarılı bir şekilde gösteren elde edilen paleosıcaklık rekonstrüksiyonu (REC), aynı zamanda GATC ile önemli bir korelasyon gösterir (R^2 = 0.63). GATC' ye kıyasla hem AVE[Br-Cl-Zr] / CA hem de REC kullanılarak, iki nispeten daha sıcak (yaklaşık 1890-1860 CE ve 1630-1600 CE) ve bir nispeten daha soğuk (yaklaşık 1770-1800 CE) dönem Köyceğiz varv çökellerine dayalı paleosıcaklık kayıtlarında tespit edilmiştir.

Anahtar Kelimeler: Paleoiklim, Paleosıcaklık Yeniden Yapılandırması, ITRAX mikro-XRF Taraması, Temel Bileşen Analizi, Çoklu Regresyon Analizi

To my beloved niece, Mabel

ACKNOWLEDGMENTS

This study uses data obtained within the scope of the project titled “Köyceğiz Gölü (Muğla) Varvlı Sedimanlarında Sedimanter Deprem Kayıtlarının İncelenmesi”, which was funded by the Scientific and Technological Research Council of Türkiye (TÜBİTAK, Project No: 117C021).

Firstly, I would like to express my deepest gratitude to my supervisor Assoc. Prof. Dr. Ulaş Avşar for his advice, guidance, patience and supports throughout the study.

I would like to thank Emrah Ürün and Sinan Altıok from Muğla Sıtkı Koçman University and also Emre Çetinkaya from Middle East Technical University for taking the core from Köyceğiz Lake. I would also like to thank Assoc. Prof. Dr. Şule Gürboğa from the General Directorate of Mineral Research and Exploration (MTA) for her close attention and help during the ITRAX core scanning process. I am also grateful to my colleague Zeynep Bektaş for her help during the core preparation process.

Finally, I would like to express my special thanks to my parents, my brother, my sister, and my friends who have always been by my side, given me strength and encouragement.

TABLE OF CONTENTS

ABSTRACT v

ÖZ vii

ACKNOWLEDGMENTS x

TABLE OF CONTENTS xi

LIST OF TABLES xiii

LIST OF FIGURES xiv

LIST OF ABBREVIATIONS xvii

CHAPTERS

1 INTRODUCTION 1

1.1 Climate Proxy Records of Lacustrine Sediments 6

1.2 Previous Paleoclimatic Studies in Anatolia and the Neighboring Areas . 10

1.3 Study Area 33

2 MATERIALS AND METHODS 35

2.1 Bathymetric Survey and Sediment Coring 35

2.2 Core Splitting 37

2.3 ITRAX Micro-XRF Core Scanning 37

2.4 Construction of Varve Chronology 41

2.5 Principle Component Analysis (PCA) 41

2.6 Multiple Linear Regression Analysis 42

3 RESULTS 43

3.1 Optical Image 43

3.2 ITRAX Micro-XRF Data 45

4 DISCUSSION 61
4.1 Paleotemperature Record by Element-ratio Profiles 61
4.2 Paleotemperature Record by Multiple Regression Analysis 66
5 CONCLUSIONS AND RECOMMENDATIONS 73
REFERENCES 75

LIST OF TABLES

TABLES

Table 4.1 Results of multiple linear regression analysis using elements and PCs as independent variables. Constant values and multipliers for regression equations, and achieved R^2 values are presented. 68

LIST OF FIGURES

FIGURES

Figure 1.1. a) Location of Köyceğiz Lake in Anatolia. J: Jsibeli Forest and N: Nar Lake. b) Relief-shaded topography and lithological units in the catchment of the lake (Modified from Avşar et al., 2016). The locations of the cores investigated in this study (KYC-J) and in Akçer-Ön (2017) (G04) are also shown. The core studied by Avşar et al. (2016) is 300 m to the west of KYC-J. c) Meteorological stations of which data is used in this study. 34
Figure 2.1 Steps of the gravity coring operation (Avşar, 2013). 36
Figure 2.3. a) Front view of the ITRAX micro-XRF core scanner. b) Components of ITRAX micro-XRF system. A: optical line-scan camera, B: triangular laser system, C: motorized XRF Si-drift chamber detector, D: 3 kW X-ray tube, E: flat-beam X-ray waveguide, and F: The X-ray line camera (Croudace et al., 2006). 39
Figure 3.1. Optical image of the uppermost part of the core. Profiles of Red (R), Green (G) and Blue (B) values and their ratios to each other. Red and purple bars represent the yellowish carbonaceous laminae along the LS. 44
Figure 3.2. XRF data showing each element profile along the core. R/G profile is also plotted. Red bars show yellowish carbonaceous laminae. 46
Figure 3.3. Varve counting along profiles of R/G, Ca/Ti and [R/G]x[Ca/Ti] for the first 15 cm of the core. Varve numbers at every five varves are shown on the right-hand side. 48
Figure 3.4. Figure 3.3 continues for 15-30 cm of the core. 49
Figure 3.5. Figure 3.3 continues for 30-45 cm of the core. 50
Figure 3.6. Figure 3.3 continues for 45-60 cm of the core. 51
Figure 3.7. Figure 3.3 continues for 60-75 cm of the core. 52
Figure 3.8. Figure 3.3 continues for 75-90 cm of the core. 53
Figure 3.9. Figure 3.3 continues for 90-105 cm of the core. 54
Figure 3.10. Figure 3.3 continues for 105-120 cm of the core. 55
Figure 3.11. Figure 3.3 continues for 120-124.95 cm of the core. 56

Figure 3.12. Close-up views of KYC-J, as examples of detection of distinct varves on the profiles and the full-width optical image (a) and missing varves along the LS (b). 57
Figure 3.13. a) Age-depth model of KYC-J. b) Comparison of profiles of varve thickness. c) $[Cr/Ni]_{av}/[Ti,K,Fe]_{av}$ along KYC-J and the core studied by Avşar et al. (2016). Note that blue and red lines in the $[Cr/Ni]_{av}/[Ti,K,Fe]_{av}$ profiles represent the raw data where black lines that overlap them indicate 21-point moving average. . 58
Figure 3.14. Profiles of individual elements and proxy ratios with respect to time. The profile of GATC was also plotted (PAGES2k Consortium, 2019). Note that grey lines on element profiles represent the raw data where black and blue lines overlapping them indicate 21-point moving average. 60
Figure 4.1. Comparison of proxy ratio profiles with average summer temperatures (JJAS) recorded at Muğla, Köyceğiz and Dalaman meteorological stations whose locations are shown in the lower right. 62
Figure 4.2. Matrices showing R^2 values of all possible element ratios with the JJAS temperatures recorded in Muğla (a), Köyceğiz (b) and Dalaman (c) meteorological stations. d) Average of matrices in a, b and c. 63
Figure 4.3. Comparison of Ca/CA, Sr/CA, Ni/Tİ, Cl/CA, Br/CA and Zr/CA profiles and GATC profile. Scatter plots and R^2 values are also shown. All data in the figure are standardized. 64
Figure 4.4. a) Overlapped profiles of Cl/CA, Br/CA, and Zr/CA, and their average. b) Comparison of the averaged profile and GATC profile. Colder and warmer periods relative to GATC are highlighted as blue and red bars, respectively. 65
Figure 4.5. Results of Principle Component Analysis (PCA) on ITRAX summer data. a) Correlation coefficients of each element with five PCs. b) Plot of principle components and corresponding elements with respect to time. Note the red arrows showing warmer periods ca. 1850-1880 and 1600-1620 presented in Figure 4.4b. 67
Figure 4.6. a) Overlapped plots of elements-based reconstructions from three stations and GATC profile. b) Overlapped plots of principle component-based

reconstructions from three stations and GATC profile. c) correlation between reconstructed temperatures from different stations. 69
Figure 4.7. Overlapped plot of $AVE_{[Br-Cl-Zr]}$ / CA and GATC on the left, and REC and GATC on the right. Note that 41-years moving average was applied on GATC profile, where 5-years moving average was applied on $AVE_{[Br-Cl-Zr]}$ / CA and REC profiles (black lines). 70
Figure 4.8. Comparison of reconstructed summer (JJAS) temperatures of this study with the other paleoclimate records obtained in Anatolia. 71

LIST OF ABBREVIATIONS

ABBREVIATIONS

AD	Anno Domini, refers to in the year the Lord Christ was born
BC	Before Christ, indicates the years before the birth of Lord Christ
BCE	Before Common Era, equal to BC
BP	Before present, before the year 1950
Ca.	Circa, the Latin word means approximately
Cal	Calibrated
CE	Common Era, equal to AD
GATC	Global Average Temperature Change
GISS	NASA's Goddard Institute for Space Studies
IPCC	Intergovernmental Panel on Climate Change
JJAS	Average of June-July-August-September temperatures
Kyr	Kilo annum, a thousand years
NCEI	National Centers for Environmental Information
NOAA	National Oceanic and Atmospheric Administration
PCA	Principle Component Analysis
REC	Reconstructed
WMO	World Meteorological Organization

CHAPTER 1

INTRODUCTION

Every living thing on Earth is in close interaction with climate. It is the main factor that ensures the continuity of life and determines the behavior of all living organisms (Baykara, 2014). The climate has changed several times throughout the history of Earth. It has gone through many ice ages and warm periods due to natural factors. These factors are mainly variations in the Earth's orbit, the intensity of solar energy, concentrations of naturally occurring greenhouse gases, and volcanic eruptions. They changed the Earth's temperature in the past very slowly over thousands of years. However, although these natural factors are still in action today, their effects are not sufficient to explain the rapid warming trend we have experienced in the recent years (Riebeek, 2010). According to records of the NOAA National Climatic Data Center, GISS, the Berkeley Earth research group, and the UK Meteorological Office's Hadley Centre, annual temperature anomalies from 1880 to 2020 showed a rapid warming over the past few decades (NASA Earth Observatory, 2022). The IPCC revealed that human activities, mainly burning fossil fuels and deforestation have impacted the climate of Earth since the industrial revolution. Greenhouse gases, especially CO_2, occur naturally in the atmosphere and make the world a warmer and more livable place. Their concentrations have started to increase because of human activities, causing accelerated warming compared to usual. According to the IPCC, the global average temperature increased by around 1.1 degrees Celsius above pre-industrial (1850-1900) levels (IPCC, 2021; IPCC, 2022; WMO, 2022).

The world has recently begun to experience devastating effects of climate change in every part of the globe, with a warming of only 1.1º Celsius. It has led to changes in precipitation patterns. These changes caused more intense, frequent, and prolonged weather events such as droughts, heat waves, storms, floods, and wildfires that

occurred in several different locations. They have potential to alter the environment, create difficulties for species on Earth to access clean water and food, affect the health of organisms, and destroy their habitats and even their lives (U.S. Environmental Protection Agency, 2021; IPCC, 2022). Floods are one of the most noticeable and destructive consequences of climate change. One of the most recent examples occurred in South Africa during April 11 and 12, 2022. Heavy rains devastated the eastern coast of South Africa by bringing in floods and causing landslides in the provinces of the Eastern Cape and KwaZulu-Natal. These floods killed around 400 individuals, destroyed over 12,000 homes, and caused likely 40,000 people to flee from their homes (Tandon, 2022; Naidoo, 2022). In addition, these effects may appear as a decrease in the productivity and quality of crops. For example, crop yield has decreased by 33% in Africa since 1961 due to negative climatic conditions (IPCC, 2022). Numerous studies have shown that climate change has increased the severity, extent, and frequency of fires related to elevated temperature, longer dry summers, and drier vegetation and soils. Wildfire smoke also affects air quality in a negative way, leading serious health consequences (U.S. Environmental Protection Agency, 2021). Wildfires in Australia, which lasted from June 2019 to February 2020, are one of the worst in the recorded history of the country. The fire burned tens of millions of hectares, polluted the air to unhealthy levels, killed about a billion animals, and displaced approximately 90,000 people (Munroe and Taylor, 2020). In addition, heat waves or hot weather, that can last for long days, can lead to an increase in heat-related deaths. More than 70,000 people died during the 2003 heat wave in Europe. According to World Health Organization, more than 166,000 people died due to heat waves between 1998 and 2017, including this event (World Health Organization, 2022). Aforementioned extreme weather events cause alterations in water cycle, leading to pollution of water resources, increasing water scarcity, and raising the risk of developing diseases like typhoid and cholera, to which children are especially sensitive (UNICEF, 2022).

Since the past, people have been aware of the impact of the climate on their activities, primarily economic and agricultural and their political and social consequences.

They observed and kept written records of weather events such as the timing and frequency of frosts; weather related natural events such as floods and droughts; recurrent weather-related periods such as the arrival of migratory birds in the spring or the time of flowering of trees (Bradley, 1999). Then, the instrumental period of climate history started with the developing technology. During this period, scientists have started to closely monitor and record regional and local temperatures with ground based meteorological devices or meteorological instruments fixed on a satellite platform (Hulme and Jones., 1994). Although the western Europe has the longest instrumental records, some of them date back to the beginning of the 18th century or even to the end of the 17th century. Continuous instrumental records for most regions rarely extend back to the early 19th century, and some distant regions, polar and desert, have much shorter measurements (Bradley, 2011). According to NASA, the most complete global temperature records started in 1880 because before that date there was not enough data to measure global temperatures for the entire planet (NASA Global Climate Change, 2022). Consequently, the instrumental viewpoint on climate variation is very limited to understand the mechanisms of climate variability in the history of Earth (Bradley, 2011).

It is imperative to realize how the Earth's climate has changed in the past to understand the present climate change. One of the main principles of geology, uniformitarianism, states that "present is key to the past". It is assumed that the same natural geological processes on Earth occuring now have always operated in the past and they are valid all around the world. Now with the insight into this principle, the following question arises: can the past also be the key to the future. The comprehension of climate mechanisms in the past makes it possible to make predictions about how increased amounts of greenhouse gases in the atmosphere and other changes may affect the Earth's climate in the future. In contrast to instrumental records, paleoclimatic data allow to have the idea of how the climate has changed over time and today's climate evolution far beyond the instrumental records (National Geographic, n.d.). Paleoclimatic data are obtained from natural geological

archives which are mainly ice cores, speleothems, tree rings, corals, and lacustrine sediments.

Ice cores are taken from polar ice caps and glaciers. Water, impurities, and gas content trapped in the ice provide information about temperature, solar activity, past volcanism, composition of atmospheric and greenhouses gases (Riebeek, 2005).

Corals living in shallow water regions of tropical oceans build their skeletons by extracting calcium carbonate from the sea water as they grow (Walker, 2005). Changing in the light, water temperature and nutritional conditions affects the density of their skeletons. Therefore, coral skeletons formed in the summer have different densities than coral skeletons formed in the winter. Seasonal fluctuations in density produce growth bands. They can be used to identify how the climate was like throughout the seasons when the coral grew (NCEI, 2016).

Tree rings are used to study the local climate of that region in the past since trees are easily affected by temperature and precipitation. They are thinner in dry and cold years, and they generally grow wider in wet and warm years. The tree may grow hardly under stressful conditions like drought. Burn marks observed in tree rings can also indicate forest fires during hot periods (Stoller-Conrad, 2017).

Speleothems are cave deposits. They grow in thin layers when dissolved calcium carbonate ($CaCO_3$) redeposited in caves as the water flows. The amount of growth reflects the amount of ground water that dripped into the cave. Rapid growth may indicate heavy precipitation whereas little growth may show a drought period (Riebeek, 2005; Göktürk, 2011).

Lacustrine sediments serve as an excellent continental archive for the climatic and environmental variations on a decadal or even annual time resolutions. They provide a wealth of information that reflects many environmental changes occurring in the water column and the catchment area. Geochemical, sedimentological, and biological methods can be used to investigate them. The collected data referred to as climate proxies are used to examine the past environmental and climatic changes,

human activities on the lake and its catchment area. Unlike other archives, lacustrine sediments are more widespread and exist in a variety of environmental settings. The multiple proxy data of lake sediments combined with accurate dating and high resolution allow for more comprehensive climatic interpretations than other continuous continental records such as speleothems and tree rings (Zolitschka and Enters., 2009).

If fine laminations are found in lacustrine sediments and these are proven to be annual layers, these annually laminated lake sediments are called as varved sediments (Zolitschka, 1991). The rhythmicity of annual layers is mainly driven by seasonal temperature and precipitation changes. Different varve types (e.g., clastic, organic/biogenic, endogenic or mixed varves) may be formed based on the location, geomorphology and geology of the lake catchment (O'Sullivan, 1983; Zolitschka et al., 2015). Each varve consists of at least two or more thin seasonal laminae with noticeably different color, texture, composition, structure, and thickness. The alternating pale and dark sedimentary laminae reflect one year of deposition. Two conditions are required for varve formation. The first condition is that there should be seasonal rhythmic changes in sediment composition. The other condition is the low oxygen bottom waters so that burrowing animals cannot mix the sediment and destroy the laminated structure (Weinheimer and Biondi, 2003). Most importantly, they provide the best time control. The downcore count of annual layers in a varved sequence offers an exact chronology in calendar years. Therefore, combining varve sediments with seasonality and precise time chronology makes varved sequences invaluable climate archives at high resolutions (Zolitschka, 2003; Tylmann et al., 2013; Zolitschka et al., 2015).

Aforementioned natural archives preserve indicators of past climates known as climate proxies. They are very sensitive to various climatic and environmental influences. Within the scope of this study, proxies obtained from lacustrine sediments will be briefly explained as follows.

1.1 Climate Proxy Records of Lacustrine Sediments

Proxies can be divided into three different major groups as sedimentary, biological, and chemical.

Sedimentary proxies such as mineral compositions and magnetic characteristics, provide insights on the significant environmental and climatic changes in the lake and the catchment area (Zolitschka and Enters, 2009). Minerals such as evaporites, clay minerals (kaolinite and chlorite), and carbonates (calcite and aragonite) can be utilized to infer past climate changes over time. Evaporites are usually indicators of arid or semiarid climates. While kaolinite usually forms by chemical weathering under humid and warm climates, chlorite generally forms in colder regions by physical weathering (Gornitz, 2009). Aragonite, one of the usual polymorphs of calcium carbonate, is precipitated by intense evaporation (Jones et al., 2006; Ülgen et al., 2012; Akçer-Ön, 2017). Magnetic characteristics of sediments can be determined by magnetic susceptibility measurements. It indicates the transportation of terrigenous input with magnetic particles from catchment into lakes. Higher magnetic susceptibility values can be related to runoff related rainfall under warm and wet periods. On the other hand, low values can be linked to formations of carbonates and evaporates under less rainfall periods (Ülgen et al., 2012; El Ouahabi et al., 2016).

Biological proxies contain residues of living organisms mainly pollen, charcoal and ostracods. Climate has a strong impact on the distribution of terrestrial vegetation. Every plant on Earth has evolved differently for the optimum photosynthesis because their tolerances for extreme temperatures are not the same. Therefore, the record of pollen data indicating changes in vegetation distributions allows to interpret the climate of that time (Brewer et al., 2007). Charcoal is carbonized matter and formed by incomplete burning of organic substances like plant tissues. Examination of charcoal particles transported and deposited in sediments provide information on fire history and fire frequency during past climate variations (Brunelle-Daines, 2002; Schlachter, 2005). Shelled organisms of ostracods record past environmental

conditions in their shells. When these organisms die, their skeletons are buried and preserved in sediments. The existence of these creatures enables both to predict the past climate changes by geochemical analysis and to produce accurate radiocarbon dates in sedimentary sequences (Bruckner,2021).

Chemical proxies are geochemical data from stable isotope and elemental analysis measurements. Isotopes are elements that differ in the number of neutrons but have the same number of electrons and protons. Stable isotopes do not decay radioactively over time, whereas radiogenic isotopes ultimately decay to another element or isotope. Since the masses of two isotopes of the same element are different, they act differently in any mass-affected biological processes like photosynthesis and physical processes like evaporation. That results in concentration of one isotopic form relative to the other one and relative depletion of the same isotope in the resulting product. For example, in a liquid being subjected to evaporation, the heavy isotope of an element with two isotopes will show depletion in the gas and an enrichment in the remaining liquid, just as the depletion and enrichment pattern for the lighter isotope is reversed. This is known as isotope fractionation. Fractionation mechanisms for oxygen and carbon stable isotopes are strongly related to regional climatic and environmental factors. Therefore, they are the most preferred stable isotopes in paleoclimatic and paleoenvironmental studies (Cohen, 2003).

Oxygen has three naturally occurring stable forms which are oxygen-16, oxygen-17, and oxygen-18. However, only oxygen-16 and oxygen-18 can be measured. Carbon has two stable isotopes which are carbon-12 and carbon-13. Oxygen-16 and carbon-12 are light isotopes founding in abundance in nature, oxygen-18 and carbon-13 are heavy isotopes and their amounts in nature are very less (Cohen, 2003; Riebeek, 2005). Oxygen and carbon isotope values are measured by a mass spectrometer. They are compared to a reference standard which is a sample of known isotope values. Stable isotope values are indicated by δ (delta) notation which is the parts per thousand (per mil, ‰) difference of the heavy isotope to light isotope ratio of the sample relative to the standard. Oxygen and carbon stable isotopes are commonly obtained from calcium carbonate deposited mostly found in lakes and speleothems

(Jones, 2004; Göktürk, 2011). In lakes, the composition of carbonates can be either skeletal (biogenic) or authigenic mineral precipitation (Leng and Marshall, 2004).

The stable oxygen isotope compositions reflect the regional precipitation and evaporation changes. During evaporation, the lighter isotope ^{16}O evaporates more quickly, leaving the heavier isotope in the water. The composition of water shifts to more positive $\delta^{18}O$ values. While carbonate precipitates from the water column or organisms form their shells, the heavy ^{18}O in the water is used. This makes the oxygen isotope values obtained from them more positive. During precipitation, the first raindrops are enriched in light isotopes. That results in more negative $\delta^{18}O$ values. $\delta^{18}O$ values of authigenic carbonates or shelled organisms are also used to estimate past temperatures. (Cohen, 2003; Leng and Marshall, 2004; Gillikin et al., 2017). In addition, speleothem $\delta^{18}O$ values directly indicate the deposition temperature and the $\delta^{18}O$ of water precipitated in the speleothem (Bar-Matthews et al.,2003; Fleitmann et al., 2009).

The carbon isotope compositions provide record of past environmental changes such as vegetation cover and productivity in the lake. The carbon isotopic composition of terrestrially originated plant material entering the lake as organic matter is related to photosynthesis. Terrestrial plants prefer to absorb ^{12}C from the atmosphere during photosynthesis, resulting in negative $\delta^{13}C$ values in terrestrial organic material. Plants are separated into two groups as C3 and C4 based on the carbon fixing pathways. C3 plants include trees and shrubs, C4 plants include grasses. C3 and C4 plants living on land can be recognized isotopically because $\delta^{13}C$ values for C4 plants are between -8 and -22 ‰ and C3 plants are between -22 and -33‰ (Meyers and Teranes, 2001). C4 pathways consume less water and is hence preferred under circumstances of poor CO_2 level, high temperature or water scarcity. In arid environments, C3 plants having high water stress conditions cause more positive $\delta^{13}C$ values. On the other hand, C3 plants with limitless water availability result in more negative $\delta^{13}C$ values under warmer settings (Bar-Matthews et al.,2003; Cohen, 2003; Fleitmann et al., 2009). In addition to external organic material inputs, organic production and photosynthesis occur within the lake itself. During photosynthesis,

^{12}C is preferentially used by photosynthetic organisms. More ^{13}C is left in the water column. As with the oxygen isotope, ^{13}C in the water is used by shell forming organisms or precipitated carbonate. That results in more positive $\delta^{13}C$ values (Cohen,2003).

Identifying the source of organic matter is also important for interpreting past climate and environmental conditions. Plants that live in the lake and its watershed are the primary source of organic matter in lake sediments. Plants are categorized in two geochemically separate groups; non-vascular plants like phytoplankton, and vascular plants such as macrophytes in lakes and grasses, trees, shrubs, and grasses on land. Terrestrial vs aquatic sources of organic matter can be identified by carbon/nitrogen atomic ratios and the $\delta^{13}C$ isotope measurements. C/N values of pure organic matter from phytoplankton are typically between 4 and 10, while C/N ratios of vascular land plants are 20 and more. As a result, a relative rise in C/N values along a sedimentary sequence can be interpreted as an increase in the influx of terrestrial organic matter into the lake (Meyers and Teranes, 2001; Avşar, 2013). The amount of organic matter in sediments is also represented by total organic carbon (TOC) which can be used as an indicator of organic matter production (Cohen, 2003; Ülgen et al., 2012).

Another important chemical proxy is the geochemical measurements of specific elements or their elemental ratios. They are mostly obtained from the X-ray fluorescence scanning. It provides information to understand how the sediment deposited in the lake changes over time under the influence of climatic and environmental factors. Lake sediments can be compositionally classified in three different ways. They can be detrital clastic material from external sources, or they can be directly precipitated either geochemically or biologically from the water column. Clastic materials can be deposited by transportation from catchment of the lake or by atmospheric deposition such as volcanic ash, pollen, and dust (Zolitschka et al., 2015). Clastic input is characterized by elements of Si, Fe, Ti, Al, K, Zr and Rb which are geochemically stable and found in resistant minerals. The elements Ca and Sr refer to calcium carbonate precipitation. Calcium carbonate can be precipitated from the water column by geochemical processes, or it can be formed

from the skeletal remnants of aquatic organisms as biogenic carbonate. The downcore variation in elemental ratios to each other allows to make interpretations on past environmental and climatic conditions. For example, increases in clastic input may indicate periods of rainfall. Warm periods may favor geochemical carbonate precipitation or biological blooms of organisms. During these periods, the related elements show significant peaks in the element profiles (Davies et al., 2015).

1.2 Previous Paleoclimatic Studies in Anatolia and the Neighboring Areas

Previous paleoclimate studies covering the last Holocene in Anatolia and the surrounding area are summarized below. These studies represent the records of tree rings, speleothems and mostly lacustrine sediments. Although there are more records from different studies, only records covering the last millennium were selected in this study.

Eastwood et al. (2007) carried out a study on stable isotope data from authigenic calcite in sedimentary record of Gölhisar Lake in southwest Anatolia. They aimed to shed light on past climatic changes during Holocene. In their study, they also considered previous works on the lake conducted by Eastwood et al. (1998, 1999b, 2002); Jones et al. (2002). They made measurements on an 8.13 m long sedimentary core. Sample intervals are approximately 10 cm for the stable isotope analyzes. They dated the core by radiocarbon dating and tephra layer. They observed that the covariance degree between oxygen and carbon isotope values in carbonates is high in the lake. They suggested stable isotope records can be interpreted with regards to variations in precipitation/evaporation ratios. Through the Holocene, oxygen and carbon isotope values were mostly negative indicating wetter climatic conditions than today. During the early Holocene from ca. 10 600 to 8800 cal. yr. BP, low isotope values are especially notable, implying drier conditions than today based on pollen data. This disparity between isotope and pollen data suggests that it may have taken many millennia for vegetation to achieve climatic equilibrium at the beginning of the Holocene. During the early to middle Holocene from 8800 to 5100 cal. yr. BP,

isotopic variations suggest aridity and humidity oscillations. Higher carbon and oxygen values for the last half of the Holocene show mostly drier conditions than before ca. 5100 cal. yr BP. However, especially during the Classical and early Byzantine periods (so-called Beyşehir Occupation Phase), there is some proof for increased humidity coinciding with pollen evidence for increased human influence and agricultural intensification. They concluded that a shift towards more positive isotope values indicating an increase in aridity over the last 1300 years.

Danladi et al. (2021) carried out a study of sediments of Gölcük Lake in southwest Anatolia to show precipitation and temperature changes since 1730. They obtained two cores from the lake and used multiple proxies to determine dry and wet periods. These proxies are lithological description, magnetic susceptibility, micro-XRF and factor analyzes. They constructed the age depth model by ^{210}Pb and ^{137}Cs dating methods. They performed magnetic susceptibility and micro-XRF scanning measurements at 1 mm intervals. They applied the factor analysis to elements (Sr, Fe, Ca, K, and Zr) obtained by micro-XRF measurements. They stated that wet periods were indicated by dark olive-green sand and silty mud, high values in magnetic susceptibility and log (Sr/Ca) values. Dry periods were related to olive green laminated and clayey mud and higher log (Ca/K) values. They observed dry periods occurred between the years around 1730-1830, 1842-1885 and 1925-1977, wet periods occurred during the years around 1830-1842, 1885-1925, and 1977-2000. They concluded that climate record of the lake also provides the evidence of solar activity and North Atlantic Oscillation teleconnection. They discovered that wet phases are associated with low solar activity and negative NOA, and dry phases, except for the Dalton minimum, are related to time of high solar activity and positive NOA.

Wick et al. (2003) performed a study on varved sediments of Lake Van in eastern Anatolia to understand past climate variations and anthropogenic activities in the region. They performed measurements using sediment cores for multiple proxies of charcoal, pollen, oxygen isotope and Mg/Ca ratio at around 16.7-year resolutions. They found that varve records cover the last 13 000 years based on the varve

chronology constructed by varve counting. They interpreted Mg/Ca and oxygen stable isotope ratios in the carbonates for regional lake level and relative humidity changes. Charcoal and pollen data were evaluated for the reactions of vegetations to climate changes. They found that geochemical data were correlated with records of vegetation changes. During the period of Late glacial, the climate was dry and cold with saline lake water and steppe vegetation. During the period of Younger Dryas, the vegetation changed to semi desert and lake level fell suddenly. At the start of the Holocene, an important increase in humidity was indicated by isotope and geochemical data, and Pistacia and nonarboreal vegetation were observed. The weather was dry during the early Holocene which was supported by the intense steppe fires and delay of the expansion of another pollen data deciduous oak woodlands. At 8.2 ka BP, a shift was observed in the climate pattern which increased the seasonal precipitation distribution in the area. That resulted in the expansion of deciduous oak forest and a significant decrease in steppe fires. Optimum climatic conditions with high lake levels and low salinity were observed between 6.2 ka and 4 ka BP. After 4 ka BP, aridity increased in the region and the weather reached to modern climatic conditions. Additionally, they stated that human activities were started in the catchment of the lake since 3.8 ka BP and intensified for the last 600 years.

Şimşek and Çağatay (2018) carried out a study of sedimentary record of Lake Van for the past 3500 years. They retrieved one core from the lake and used multiple proxies to reveal environmental and climatic changes. These proxies include measurements of magnetic susceptility, stable isotopes of oxygen and carbon, geochemical analyses (micro-XRF, total inorganic carbon and organic carbon), and ostracod counting. They constructed the age model by ^{210}Pb and ^{137}Cs radionuclide dating and varve counting. Multiple proxies (Ca, Sr, Ti, Ti /Ca and Sr/Ca) reveal that drier conditions occurred in Lake Van between 3.5 ka and 1.6 ka cal BP than the past 1.6 ka cal BP. In the last 3.5 ka, 16 periods of dry/cold and warm/wet periods lasting 100-350 years are observed. They found that climate records of Lake Van are consistent with Sofular cave speleothem record, Nar Lake, and the historical

European climate periods such as the Roman Warm Period, Dark Age Cold Period, Medieval Warm Period and Little Ice Age. They also observed dramatic increase in the clastic input proxies of magnetic susceptibility, Ti/Ca and Ti in the record. They concluded a dramatic increase in the clastic input proxies of magnetic susceptibility, Ti/Ca and Ti in the records is caused by human activities for the past 700 years.

Ocakoğlu et al. (2015) investigated the sediments of Lake Çubuk in the northwest Anatolia. They retrieved 303 cm long sedimentary core from the lake and obtained multiple proxies. They are sedimentological, stable isotopes, elemental data measurements and diatoms, pollen and ostracods. They subsampled the core at 4 cm intervals for the measurements. They constructed the age depth model by radiocarbon dating on organic material of bulk mud and charcoal fragments. They found that the core they studied covers the last 2800 years. They observed that at the end of the Near-East Aridification Phase, the driest period occurred at around 200 BC when the oxygen isotope values shifted to more negative values and the planktonic diatom ratio declined significantly. The periods of Dark Ages and late Byzantine from 670 AD to 1070 AD are marked by more positive oxygen isotope values, rising lake levels, and the most widespread arboreal cover on the record. The Little Ice Age occurred abruptly at about 1350 AD. During this period, they observed more positive oxygen isotope values, a dramatic fall in pollen data and a sudden rise in diatom abundance implying a decrease in lake level. They concluded that climate is the dominant factor for the vegetation cover in the area based on the close relation between pollen assemblages and stable isotope results in many sections of the record over the last 2800 years.

Ön et al. (2018) studied the sediments of Lake Hazar in the eastern Anatolia. They used the independent component analysis (ICA) method to find statistically independent records of past climates from micro-XRF element data (Ca, Mn, K, Ti, Fe and Sr). They performed element analysis at 1 mm resolution along a 3.8 m long sedimentary core. They also measured magnetic susceptibility at 1 cm resolution. The core was subsampled at 30 mm intervals for oxygen and carbon isotope analyzes from ostracods. They established the age model by radiocarbon dating on mollusks

and wood material. They found that the core they studied covers the last 17.3 ka. They used the distance correlation to select the convenient components by a similarity measure between records of past climates and independent components for the ICA method. For the past climate records, they selected high resolution, well dated oxygen isotope record of North Greenland Ice Sheet Project and carbon isotope record of Sofular Cave. Based on the distance correlation similarity, they selected two of six independent components. They proposed that these two components are associated with temperature and precipitation-evaporation. They found that the records of the cold period between17.3 ka and 13.8 ka BP, warm and wet Bolling Allerod period between 14.8 ka and 12.85 ka BP, the Younger Dryas Cold event caused a fall in lake levels during 12.49 ka and 11.76 ka BP, the start of the Holocene and reaching Holocene normal at approximately 8 ka BP. According to precipitation record, the region experienced its driest period from 8 ka and 5 ka BP during the Holocene. Then, climate reached to the Holocene normal between 5 ka and 3.5 ka BP. Around that period, the temperature fell suddenly, cold, and dry periods observed around 3.5, 2.8 and 1.8 ka BP. They also suggested that Hazar Lake has no proof for the 4.2 ka event.

Danladi and Akçer-Ön (2018) investigated the sediments of Salda Lake in the southwest Anatolia to understand the relation of solar forcing and climate variability. They recovered four cores and used high resolution multiple proxies containing magnetic susceptibility, geochemical data (Mn/Fe, Ca/Fe, Ca, Inc./Coh.) by micro-X ray fluorescence, carbon and oxygen stable isotopes, total inorganic carbon, and total organic carbon. They measured magnetic susceptibility at 5 mm and geochemical data at 2 mm resolutions. They used different cores and subsampled them for stable isotopes of oxygen and carbon measurements at 10 mm intervals, and TIC, TOC analyses at 3 cm intervals. The age depth model was constructed by radionuclide (^{210}Pb and ^{137}Cs) and radiocarbon dating. According to radiocarbon measurements they made on ostracod shells, they found that sedimentary record of the lake covers the last 1400 years. According to results of multiple proxies, they characterized alternations of wet periods between the years 550-600, 770-850 and

900-1000, 1150-1250, 1720-1780 and 1850-2014) and dry periods between 600-770, 850-900, 1000-1150, 1250-1720, and 1780-1850) in Salda Lake. They discovered that wet periods are associated with higher lake levels and high values in magnetic susceptibility and TOC, low values in Mn/Fe and carbonate content (TIC and Ca/Fe). They stated that these dry periods correspond to time periods with low solar activity such as Grand, Oort, Wolf, Spörer, Maunder, and Dalton Minimums. Wet periods are consistent with high solar activity such as Medieval and Modern Maximums. They also found the records of Dark Ages Cold Period, Medieval Climatic Anomaly, Little Ice Age, and Modern Warm Period in Salda Lake by using Ca/Fe ratio.

Ülgen et al. (2012) examined the sedimentary record of İznik Lake in northwestern Anatolia to reveal climate changes for the last 4700 years. They performed multiple proxy analyzes including magnetic susceptibility, palynology, geochemistry, and mineralogy on approximately 5 m long sedimentary cores. They measured magnetic susceptibility, element analyzes (Rb, Ca, Al, Ti, Sr) by XRF core scanner at 1 cm resolution and pollen data in 10 cm intervals. They subsampled cores at 2 cm and 4 cm intervals and used them for mineralogical and other geochemical measurements. They established the age depth model based on radionuclide (^{210}Pb and ^{137}Cs) and radiocarbon dating. The radiocarbon dating was carried out on bulk sediments and plant materials. They characterized five dry periods and six wet periods. Dry periods include 4.4-4.2 ka (4.2 ka event), 3.65-3.3 ka (collapse of Bronz Age), 2.6-1.95 ka, 1.35-1.1 ka (Dark Age Cold Period), 0.7 ka-30 a cal BP (Little Ice Age) and 30 a cal BP-2005 AD. Wet periods include 4.72-4.4 ka, 4.2-3.65 ka, 3.3-2.6 ka, 1,95-1.35 ka (Roman Warm Period), 1.1-0.7 ka cal BP (Medieval Warm Period). They observed that wet periods are consistent with high values in magnetic susceptibility, (Rb+ Zr)/Sr and clay content, low values in TIC, C/N, Ca/Ti and the ratio of aragonite and calcite.

El Ouahabi et al. (2017, 2018) investigated the six-meter-long sedimentary record of Amuq Lake in southern Turkey. The Amuq plain has a long history of varied, dense, and well-defined human settlements. They aimed to shed light on enormous environmental variations over the last 4000 years concerning the different phases of

human occupation. The radiocarbon dating on terrestrial remains, ostracods, shells, micro charcoals, and radionuclide (^{210}Pb and ^{137}Cs) dating were performed for the age depth model. El Ouahabi et al. (2017) used magnetic susceptibility and clay minerology as proxies. They performed magnetic susceptibility measurements at 1 cm intervals, clay mineralogy between 10-20 cm intervals. They observed important changes in clay minerals, illite, kaolinite, smectite and chlorite. They used them as weathering proxies. They stated that kaolinite and smectite are the product of chemical weathering, chlorite and illite are the physical weathering products. Furthermore, they observed magnetic susceptibility values become higher under warm conditions with high chemical weathering. In addition to this study, inorganic geochemistry obtained from XRF scanning was performed at every 5 and 10 cm at the bottom of the core by El Ouahabi et al. (2018). They used variations in NiO, ZnO, Cr_2O_3 and ZrO_2 and magnetic susceptibility measurements to predict the soil erosion changes triggered by human occupation. They documented many erosion phases occurred during different archeological times. They observed and concluded that the landscape of the Amuq Lake has considerably changed in connection with the human occupation and land use phases.

Additionally, Avşar et al. (2019) had a preliminary study on the sediments of Amuq Valley to reveal paleoenvironmental variations due to human activities and past climate changes for the last 31 kyr. They recovered sediments by modified piston coring method. They obtained high resolution geochemical data (Ca/Ti) and optical images by ITRAX micro-XRF core scanning at 1 mm intervals. Radiocarbon dating on charcoal samples was used to establish the age depth model. The Pleistocene-Holocene transition was observed and characterized by a significant sedimentological change in optical images and by a shift from higher Ca/Ti due to colder and drier Pleistocene climate to lower Ca/Ti due to wetter and warmer Holocene climate. They made interpretation about another Ca/Ti anomaly implying an important aridification which may be connected to archaeologically with the collapse of the Hittite Empire. Moreover, they stated that the beginning of the abundant coal content may be connected to intensive agriculture began around 1750

BC. They concluded they will improve their interpretations by paleo botanical, palynological and mineralogical measurements on multiple cores retrieved from different locations within the valley.

Nar Lake, one of the varved lakes in Turkey, in the Cappadocia region of central Anatolia has been studied in detail by Jones et al. (2005), Jones et al. (2006), England et al. (2008), Dean et al. (2015) and Roberts et al. (2018). Jones et al. (2005, 2006) presented a highly resolved stable oxygen isotope ($\delta^{18}O$) measurements on the 3.76 m long sedimentary core obtained from Nar Lake. Each varve is made up of summer precipitated light colored carbonate layer and organic material rich dark colored layer. They dated the upper part of the core by ^{210}Pb and ^{137}Cs dating methods to confirm annual laminations. The rest of the core was dated by varve counting. They found that the core they studied covered the last 1700 years. They made isotope measurements on authigenic carbonate to understand precipitation and evaporation changes. The top 900 carbonate varves were analyzed individually, the other 825 varves studied from consecutive bulk samples at a 5-year resolution. They observed a major shift to more negative values occurred in around 530 AD, while large shifts to more positive values occurred in approximately 800 and 1400 AD. They stated their observations are supported by deposition of aragonite which formed during periods of intense evaporation and more positive values (before 530 AD and from 1400 to 1960 AD). On the other hand, they observed calcite deposition during times of more negative values from 530 AD to 1400 AD. They found drier intervals occurred in 300-500 AD and 1400-1960 AD while wetter periods were observed in 560-750 AD, 1000-1400 AD and after 1960. They stated that isotope record of Nar Lake is associated with summer drought intensity and the precipitation amount changes. They also observed changes are compatible to proxy and instrumental records of Indian monsoon. Dry summers in the Eastern Mediterranean are related to the periods of increased monsoon rainfall. In addition, they stated that the large shifts are consistent with the North Atlantic winter climate changes with wet and cold periods in the Alps during the dry climate of Turkey (Jones, 2006).

England et al. (2008) carried out a palaeoecological study on a 1700 year sedimentary core from annually laminated sediments of Nar Lake. Pollen measurements were done on the sedimentary core that was previously studied in the area (Jones et al., 2005; 2006). Sample resolution for the pollen data was 18 years. They combined their pollen data with the stable isotope data (Jones et al., 2005; 2006), the archaeological and historical records to interpret the role of various human and natural factors in changing Late Holocene landscape in Cappadocia. They observed vegetation and land use changes indicated by pollen data did not overlap with the staple isotope record. They interpreted landscape variations are mainly driven by human influences. Based on pollen data, they determined four land use phases. First one represents the early Byzantine period marked by tree crops and cereal and the final term of Beyşehir Occupation phase. In the second phase, the landscape was abandoned, and secondary woodland was established between 670-950 AD. That period was corresponded to the Arab attacks on Anatolia. In the third phase, pastoralism and the cereal related farming were established again from around AD 950. This cultural environment was preserved through the 'Golden Age' of Byzantine, the Seljuk, and Ottoman Empires. In the last phase, agriculture intensified in the late Ottoman period and the Turkish Republic (1830 AD to present). They concluded that pollen data of Nar Lake and historical records are compatible with each other regarding timing of landscape alterations.

Dean et al. (2015) presented a high resolution stable oxygen and carbon isotope record and carbonate mineralogy from Nar Lake. They aimed to reveal the centennial scale climate change and climate shifts during the Holocene. They obtained three cores from the deepest part of the lake. They dated the core by varve counting and uranium-thorium dating. Sample resolution for the measurements was almost 25 years. They also stated that oxygen carbonate record from Nar Lake indicate the regional water balance. They observed dry conditions in the Younger Dryas, relatively wet conditions during the early Holocene. Two dry periods were observed in the Early Holocene, occurring at approximately 9.3 ka and 8.2 ka. After that, a millennial scale dry period during the mid Holocene transition was seen in the record.

The centennial scale drought periods at the times of Late Bronze Age societal collapse and 4.2 ka event were observed during the relatively dry Late Holocene. They stated that dry periods in their record were compatible with records of cooling events in North Atlantic. They suggested there is a teleconnection between these two regions due to cyclonic activity changes and the route and frequency of storm tracks changes from Atlantic. However, they observed that the duration of Mid Holocene transition and 9.3 and 8.2 ka periods were longer than the events seen in the records of the North Atlantic. They stated that the hydroclimate of the Eastern Mediterranean is driven by additional controls.

Roberts et al. (2018) reconstructed the erosion history of the catchment of Nar Lake in central Turkey. They obtained three cores and performed micro-XRF scanning measurements along split cores. They also used oxygen isotope and pollen proxies. The measurement resolution of XRF scanning was 200-µm. According to result of varve counting and U-Th dating, they found that the record they studied covered the last 13.800 years. They identified clastic laminations by ITRAX data. They observed that clastic laminations are well defined with Ti and K, while concentration of Ca is low. They found Ti peaks with other clastic elements and clastic lamination changes show increasing sediment inflow to the lake from 9300 to 8000 cal BP and during the past 2500 years. When they made multiple proxy comparisons, they revealed that these periods were linked to periods of released human influence on the soils and vegetation around the lake.

Akçer-Ön conducted a study in 2017 on the sedimentary record of Köyceğiz Lake. She aimed to reveal the Late Holocene environmental and climatic changes in western Turkey by using multiple proxies. They are magnetic susceptibility, geochemical data (Ca, Fe, Ca/Fe, Mn/Fe, Sr/Ca, Inc/Coh) by ITRAX micro-XRF core scanning and carbon and oxygen stable isotope measurements. She recovered two cores from northern and one core from southern basins of the lake and one core from the ridge that separates these two basins. She constructed the age model by radiocarbon dating on shell fragments. She found that the sedimentary record covers almost the last 500 years. Geochemical data and magnetic susceptibility were

measured at 5 mm resolutions. Stable isotopes were analyzed at 20 mm resolutions. She applied the factor analysis on micro-XRF data (elemental profiles of Ca, K, Ti, Sr, Fe, Mn and Inc./Coh ratio). She obtained three different factors. Factor 1 showed that Ti, K and Fe represent clastic material input were inversely correlated with Ca and Sr. Factor 2 referred to Mn and Ca. Mn indicates redox conditions, on the other hand, Ca also shows biological and/ or chemical precipitation in the sediment. She observed that the correlation was not so high in F2. Factor 3 showed that Ti, K and Fe were inversely related to Inc/Coh ratio which is considered as total organic carbon. That was interpreted as the enrichment of total organic carbon during drier and colder periods. In her study, she used Fe for detrital input and Ca for carbonate precipitation. Decreasing in carbonate precipitation and increasing in clastic input occur under warmer and wetter periods. The Sr/Ca ratio indicates the ratio of aragonite and calcite. Wet and warm periods lead to increase in this ratio. She observed the covariance of $\delta^{18}O$ and $\delta^{13}C$. While stable isotope values have higher values during drier conditions, they are low in warmer periods. Based on her findings, she found that Köyceğiz Lake record covers the Little Ice Age (1450 AD-1850 AD). During this period, she observed three dry and cold periods called as Spörer Minimum (1460 AD-1550 AD), Maunder Minimum (1645 AD-1715 AD) and Dalton Minimum (1790 AD-1830 AD). She stated that the variability in sunspot numbers affects the climate of the region.

In addition to these studies, paleoclimate record was also used as a tool to enhance the sedimentary chronology in the study by Avşar et al. (2014a). They studied the sedimentary record of Yeniçağa Lake located at the western part of the North Anatolian Fault to reveal traces of paleo earthquakes. They measured inorganic geochemistry of the sediments by ITRAX micro-XRF core scanning along a 4.6 m long sedimentary core at 2 mm resolution. They constructed the sediment chronology by radiocarbon measurements and time stratigraphical correlation with highly resolved and well dated speleothem $\delta^{13}C$ record of Sofular cave (Fleitmann et al., 2009) which is 70 kilometers north of the lake. They measured radiocarbon on bulk samples and various organic fragments such as pollen, charcoal, remains of

phragmite and Daphnia ephippia. They found that the core they studied covers the last 3400 years. To establish the sediment chronology, they analyzed ITRAX data of the lake to identify the most compatible paleoclimatic proxy with the Sofular record using a matrix of correlation coefficients. Relatively higher correlation coefficients with the Sofular record were observed in the ratios of detrital elements (Ti, Si, Co, K, Rb, Zn and K) to sulphur. Therefore, these ratios were averaged and tuned to speleothem data through tie points. After tuning, they compared two records and observed they were overlapped specially after 300 AD. They noticed that the more negative $\delta^{13}C$ values in the record of Sofular cave are conformed with relatively higher sulphur contents in Yeniçağa Lake under wetter and warmer climatic conditions. They stated that wetter and warmer climates appear to favor high primary production in the lake which results in organic sulphur enrichments. Moreover, they found eleven seismicity events in the sedimentary sequence of the lake. These events were characterized by siliciclastic-enriched intercalations. They concluded that the chronology of the events and the correlation between Yeniçağa Lake and Sofular cave records are almost the same. It is suggested that event deposits are independent of climate effect.

Besides the paleoclimate records of lake sediments, tree rings provide helpful information about the past climates. They have been used extensively to reconstruct the precipitation during the last decade in different regions of Anatolia. These studies identified past wet and dry periods and their durations (Köse et al., 2017).

Touchan et al. (2003) and (2007), and Köse et al. (2013) studied southwestern Anatolia by reconstructing May-June precipitation on tree ring data. Touchan et al. (2003) conducted a preliminary study covering the last 660 years (between 1339 and 1998 AD) in the Burdur and Antalya districts. They correlated the gridded precipitation records and the first and third principal components of three tree ring records from 1931 to 1998 for the reconstruction of May-June precipitation. They aimed to reveal the frequency, duration, and intensity of drought periods, as well as the possible range of extended wet and dry periods. They observed 139 drought events with an average interval of 4.8 years between them. They found that the single

driest spring in 1746 and droughts lasting more than three years were extremely rare, occurring only once between 1476 and 1479. Extended wet spells were also prominent mostly from 1532 to 1535 and from 1688 to 1690. They stated that the existence of extended spring wet periods and the lack of extended droughts in 16th and 17th centuries indicate a probable climate regime shift. Touchan et al. (2007) also developed the reconstruction of May-June precipitation in Mersin and Antalya districts. Their study covered the last 900 years (between 1097-2000 AD). They used response function analyses for the correlation between monthly temperature and precipitation data and tree ring chronology. They observed three wettest and three driest 70-year periods in the reconstruction. These wettest periods occurred in years between AD 1098 and 1167, 1518 and 1587 and 1743 and 1812, driest periods occurred in years between AD 1195 and 1264, 1434 and 1503, and 1591 and 1660. They found that the most humid period from 1518 to 1587 AD were coincident with a notable shift in the European climate. On the other hand, the driest period from 1591-1660 AD was characterized by political, social, and climatic instability in Anatolia. In addition to these studies, Köse et al. (2013) reconstructed the May-June precipitation for southwestern Anatolia spanning the years 1692-2004 AD. Their purpose was to understand the rainfall regime of the region and examine the connection between reconstructed precipitation patterns and significant volcanic eruptions. They calibrated tree ring data with meteorological data. For the reconstruction, they built three tree ring chronologies, and used previously published four tree ring chronologies. They observed 48 wet and 41 dry years between AD 1692 and 1938. While the very dry years were observed in AD 1725, 1814, 1851, 1887, 1916, and 1923, the very wet years were observed in AD 1736, 1780, 1788, 1803, and 1892. They claimed that the longest dry period lasted sixteen years between AD 1860 and 1875. They also found that wet conditions developed after major volcanic eruptions.

Akkemik et al. (2005) conducted a preliminary study on the reconstruction of March-June precipitation in the western Black Sea region of Anatolia covering the years 1635-2000 AD. They examined the widths of trees to figure out drought patterns,

especially patterns of wet and dry years. As a preliminary step in the reconstruction, they investigated the relation between tree ring indicators and monthly precipitation data by using simple correlation coefficients. According to their findings, drought events in this area did not exceed two years, and extremely wet and dry events occurred mostly at one year intervals. They observed that historical drought records in Turkey and neighboring countries confirmed the data provided by tree ring widths. They found major famine and drought events occurred in 1725, 1757, 1887, 1890–1891,1893–1894 and 1927–1928.

Akkemik et al. (2008) presented a reconstruction of May-June precipitation for the western Black Sea region of northwestern Anatolia from AD 1650 to 2000. They also described a spring-summer (May-August) streamflow reconstruction for the first time, apart from other dendroclimatological studies in Turkey. They correlated tree ring widths with gridded monthly precipitation data. They tried to validate the reconstruction of streamflow using the precipitation data for the same period from May to August. In the precipitation reconstruction, they observed 35 one year wet and 61 dry events from 1650 to 1930. Permanent dry anomalies observed in only ten events for at least 2 years which are 1696–1697; 1707–1708; 1715–1716; 1731–1732; 1745–1746; 1819–1820; 1827–1828; 1861–1862; 1893–1894; 1927–1928. They found that the longest interval between dry events was twenty-two years (1905-1926) while it was 27 years for the wet events. Furthermore, longer wet events lasting two years were also rare and occurred in 1729–1730 and 1816–1817. They stated that since the region is mostly humid, dry events have shorter duration compared to other regions.

Akkemik and Aras (2005) presented a study on the April-August precipitation reconstruction by using tree rings in the southern part of central Anatolia. Their purpose was to reveal the wet and dry years and their durations in the region from AD 1689 to 1994. They established the chronology by a linear regression. They observed 23 dry years lasting generally one year, 4 dry years rarely lasting two years and very rarely only 1 dry year lasting three years. The last one was seen in AD 1745-1747. Two wet events with three years duration occurred only between 1727

and 1729, and 1900 and 1902. During three centuries, 2 year dry events 1725-1726, 1796-1797, 1819-1820, 1862-1863 and 1927-1928; two years of wet events occurred in 1770-1771 and 1901-1902. They also observed extreme dry events in 1890 and 1925-1928 AD. They found that the distribution of wet and dry years was not regular, and the interval between two dry periods was less than six years.

Köse et al. (2011) examined past wet and dry events for the western Anatolia by developing spatial and local May-June precipitation reconstructions. They studied the period from AD 1786 to 2000. They observed generally one year and rarely 2-year drought events. The longest dry event lasted four years in AD 1925 and 1928. According to spatial reconstructions from AD 1786 to 1930, extreme dry events occurred in AD 1740, 1794, 1887 and 1893. They found 1887 was the driest year during the 215 years. The wettest events occurred in AD 1835, 1876, 1881 and 1901 for all western Turkey. They concluded that there is a significant overlap between dry years and the years of agricultural famine.

Previous tree ring studies conducted in Turkey were based on measurements of tree ring widths and they aimed to reconstruct the precipitation and find drought events. On the other hand, Heinrich et al. (2013) reconstructed the January-May temperatures by stable carbon isotope ($\delta^{13}C$) chronology in southwestern Turkey. They used tree rings from Jsibeli in Antalya. They found that the chronology goes back to 1125 AD. They stated thay the study is the first isotope record based on tree rings from Turkey, so they evaluated its utility for future palaeoclimatological studies. They aimed to detect high and low frequency climatic signals from the record. They identified the Little Ice Age and the Medieval Warm Period which were related to low frequency signals. However, they could not observe the warming trend of the 20th century observed in other studies in their proxy record and relevant meteorological data used for their study. Moreover, they correlated the reconstructed temperatures with different climate indices such as Mediterranean Oscillation, Arctic Oscillation and North Atlantic Oscillation. They found that atmospheric oscillation patterns have an influence on the temperature variability in southwest Anatolia.

Köse et al. (2017) also presented a reconstruction of March-April spring temperatures by using twenty three tree ring chronologies from Turkey. The study covered the period between 1800 and 2002. They compared their findings to previous precipitation and temperature reconstructions to have a more clear knowledge of climate conditions in the nineteenth and twentieth centuries. The study area covered the western Anatolia, Marmara, the western part of Mediterranean and Black Sea regions. Beside the 15 chronologies produced by previous studies,they developed tree ring chronologies for eight study areas. They measured widths of tree rings and cross dated them visually. Then, they reconstructed the climate by principal components of twenty three chronologies. Between 1800 and 1929, they identified periods of severe warm and cold that usually lasted 1 year or seldomly exceeded 2 to 3 years. The warmest and coldes years occurred for the western Anatolia in the 19th century. Moreover, they stated that the 20th century was characterized by an increased temperature. They concluded that in addition to precipitation signals, temperature signals obtained from tree rings can be helpful climate indicators to reconstruct the past temperature changes.

Fleitmann et al. (2009) studied stalagmite record of Sofular Cave in northwestern Anatolia. Their purpose was to understand the timing of abrupt climatic oscillations occurred in the last glacial period. These are termed as Greenland Interstadials. They collected three active large stalagmites from the cave. The stable isotopes of oxygen ($\delta^{18}O$) and carbon ($\delta^{13}C$) were measured at about twenty-year resolutions. They dated the stalagmites by uranium-thorium dating to develop a precise chronology. They found their record covered the last 50 kyr BP. Although they stated that they do not know exactly how climatic factors impact the $\delta^{18}O$ values in stalagmites, they observed that for longer timescales, $\delta^{18}O$ values are mainly affected by $\delta^{18}O$ changes in the surface water of Black Sea. On the other hand, denser vegetation, higher amount of C3 plants, increased soil productivity occurred in generally wetter and warmer climatic conditions in northwestern Anatolia. That leads to more negative $\delta^{13}C$ values. Therefore, they considered $\delta^{13}C$ record as a sensitive proxy for the local ecosystem changes. According to their findings, they concluded that Sofular Cave

stalagmite record gives clear evidence of a rapid ecosystem and climate response to Greenland Interstadials in the eastern Mediterranean.

Jex et al. (2011) carried out a study on a 500 year long stalagmite record of Akçakale Cave from northeast Turkey. They reconstructed the winter precipitation by extrapolating the relation between the winter (ONDJ) precipitation and the stalagmite $\delta^{18}O$ record in Gümüşhane from 1933 to 2004 AD. They found that the record extended back to 1500. They observed that reconstructed precipitation was lower between years of 1540 and 1560 when higher pressure is estimated over the Caspian Sea. They also stated that present day winter rainfall is assosiciated with pressure fields over Western Russia. They stated that based on the isotope record and meteorological data confirmation, the pressure fields in the Caspian Sea and Western Russia have an impact on the winter precipitation variations in northeastern part of Turkey.

Jacobson et al. (2021) presented a highly resolved, late Holocene record of Kocain Cave from southwest Turkey. They performed multiple proxy measurements on actively growing stalagmite to reveal past climate variations. These are measurements of trace metals, carbon, and oxygen isotope ratios. Trace metals of Mg, Sr, P and Ca were measured at approximately 5 μm resolution. $\delta^{18}O$ and $\delta^{13}C$ isotope measurements were done at 0.5 mm intervals. They constructed the age model by uranium-thorium dating method. They observed that groundwater with longer residence times during drier periods enhance the Mg/Ca ratio. When $\delta^{18}O$ was compared with Mg/Ca ratios, they observed that low Mg/Ca values coincide with more negative $\delta^{18}O$ values. They implied that wetter climates in southwest Turkey are indicated by increases in P/Ca and decreases in Sr/Ca, Mg/Ca, $\delta^{18}O$ and $\delta^{13}C$. They found arid conditions occurred in 1150 and 800 BCE, a wet period in about 330 – 460 CE. This is followed by an abrupt shift to drier intervals between 460 and 830 CE. Finally, a dry/wet pattern of Medieval Climate Anomaly/Little Ice Age was observed.

Cheng et al. (2015) carried out a study on the accurately dated and high resolution speleothem record covering the last 20 ka from Jeita Cave in northern Levant. They used multiple proxies of Sr/Ca ratio and oxygen and carbon stable isotopes. Sample resolution of stable isotope analyses was around 7 years. Sr/Ca profile was developed using XRF scanning. They established the chronology by thorium dating. They implied that changes in $\delta^{18}O$ record are affected by precipitation amount and the east Mediterranean Sea surface $\delta^{18}O$ changes. $\delta^{13}C$ changes in speleothem record are also related to variations in precipitation and evaporation conditions. Lower P-E results in sparse vegetation and less amount of light organic carbon in speleothems, leading to increased $\delta^{13}C$ values. They implied that Sr/Ca ratios are affected by growth rate and prior calcite precipitation process. Precipitation of calcium carbonate is promoted under drier periods. Increased precipitation leads to higher values in Sr/Ca ratio and $\delta^{13}C$ in the dissolved inorganic carbon. They stated that changes in Sr/Ca and $\delta^{13}C$ in speleothems reflecting the dewatering degree in soil and aquifer above the cave is inversely linked to precipitation and evaporation conditions. When they compared long term changes in $\delta^{18}O$ record with Sr/Ca, they observed some offsets. This was interpreted as $\delta^{18}O$ values driven by additional controls such as changes in vapor sources and seasonality. According to their findings, Bond events known as dry events were observed in Jeita $\delta^{18}O$ and $\delta^{13}C$ records. They also found evidence of additional dry events occurred at approximately 7.1, 8.9 and 10.1 ka. They characterized the early Middle Holocene by a trend to higher precipitation-evaporation state, peaking between 7 and 6 ka. Two important drought periods from 5.3 to 4.2 ka and from 2.8 to 1.4 ka were observed in the middle late Holocene. Moreover, they found that a 500-year periodicity dominates the climate variability in the northern Levant.

Zanchetta et al. (2012) studied a multiple proxy record from the sediments of Lake Shkodra in Albania, Montenegro. They performed measurements of multiple proxies using 7.8 m long sedimentary core. They used pollen data and stable isotopes of oxygen and carbon as proxies. The sample resolution of isotopes was approximately between 30 and 50 years. They prepared pollen samples at about 10 to 20 cm

intervals. They developed the age depth model by tephra layer and by radiocarbon dating on macrofossils of terrestrial plant. They found that the lake record covers the last 4500 BP. They stated that since the other proxies are difficult to interpret due to relatively less information on the lake behavior, the oxygen isotope record on carbonate was chosen as the most reliable proxy. $\delta^{18}O$ showed that two significant wet phases were observed approximately at 4300 BP and from 2500 to 2000 BP. During the last 2000 years, four minor wet intervals occurred approximately from AD 150 to 450, 600 to 700, 850 to 1150 and approximately at AD 1860. $\delta^{18}O$ values showed three major peaks indicating drier intervals at around 4100-4000 BP, 3500 BP and 3300 BP. They also identified four drier phases at AD 100, 550, 800 and 1200. They stated that although pollen record did not change due to poor vegetation during these periods, decreasing in pollen data since about 900 BP suggest significant deforestation caused by human activities.

Sharifi et al. (2015) presented a multiple proxy reconstruction of past hydrological variations and aeolian input by using the sediment record of Neor Lake in northwestern Iran. They developed the age model by radiocarbon dating and found that their record covers the last 13000 years. They measured trace and major elements using XRF scanning at approximately 3. 5 year resolution. They used changes in Ti concentrations as proxy for the aeolian input. They observed a transition between Younger Dryas and the early Holocene. While drier and dusty condition occurred during Younger Dryas, a wetter period with low aeolian input and increased carbon accumulation was observed in the early Holocene. During the mid to late Holocene, relatively dustier and drier conditions occurred. Several increased aeolian input events spanning several decades to millennia also occurred in this period. Over the last 13000 years, the wavelength analysis on Ti changes showed considerable periodicities at 230, 320, and 470 years with remarkable periodicities concentrated around 820, 1550, and 3110 years. Moreover, they compared their findings with archaeological and historical records from this region to examine the possible impact of rapid climate changes on significant human settlements. They stated that power transitions, famine and drought periods across

the Mesopotamia, Iranian Plateau and the eastern Mediterranean region coincided with almost all recorded episodes of increased dust deposition during the mid to late Holocene.

Bar-Matthews et al. (2003) conducted a study to reveal paleoclimate conditions in the Eastern Mediterranean by comparing speleothem oxygen and carbon isotope records from two caves with the previously published marine planktonic foraminifera oxygen isotope record. They studied speleothem records of Peqiin Cave in northern Israel and found that the record covers the last 250 kyr. When they compared it to the well studied 185 kyr-long record from Soreq Cave in central Israel, and strong similarities were observed over the last 185 kyr. They stated that both speleothem records indicate a strong regional climate signal caused by fluctuations in temperature and precipitation amount. They also found that the combined Peqiin and Soreq oxygen isotope record perfectly matched with the marine oxygen isotope record. Their research showed a strong relation between sea and land regions. Precipitation in the land region and $\delta^{18}O$ values of precipitation were estimated by using sea surface temperatures as a proxy data for land temperatures. They characterized the low $\delta^{18}O$ speleothem and planktonic foraminifera values with increased precipitation in the Eastern Mediterranean sea and land regions. They concluded that the record for the past 7000 years shows an increasing trend of aridity.

Litt et al. (2012) studied the pollen record of Dead Sea to understand variations in Holocene climate. They used a twenty-one-meter-long sedimentary core retrieved from the western coast of the Dead Sea. According to radiocarbon measurements, they found that sedimentary record covers the last 10,000 years. They applied the botanical-climatological transfer functions to pollen data to reconstruct annual precipitation and winter temperatures. They found three main periods of climate variation. The area was warm and arid in the early Holocene, approximately from 10 to 6.5 ka cal BP. In the middle Holocene, the area was colder and wetter from 6.3 ka to 3.3 ka cal BP. Then, it was warmer and drier in the late Holocene, approximately from 3.2 ka to present.

Kaniewski et al. (2013) conducted a study on Larnaca Lake near Hala Sultan Tekke in Cyprus for the Late Bronze age (LBA) collapse, also known as 3.2 ka event. They aimed to reveal effects of famine caused by sudden climate change by using paleoclimate and archeological proxies. They obtained one core from the lake. They used pollen data for agricultural activity and established the chronology by radiocarbon dating. They applied principal component analyses on pollen data. They observed that positive values indicate increased precipitation whereas negative values reflect dry periods. The integration of archaeological and environmental data showed that the LBA collapse coincided with the start of the 300 year drought event 3200 years ago. They claimed that climate change resulted in crop failures and famine which resulted in accelerated socio-economic crises and regional human migrations.

Emmanouilidis et al. (2022) investigated the sediments of Lake Vouliagmeni in Greece to reveal Holocene climate fluctuations. They obtained a 6 m long sedimentary core from the lake and used multiple proxies. They are stable isotopes of $\delta^{18}O$ and $\delta^{13}C$ on bulk carbonate and aragonite, diatom data and elements by XRF scanning. They established the age model by radionuclide and radiocarbon dating methods. They performed radiocarbon measurements on shells, charcoal, and bulk organic sediments. They found that the core covered the last 11.7 ka cal BP. They used almost 2 g wet sediment to extract diatoms. The sample resolution was chosen as 5 mm for XRF scanning and almost 4 cm for isotope analysis. They observed laminations, homogeneous sediments, and event deposits throughout the core. They found humid and dry periods. Humid episodes were characterized by increases in siliciclastic input and low values in $\delta^{18}O_{bulk}$ from 7.4 ka to 6.8 ka, 5.2 ka to 4.2 ka, 3.3 ka, 2.4 ka and 1.5 ka cal BP. These warm periods also favor the diatom blooms. Dry periods with high summer temperatures were identified by enhanced evaporation occurred from 7.4 ka to 6.8 ka and 5.4 ka and 4.5 ka cal BP. During these periods, they observed increasing aragonite accumulation indicated by more positive values in $\delta^{18}O_{Ar}$ and increases in Sr/Ca and Ca/K ratios.

Different types of proxy data should be compared and correlated for the high-resolution paleoclimate reconstructions. That allows us to forecast the climate in the future by making healthy interpretations for past climate and environmental conditions. Therefore, it is essential to construct a precise chronology in paleoclimate studies (Zolitschka, 2003).

Although most paleoclimatic investigations have focused on lacustrine sediments, they are valuable when a reliable time scale is established. Radiocarbon dating is the most used technique to construct the age depth model (Tylmann et al., 2013). To give a summary about radiocarbon dating, radiocarbon (^{14}C) is the radioactive isotope of the carbon. It is continuously formed in the upper part of the atmosphere by the effect of cosmic ray neutrons on nitrogen atoms. It is quickly oxidized to carbon dioxide in the atmosphere and taken by living organisms for tissue formation. When an organism dies, ^{14}C in the organism immediately begins to decay. Depends on the measuring the radioactive decay level, the time of death can be estimated by using half-life of the radiocarbon isotope of 5568 years. Calcareous shells, pollen, charcoal, remnants of aquatic and terrestrial plants are some examples of organic matter used for radiocarbon dating. However, radiocarbon dating of samples taken from the aquatic environment may contain possible dating errors because of instrumental errors, the contamination of old and young materials (reworking and deposition of older organic materials, bioturbation, root penetration etc), and reservoir/hard water effect (Björck and Wohlfarth, 2002). Allochthonous organic material transported to lakes may be sourced by older organisms. Therefore, the measured radiocarbon age will give an age older than the actual sedimentation age. On the contrary, plant roots growing in higher layers of the sediment may reach the lower levels. In this case, radiocarbon mesurement on plant tissue will give an age younger than the sedimentation age (Olsson, 1991). Carbon in the lake waters used by aquatic organisms (aquatic plants or shelled organisms), can also be contaminated by input of carbon from dissolved old carbonates. This is known as reservoir/hard water effect. Radiocarbon dates measured on organic matter subjected to these effects give results that are older than their actual age (Björck and Wohlfarth, 2002).

Apart from these errors, the ^{14}C production rate is not constant in the atmosphere because of natural changes in the solar activity intensity and geomagnetic field of the Earth. Therefore, radiocarbon ages should be calibrated to convert radiocarbon ages to calendar years. It should be considered that radiocarbon dating does not provide an exact date, it produces a time range. Since fossil fuels burning, and nuclear weapon tests related to human activities have also affected the atmospheric radiocarbon levels over the past 250 years, radiocarbon dating of younger sediments has low accuracy (Walker, 2005; Tylmann et al., 2013). Additionally, constructed chronologies may not always be with the desired resolution and precision due to the lack of materials suitable for dating at all levels throughout the successions, or the lack of budget in research.

On the other hand, lacustrine varved records eliminates the errors caused by radiometric dating. After layers are proven to be annual, chronology can be established by counting of consecutive layers. The uppermost varve reflecting the year of coring allows counting back in time. It assigns an age to each depth interval of the varved record. That produces a continuous and precise chronology in calendar years. Unlike radiocarbon dating, the established chronology can be correlated with instrumental or historical records without calibration (Zolitschka, 2003; Zolitschka et al., 2015). However, they are very scarce in Anatolia and its surroundings. According to Zolitschka et al. (2015), there are two varved lakes in Turkey, namely Nar Lake, and Lake Van. After this publication, Avşar et al. (2016) discovered that Köyceğiz Lake is the third varved record in Turkey. That makes Köyceğiz Lake a priceless archive in paleoclimate studies.

The aim of this thesis is to investigate the paleotemperature information from varved sediments of Köyceğiz Lake (SW Turkey) by using geochemical data obtained from ITRAX micro-XRF core scanner along one undisturbed gravity core.

1.3 Study Area

Köyceğiz Lake is located in the southwestern part of Turkey in Muğla province in the eastern Mediterranean (Figure 1.1a). The lake has a surface area of 52 km^2 which makes it one of the 20 largest lakes in Turkey. It has a catchment area of 875 km^2 and the elevation profile of the catchment area reaches up to 2200 meters of elevation (Avşar et al., 2016; Avşar and Kurtuluş, 2017). Major streams feeding Köyceğiz Lake are Yuvarlak, Namnam and Köyceğiz Streams, and the lake drains into the Mediterranean Sea through the Dalyan Channel (Figure 1.1b). The study area is prevailed by the Mediterranean climate. Summers are hot and dry, and winters are warm and rainy. The lake was described as meromictic lake which means bottom waters are permanently anoxic (Kazancı et al., 1992; Bayarı et al., 1995; Kazancı et al., 2008). It indicates during circulation periods, just the upper portion of water column in lakes is mixed and oxygenated (Anderson et al., 1985). The study conducted by Avşar et al. (2016) report carbonaceous-organic type varved sediments in Köyceğiz Lake. They found that one year of varve deposition is represented by alternation of yellowish calcium rich lamina deposited in summer season and dark clastic sediments and organic matter rich lamina deposited in fall and winter season.

Köyceğiz Lake consists of two different basins which are Köyceğiz and Sultaniye basins (Kazancı et al., 1992). Köyceğiz Basin is in the northern part and Sultaniye Basin is in the southern part of the lake. According to the bathymetric study conducted by Avşar et al. (2016), the maximum depths of the two basins are 26 m in the northern basin and 32 m in the southern basin (Figure 1.1b).

The geology of the SW Anatolia consists of the Lycian nappes and Quaternary alluvium. Lycian nappes can be subdivided from bottom to top into three major units: Yeşilbarak nappes, carbonate nappes and Marmaris nappes. The Yeşilbarak nappe is of Late Lutetian-Early Burdigalian age, and it includes shales and sandstones. All units in the area are covered by the Lower Cretaceous Marmaris nappe (Şenel, 1997; Kurtuluş et al., 2019). It consists of peridotites which is the dominant lithology in

the catchment area with an abundance of around 60% areal extent (Avşar et al., 2016).

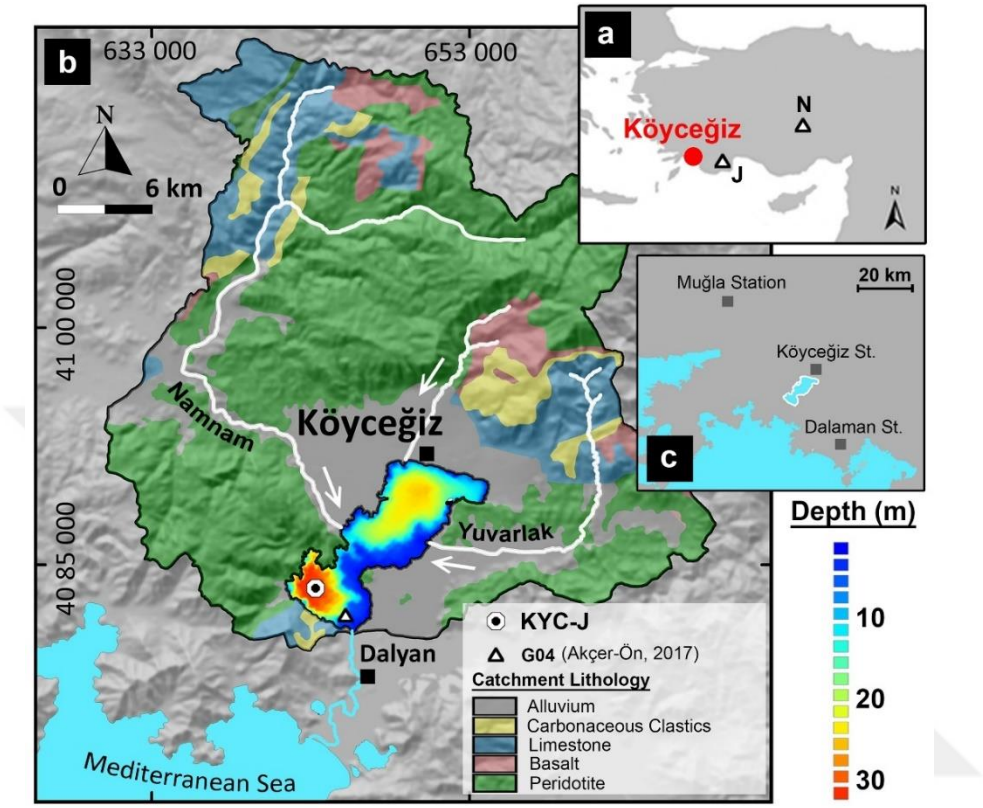

Figure 1.1. a) Location of Köyceğiz Lake in Anatolia. J: Jsibeli Forest and N: Nar Lake. b) Relief-shaded topography and lithological units in the catchment of the lake (Modified from Avşar et al., 2016). The locations of the cores investigated in this study (KYC-J) and in Akçer-Ön (2017) (G04) are also shown. The core studied by Avşar et al. (2016) is 300 m to the west of KYC-J. c) Meteorological stations of which data is used in this study.

CHAPTER 2

MATERIALS AND METHODS

2.1 Bathymetric Survey and Sediment Coring

Bathymetric survey is the first step of lake studies before coring operations. It provides information to understand the morphology of lake basin and to determine the core locations (Jones, 2004; Avşar, 2013).

A bathymetric survey of Köyceğiz Lake was conducted by Avşar et al. (2016). The bathymetric map was obtained by using the "JEOLODTÜ" floating research platform belonging to the Department of Geological Engineering of Middle East Technical University. The study showed that Köyceğiz Lake has two basins. Maximum depth for the northern basin is 26 m and for the southern basin is 32 m.

After the bathymetric map was obtained, the core location was determined. The core was taken from the flattest and deepest part of the lake basin considering two important reasons. The first reason is that a continuous sedimentation may not be observed in the core taken from the basin slopes since they can be subjected to mass movements. That creates a hiatus in the sedimentary sequence. Another reason is that the sedimentation rate in the deep and flat part of the basin is lower than the basin edges, so the cores taken from that point provide a much longer sedimentary record in terms of time.

There are different types of coring techniques to sample sedimentary records from the bottom of lakes. It is important to retrieve the sediment water interface without losing or disturbing sediments (Jones, 2004; Avşar, 2013). When recovering annually laminated lake sediments, undisturbed records enable to establish a well dated varve chronology because the topmost part of the varve record indicates the year of coring (Zolitschka et al., 2015).

In this study, gravity coring method was applied to recover the sediments in Köyceğiz Lake. Simply, a core tube penetrates vertically into the sediments under the effect of free gravitational fall in gravity coring operations.

Steps of gravity coring operation are schematized in Figure 2.1. A typical gravity corer is made up of three main parts (Figure 2.1) : (a) PVC liner, (b) brass weight, and (c) valve flap at the top of the core tube. The first step is to lower the corer to a specific height from water-sediment interface (free fall height in Figure 2.1-1) where the corer is released for the free gravitational fall. Then, valve flap is open to allow water flow into the PVC liner and to take sediment during free fall and penetration (Figure 2.1-2). After the optimum penetration is achieved (Figure 2.1-3), the corer is pulled back (Figure 2.1-4). The valve flap is closed, and it makes vacuum to prevent sediment loss (Avşar, 2013).

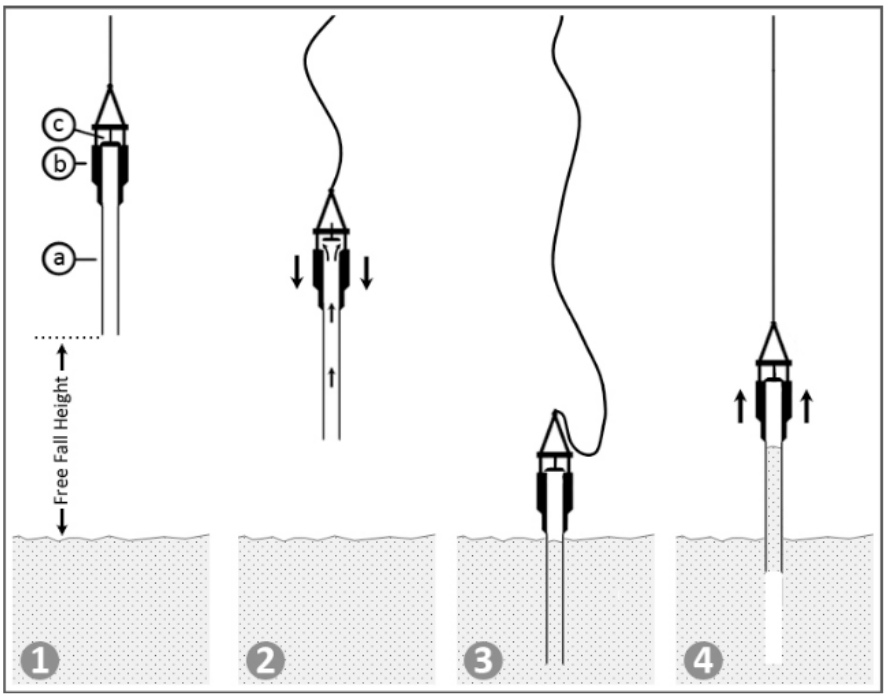

Figure 2.1 Steps of the gravity coring operation (Avşar, 2013).

The amount of recovered sediment can be affected by free fall height and the brass weight on the corer. If the free fall height is higher than a certain level, the corer may be tilted during the fall. In such a case, the penetration will not be vertical. On the

contrary, inadequate free fall height may result in insufficient sediment recovery due to poor penetration. Therefore, maximum possible brass weight should be used for minimizing the free fall height. For this purpose, several attempts could be helpful in determining the appropriate free fall height for optimum sedimentary core recovery. Valve flap should also be light and freely move to provide water flow through the PVC liner during the fall without creating turbulence in front of the liner.

Within the scope of this study, one gravity core was collected from the deepest and flattest part of southern basin of Köyceğiz Lake (E: 643080, N: 4083670) in June 2017. The gravity coring technique operated in this study made it possible to obtain 124.95 cm-long core. After the coring process was completed, the core was transported to METU Sediment Coring and Analysis Laboratory.

2.2 Core Splitting

Core splitting was performed to prepare sediments for geochemical analysis. A core cutting platform was used to separate cores into two halves. There are cutting discs on the left and right sides of the platform. The core is positioned horizontally on the platform and fixed to the platform with plastic clamps. During cutting process, to avoid damaging both the cores and sediments inside the cores, the discs moving at a slow and steady speed cut the PVC pipe equally from the outside of the core. The cut core is removed from the platform and placed on a flat surface. It is split into two halves by sliding of a fishline through the cut edges of the pipe. In order to make the core ready for further investigations, the surface of the core is cleaned and smoothed by scraping approximately 1-2 mm of sediment from the core to expose the fresh surface.

2.3 ITRAX Micro-XRF Core Scanning

The ITRAX micro-XRF core scanning is a widely used method in lacustrine, marine, and terrestrial records and drilled rock cores (Croudace et al., 2006; Avşar, 2013). It

provides RGB optical and radiographic images and down core element variations of sediments along the cores. When ITRAX core scanning is compared to conventional XRF analysis, ITRAX scanner is a very rapid method for obtaining high resolution continuous records at decadal, annual, and even sub annual scales without damaging to split sediment cores (Croudace and Rothwell, 2015). Sediments are incrementally sampled, then dried and grounded in conventional XRF methods. The sample preparation operations for conventional techniques require 2 weeks for a 1 m core at 1 cm increments. On the other hand, ITRAX core scanner is capable to analyze the same core at 200 μm increments in a few hours (Croudace et al., 2006; Avşar, 2013). Therefore, the ability of the ITRAX micro-XRF core scanner provides opportunities for studies of annually laminated sediments "varves". Since they are too thin to sample manually, it is very difficult to prepare discrete samples for chemical analyses. Hence, the application of ITRAX has a great importance in paleoenvironmental and paleoclimatic reconstruction studies (Croudace and Rothwell, 2015).

The ITRAX scanner (Figure 2.3a) is made up of a central measuring tower involving an X-ray focusing unit and a range of sensors. The components of the ITRAX system are showed in Figure 2.3b. The system works in four steps. Firstly, the RGB image is obtained by optical line camera before X-ray scanning. Secondly, radiographic image is taken. The X-rays generated by the source reach the flat-beam waveguide. The beam passes through sediments and X-ray line camera records the number of X-rays. Thirdly, the triangle laser system measures the surface topography of the core along the measuring line. Then, during scanning, the XRF detector arranges its distance from the core. Finally, the XRF scan is performed at desired increments.

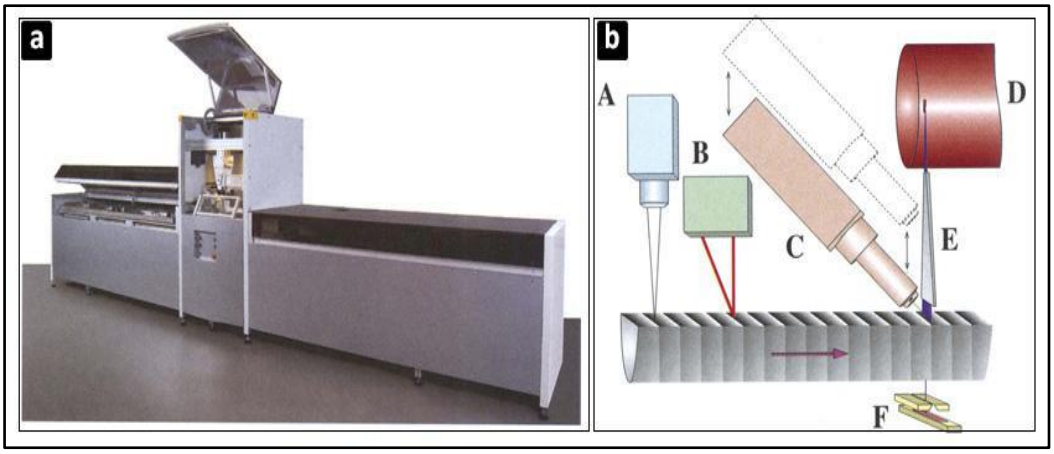

Figure 2.3. a) Front view of the ITRAX micro-XRF core scanner. b) Components of ITRAX micro-XRF system. A: optical line-scan camera, B: triangular laser system, C: motorized XRF Si-drift chamber detector, D: 3 kW X-ray tube, E: flat-beam X-ray waveguide, and F: The X-ray line camera (Croudace et al., 2006).

Based on elements of interest, the X-ray tube type used by ITRAX should be determined carefully before scanning. The most used types are Molybdenum (Mo) and Chromium (Cr). The Mo X-ray tube is more suitable to detect heavier elements. On the contrary, lighter elements are detected by the Cr X-ray tube (Croudace et al., 2006; Avşar, 2013). Measurement increments and dwell time at each measurement point can be set by the users to achieve qualified data. Increments for the measurements are entirely dependent on the needed resolution. They can be set as fine as 200 μm for finely laminated sediments. In addition, determination of optimum dwell time has a significant importance not only for the data quality but also for the budget of the analysis (Avşar, 2013).

Within the scope of this research, the sediment core was scanned in the ITRAX Laboratory constituted by the Marine Research Department of the General Directorate of Mineral Research and Exploration (MTA). The core consisting of finely laminated varved sediments was scanned at 0.02 cm resolution. The XRF scanning was done by Mo-tube with 5 seconds of exposure time.

ITRAX generates XRF spectra for each measurement point during scanning. A spectrum is a plot of incident X-ray energy (keV) vs measured photon emission intensity from a sample in terms of counts per second (cps). The XRF spectra detect elements depending on their specific level of incident X-ray energy to emit photons. The emission rate (i.e., height of the peak) is a function of element concentration in the sample. The ITRAX software automatically detects the peaks on XRF spectra and calculates their areas.

Since the ITRAX core scanners perform measurements directly on untreated bulk sediment surface, XRF measurements are strongly influenced by sediment properties such as organic matter content, water content, grain size distribution and porosity (Böning et al., 2007; Tjallingii et al., 2007; Löwemark, 2011; Avşar, 2013). Therefore, it would be misleading to directly use the ITRAX data of an element to interpret its variation along the core. To overcome this problem, the ratios of elements to each other are used so that more reliable paleoclimatic and paleoenvironmental interpretations can be made (Croudace et al., 2006; Avşar, 2013). However, comparable scales between elements should be obtained to use element ratios. Although all acquired ITRAX data is measured in counts per second, their magnitudes significantly change. For this reason, the dataset should be standardized for comparison to eliminate different magnitudes. The mean (μ) and standard deviation (σ) values of each element are calculated for standardization. The standard value (z) for each measurement point is obtained by means of dividing the difference between the data value and the mean value at that point by the standard deviation value (Equation 1). The standard scores (z) of each variable are calculated to get a dataset with mean value of 0 and standard deviation of 1, so that different elements are scaled comparably through the sedimentary sequence.

$$z=(x-\mu)/\sigma \qquad \text{Equation 1}$$

Where z: standardized value, x: data value, μ: mean of the dataset, and σ: standard deviation of the dataset.

2.4 Construction of Varve Chronology

The annual nature of laminated sediments should be confirmed to construct a varve chronology since many finely laminated sediments are sometimes attributed as varves. Therefore, independent dating methods are needed to verify annual laminations (Ojala et al., 2012; Jones, 2014). According to the study by Avşar et al. (2016), annual laminations in Köyceğiz Lake were confirmed by ^{137}Cs and ^{210}Pb dating methods.

Visual counting can be used to date varved sediments. However, it can be complicated especially when annual layers are too thin to count (Weinheimer and Biondi, 2003; Cuven et al., 2015). Recent technological developments have supplied new perspectives to counting of annual layers to construct the chronology. The advances in micro-XRF core scanning allow varve counting by using radiographic, optical images and elemental profiles of varved sequences (Zolitschka et al., 2015).

In this study, the varve chronology was constructed by counting the peaks along the elemental profile of Ca/Ti ratio and optical image obtained from ITRAX micro-XRF core scanning.

2.5 Principle Component Analysis (PCA)

The ITRAX method mentioned above produces several different variables (i.e., elements) measured on the sediment core. However, these variables are not fully independent of one another. Multivariate statistical techniques are utilized to study inter-variable relationships for this type of datasets (Davis, 2002). In this study, Principle Component Analysis was applied on the dataset of ITRAX. Simply, this statistical method reduces the number of variables. Correlated variables are grouped together, and new sets of uncorrelated variables called as principle components (PCs) are created. For this purpose, SPSS software was used to process each standardized variable of ITRAX dataset.

2.6 Multiple Linear Regression Analysis

Multiple linear regression is a statistical approach for predicting the result of one variable depending on the values of two or more variables. It is an extension of simple linear regression. In simple linear regression, single independent variable is used to predict the dependent variable. On the other hand, in multiple linear regression, the dependent variable is predicted by multiple independent variables (McKillup and Dyar, 2010). The equation is expressed as:

$$Y = a + b_1X_1 + b_2X_2 + b_3X_3 + \cdots etc \qquad \text{Equation 2}$$

Where Y is the dependent variable to be predicted. X_1, X_2, X_3… are the independent variables used to predict dependent variable. "a" is the constant value and b_1, b_2, b_3… are the multipliers that describe the degree of the effect of independent variables on dependent variable (i.e., Y).

In a regression model, R-squared (R^2, coefficient of determination) is a statistical measure that determines the proportion of variation in the dependent variable predicted by the independent variables. In other words, it indicates how well the data fit the model. The value of R^2 can range from 0 to 1. If the R^2 is equal to 1, it indicates that the regression estimatations fit the data perfectly.

Within the scope of this study, multiple linear regression analysis was applied on the element of ITRAX dataset to estimate average summer temperatures recorded at Muğla, Köyceğiz and Dalaman meteorological stations. Elements were used as independent variables, and the estimated temperature was the dependent variable in this study. The formula produced by the analysis was extrapolated down core for summer temperature reconstruction along the core.

CHAPTER 3

RESULTS

3.1 Optical Image

Firstly, optical image of the core taken from Köyceğiz Lake was visually examined. It was observed that annual laminations were repeated rhythmically throughout the core. For detailed interpretation, optical image of the topmost 12 cm was chosen and illustrated in Figure 3.1. This interval represents whole cored section, and it is suitable for showing detailed interpretations without causing any confusion. Yellowish and brownish-bluish colored laminations in the range of 1-2 mm thickness and approximately 2-6 mm spacing are easily recognized along the core. However, there are also intervals where laminations are not distinct (e.g., at the depth between 8 cm and 11 cm). These light and dark colored laminations of Köyceğiz Lake are very similar to the typical view of carbonaceous organic varve extensively defined in the literature (e.g., Zolitschka et al., 2015). During the period of increased seasonal temperature, calcite generally precipitates from the water column in two different ways. Calcium carbonate becomes less soluble with the increasing temperature in surface waters, so it directly precipitates from the water column. Temperature dependent increase in photosynthetic activity also removes CO_2 from the water. This situation results in an increase in pH of lake water. That decreases the solubility of calcium carbonate and leads to its precipitation (Kelts and Hsü, 1978; Zolitschka et al., 2015). This deposition appears as a distinct whitish-yellowish carbonate lamina. On the other hand, during fall and winter months, rainfall is high compared to summer months. Runoff events associated with the rainfall transport terrestrial clastic sediments and organic matter into the lake. This deposition seems like dark colored lamina. Laminations formed as couplets consisting of yellowish-whitish carbonate laminae and organic material rich dark laminae are described as

carbonaceous organic type varve. Avşar et al. (2016) proved annual laminations in Köyceğiz Lake by ^{210}Pb and ^{137}Cs dating methods and laminae counting. One year of varve deposition of Köyceğiz Lake is made up of alternating yellowish carbonaceous lamina and brownish-bluish clastic sediments and organic matter rich lamina.

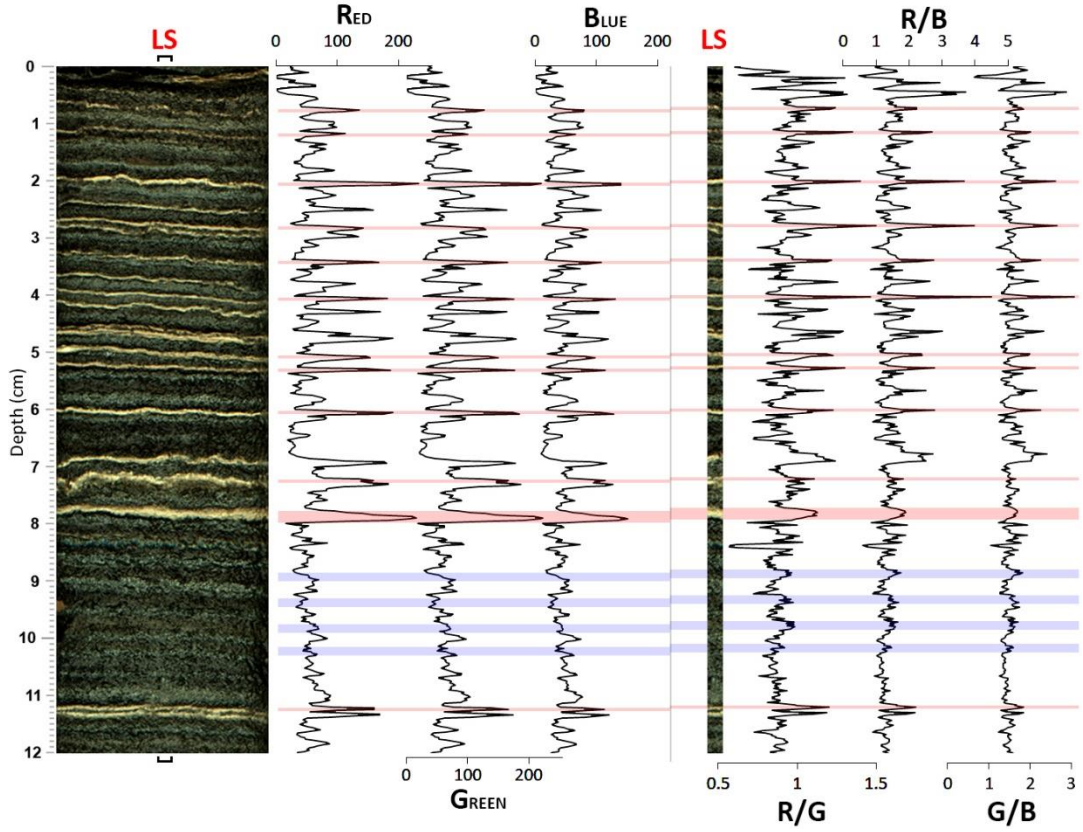

Figure 3.1. Optical image of the uppermost part of the core. Profiles of Red (R), Green (G) and Blue (B) values and their ratios to each other. Red and purple bars represent the yellowish carbonaceous laminae along the LS.

The optical RGB image of the core was converted into matrices containing RGB values for each pixel in the image by using Matlab software. Then, Red (R), Green (G) and Blue (B) values and their ratios to each other along the 20-pixel-wide Line of Scan (LS) were plotted. In Figure 3.1, individual profiles of R, G, B are shown on the left side of the LS, whereas their ratios, namely as R/G, R/B and G/B, are shown

on the right side of the LS. Profiles showing anomalies along the LS are considered to represent the yellowish laminae. However, unlike distinct yellowish laminae, indistinct ones do not show significant anomalies along the profiles. In the figure, the visually distinct yellowish laminae are indicated by red bars, indistinct laminae are marked with purple bars along the LS. At the first glance, the yellowish carbonaceous laminae seem to be represented by anomalies along profiles of R, G and B. However, when the bars are followed carefully, the anomalies along profiles of R, G and B do not coincide with the yellowish carbonaceous laminae. On the other hand, anomalies along the ratio profiles are more compatible with the yellowish carbonaceous laminae. Careful examination reveals that R/G profile is the best indicator of the yellowish carbonaceous laminae.

3.2 ITRAX Micro-XRF Data

Element profiles along the core are presented in Figure 3.2. The levels representing yellowish carbonaceous laminae (i.e., summer laminae) on the profiles are marked with red bars. It was observed that elements representing terrestrial clastic material (Si, K, Ti, Cr, Mn, Fe, Ni, V, Zn and Rb) were depleted at summer levels. On the other hand, these elements carried from the catchment to the lake by runoff events, were enriched at levels corresponding to brownish-bluish laminae (i.e., winter laminae). Since Ca and Sr elements are indicators of carbonate content, significant anomalies are observed in Ca and Sr element profiles at summer levels. Hence, correlation between elements representing clastic material and elements representing carbonate is negative. In the first 8 cm, Br and Cl elements negatively correlate with Ca and Sr (i.e., positively correlate with elements of clastic material) at summer levels, while they negatively correlate with elements of clastic material between 8 and 11 cm. Cu and Zr do not show a consistent correlation with other elements visually throughout their profiles.

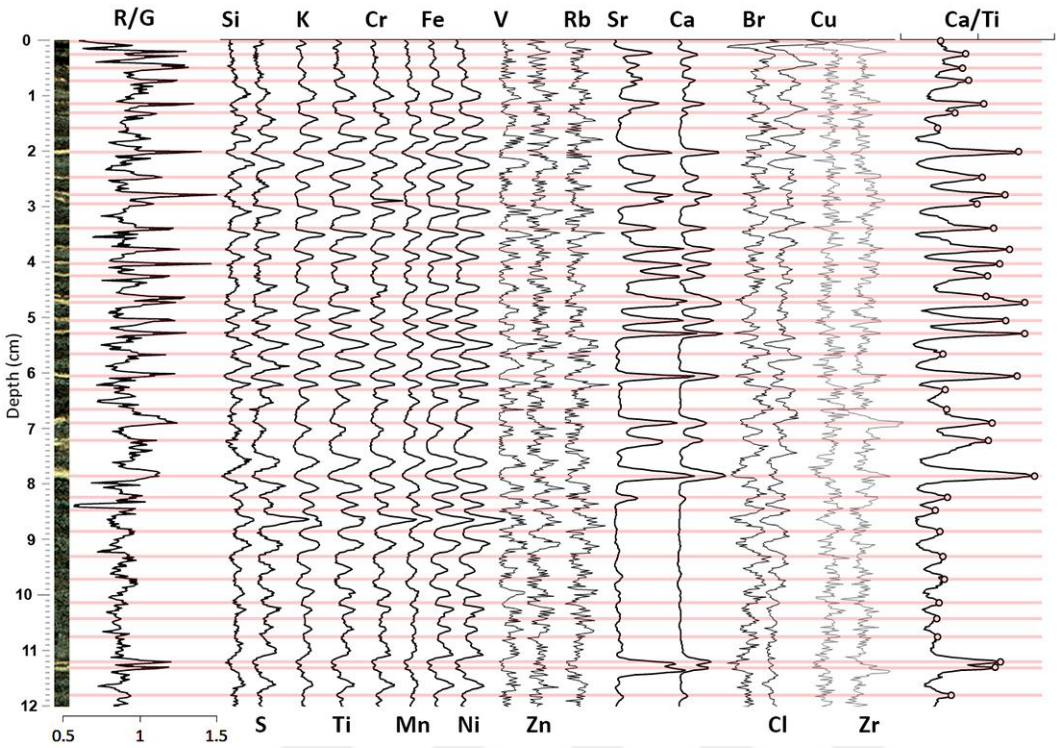

Figure 3.2. XRF data showing each element profile along the core. R/G profile is also plotted. Red bars show yellowish carbonaceous laminae.

As seen in Figure 3.2, all elements representing clastic material follow the same pattern. In this study, Ti was selected to represent allochthonous clastic input during fall and winter months. Among other terrestrial silicate elements, Ti is regarded as more reliable element in the literature. It is redox insensitive, and not affected by diagenetic and biologic processes. On the other hand, Si may be derived from siliceous organisms (e.g., diatoms). Fe and Mn may be affected by redox conditions and diagenetic processes. Ca and Sr represent calcium carbonate precipitation. Calcium carbonate can be precipitated from the water column by geochemical processes, or it can be formed from the skeletal remnants of aquatic organisms as biogenic carbonate. Sr following the pattern of Ca, indicate Sr presence in calcite crystals. Sr may also incorporate into aragonite (Croudace and Rothwell, 2015; Dulski et al., 2015). In this study, Ca was selected for the indicator of autochthonous calcium carbonate deposition during summer months. It should be considered that

the data provided by ITRAX are semi quantitative, so concentrations do not indicate the absolute element concentrations. Thus, changes along an element profile should not be interpreted as exact changes in that element. Using element ratio profiles instead of single element profiles will lead to a more precise interpretation of relative changes in elements. Figure 3.2 illustrates that element profile of Ca/Ti shows significant anomalies at levels of yellowish carbonaceous laminae (i.e., along red bars). While anomalies were almost invisible at levels between 8 cm and 11 cm in individual profile of R/G and Ca, using element ratio profile of Ca/Ti allowed to observe anomalies at these levels. In this study, profiles of Ca/Ti ratio and R/G are used to establish the varve chronology.

Varve chronology was constructed by counting summer carbonaceous laminae. They are represented by anomalies along both R/G and Ca/Ti profiles, which means more yellowish and more carbonate content, respectively. In addition, R/G and Ca/Ti profiles were multiplied in order to better illustrate levels where both conditions are satisfied (i.e., both yellowish and carbonate-rich levels). The detected varves (i.e., yellowish carbonaceous laminae) are marked with red bars on R/G, Ca/Ti and [R/G]x[Ca/Ti] profiles. These lines are also shown on optical image of the core along the LS. All of the varves were detected along KYC-J through Figure 3.3 to Figure 3.11. Varve numbers counted at every five varves are presented in each successive 15 cm of the core and they are shown on the right-hand side of these figures.

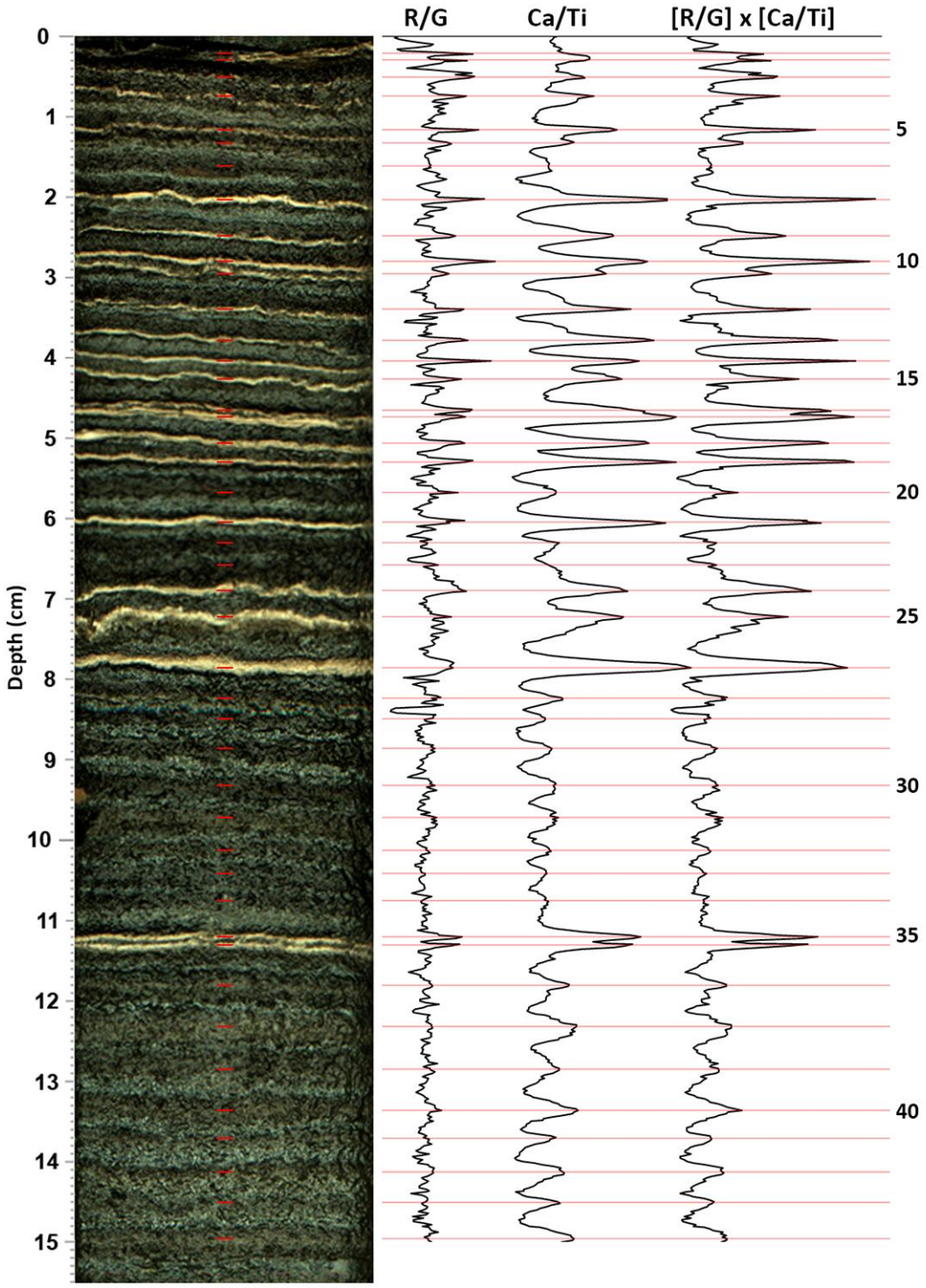

Figure 3.3. Varve counting along profiles of R/G, Ca/Ti and [R/G]x[Ca/Ti] for the first 15 cm of the core. Varve numbers at every five varves are shown on the right-hand side.

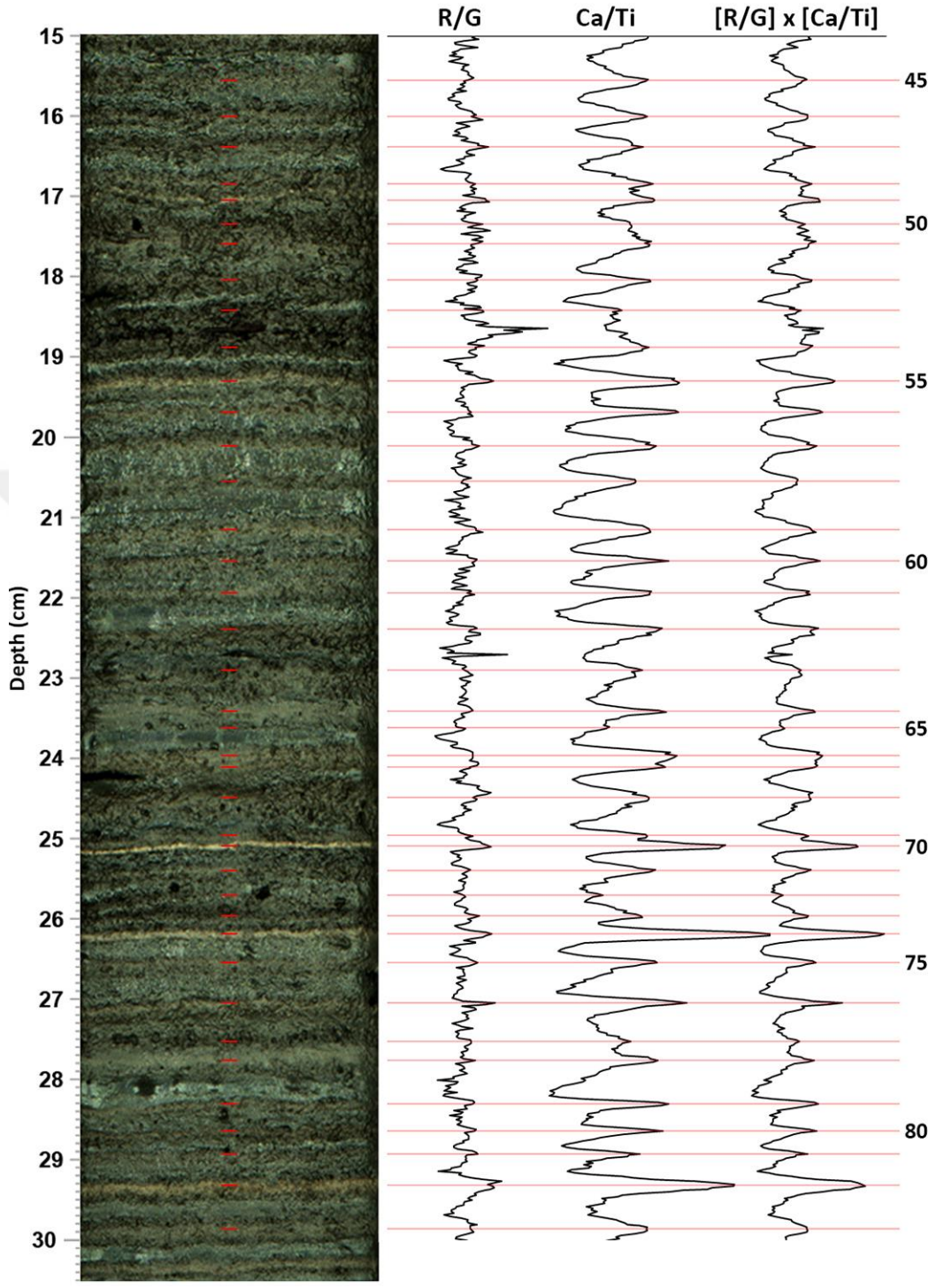

Figure 3.4. Figure 3.3 continues for 15-30 cm of the core.

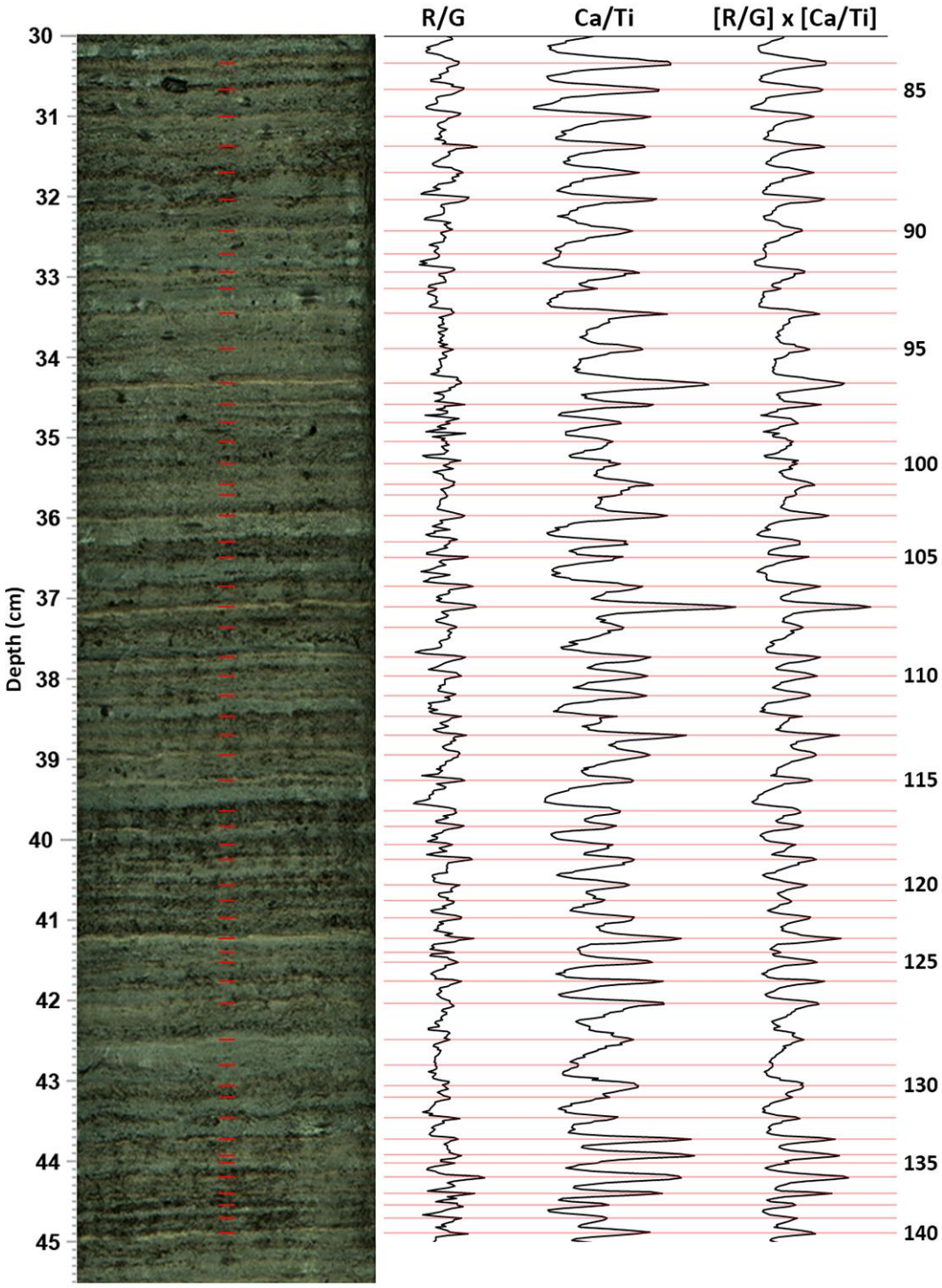

Figure 3.5. Figure 3.3 continues for 30-45 cm of the core.

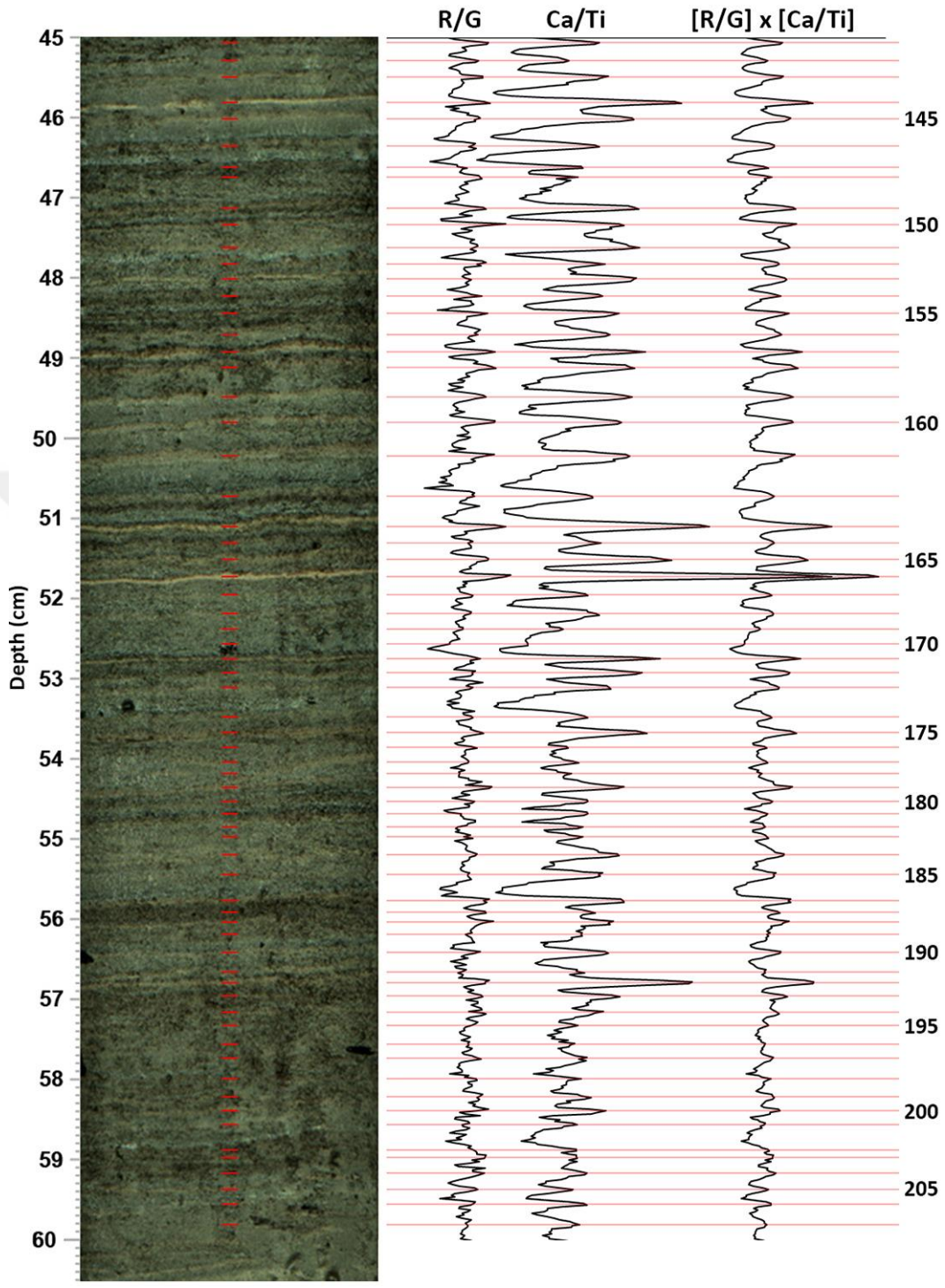

Figure 3.6. Figure 3.3 continues for 45-60 cm of the core.

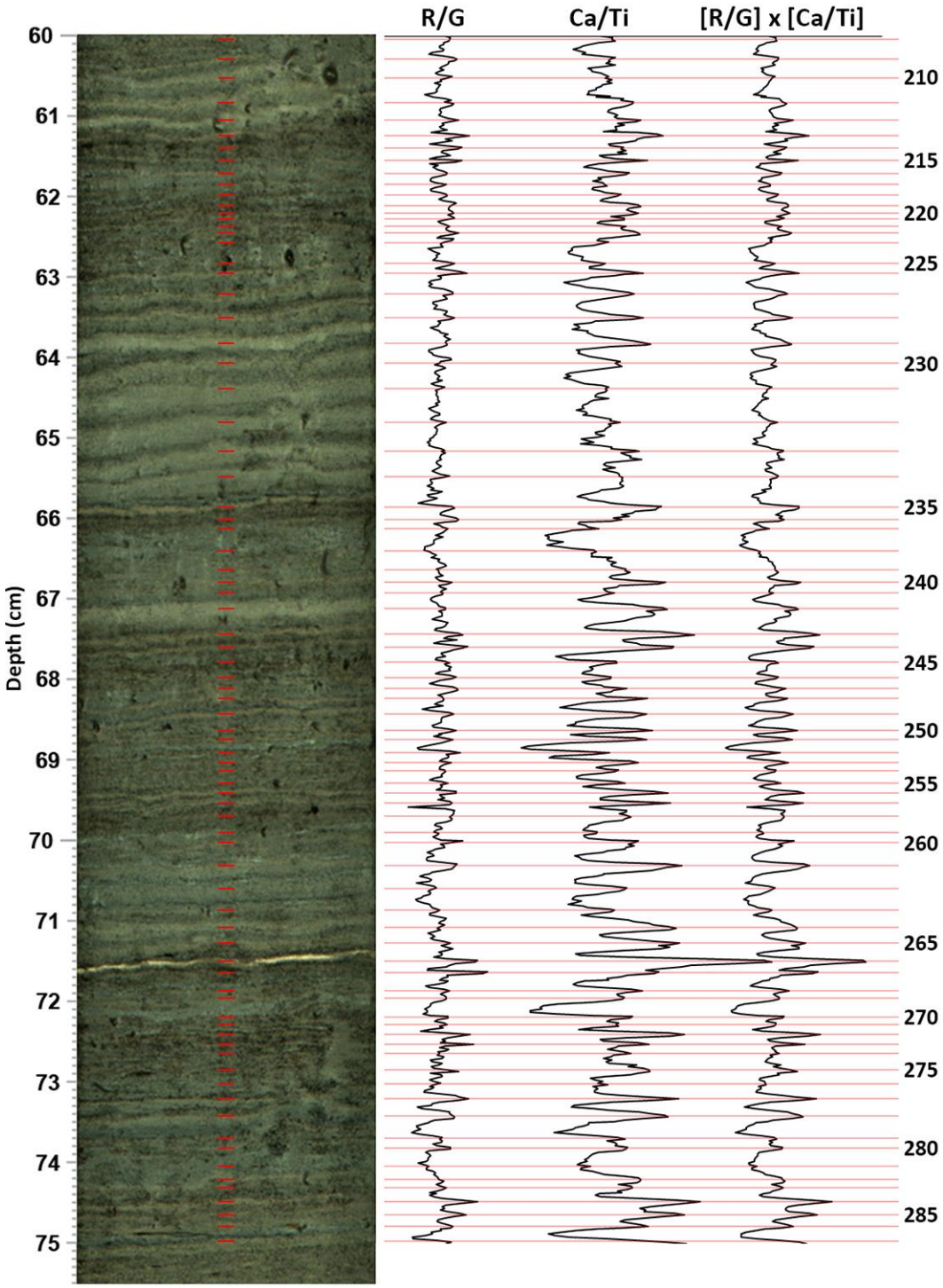

Figure 3.7. Figure 3.3 continues for 60-75 cm of the core.

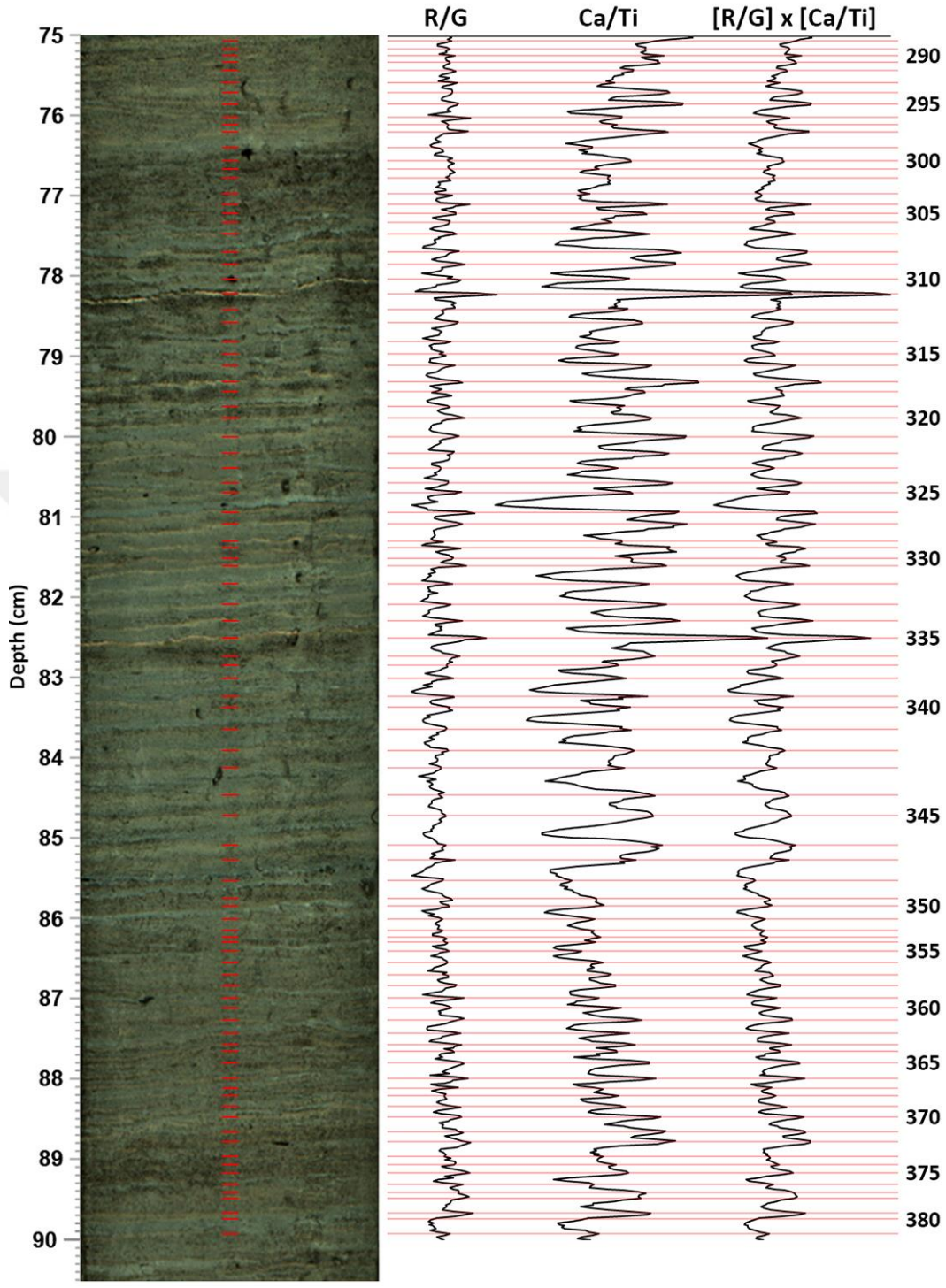

Figure 3.8. Figure 3.3 continues for 75-90 cm of the core.

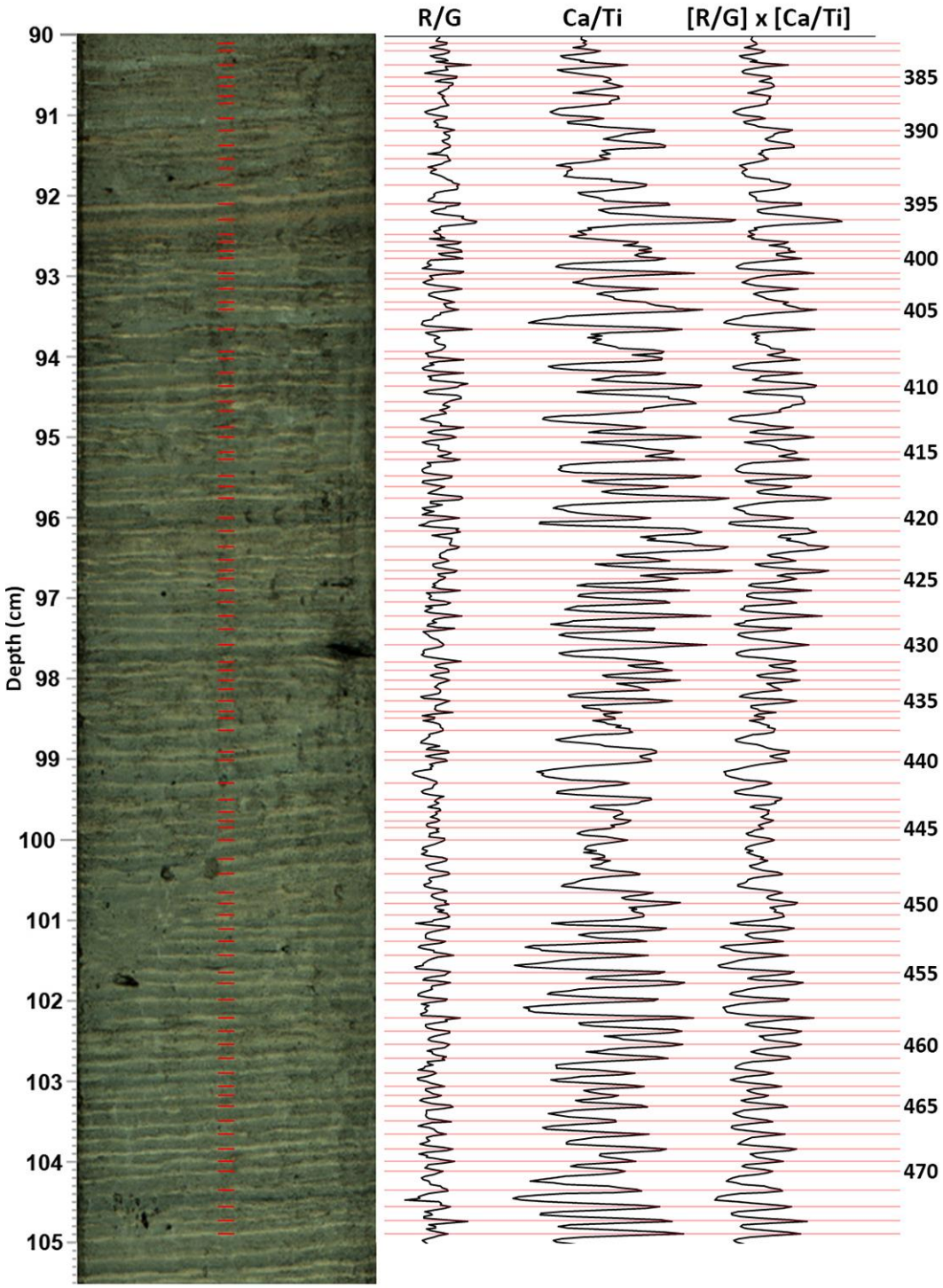

Figure 3.9. Figure 3.3 continues for 90-105 cm of the core.

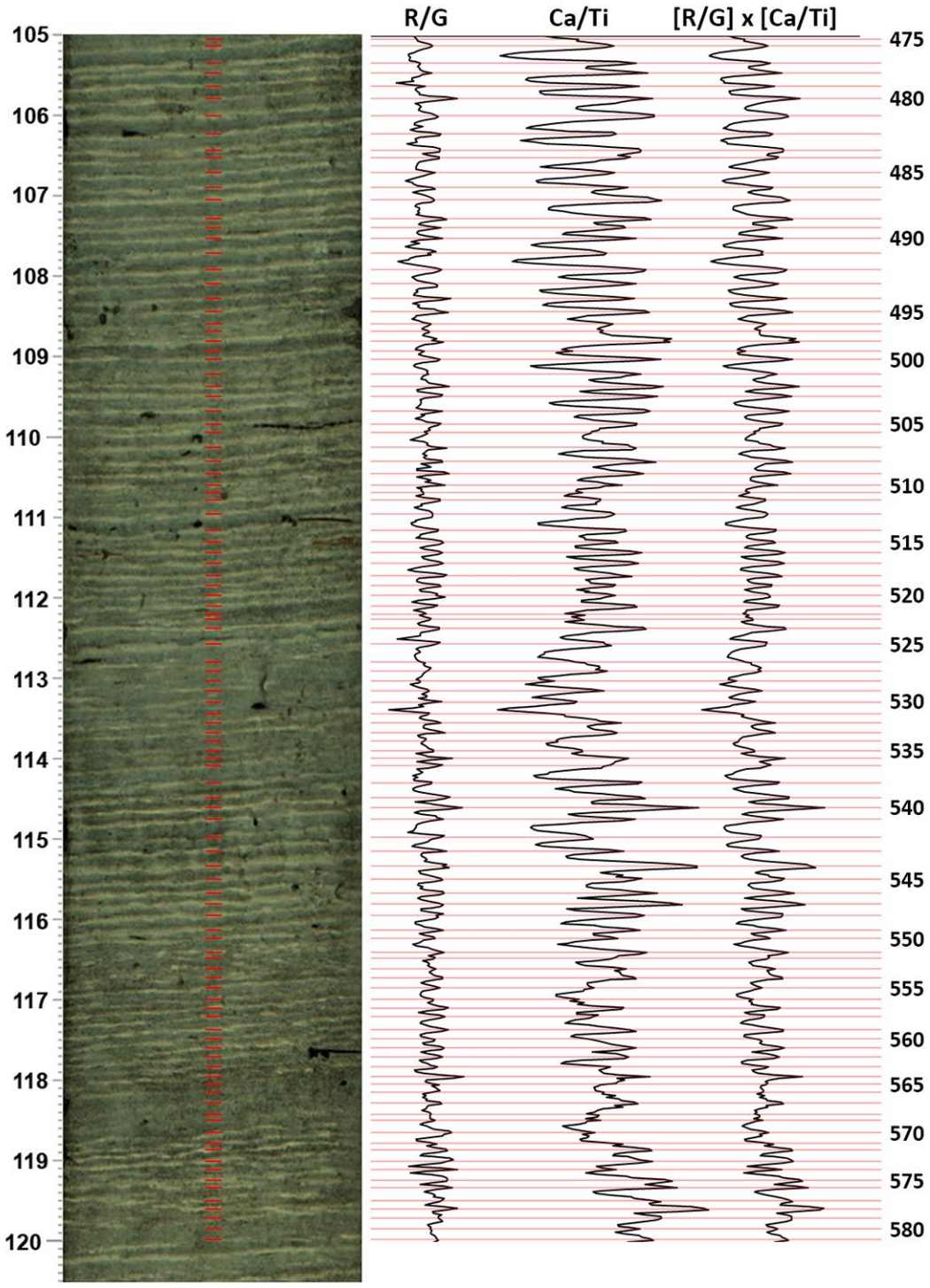

Figure 3.10. Figure 3.3 continues for 105-120 cm of the core.

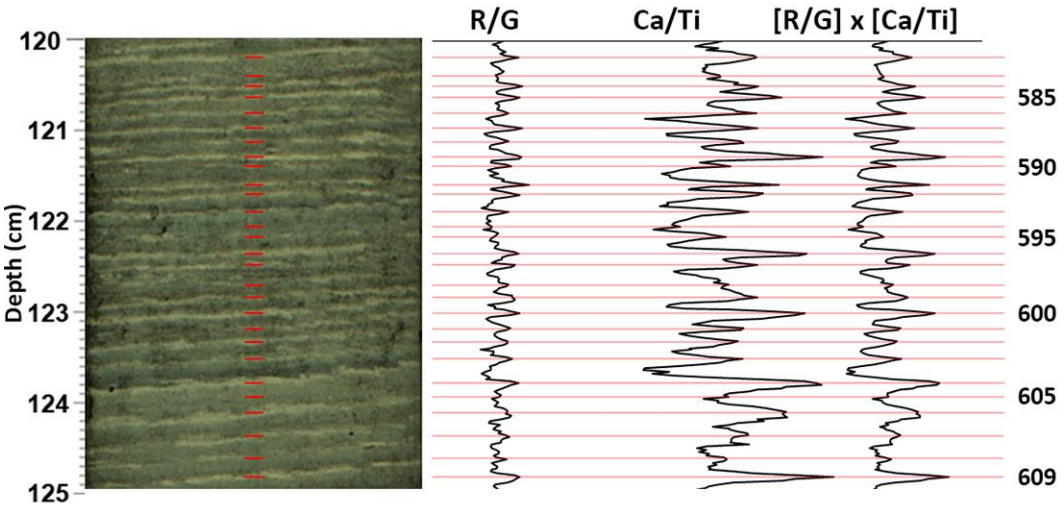

Figure 3.11. Figure 3.3 continues for 120-124.95 cm of the core.

During varve counting, in most cases, full-width optical image and R/G-Ca/Ti profiles clearly agree on the presence of varves (Figure 3.12a). However, in some cases, although the profiles do not clearly show evidence of a varve, careful inspection of the full-width optical image reveals varves missing along the LS (Figure 3.12b). In this case, firstly, prominent varves observed on the profiles and the optical image were detected. Then missing varves between these distinct varves were carefully checked and detected. For example, varve numbers 401, 403 and 405 are prominent on the profiles and the optical image. They were drawn by red lines on the optical image in Figure 3.12b. Varve number 402 was detected between varve numbers 401 and 403, and varve number 404 was determined between varve numbers 403 and 405. These missing varves were drawn by green lines on the optical image. In addition, varve thickness in adjacent levels was also considered for detecting varves in order to avoid non-reasonable sedimentation rates. It is seen that profiles and full-width optical image should be considered together in order to achieve a reliable varve counting. In conclusion, total of 609 varves were detected along 124.95 cm-long KYC-J core corresponding to 0.205 cm/yr sedimentation rate in average.

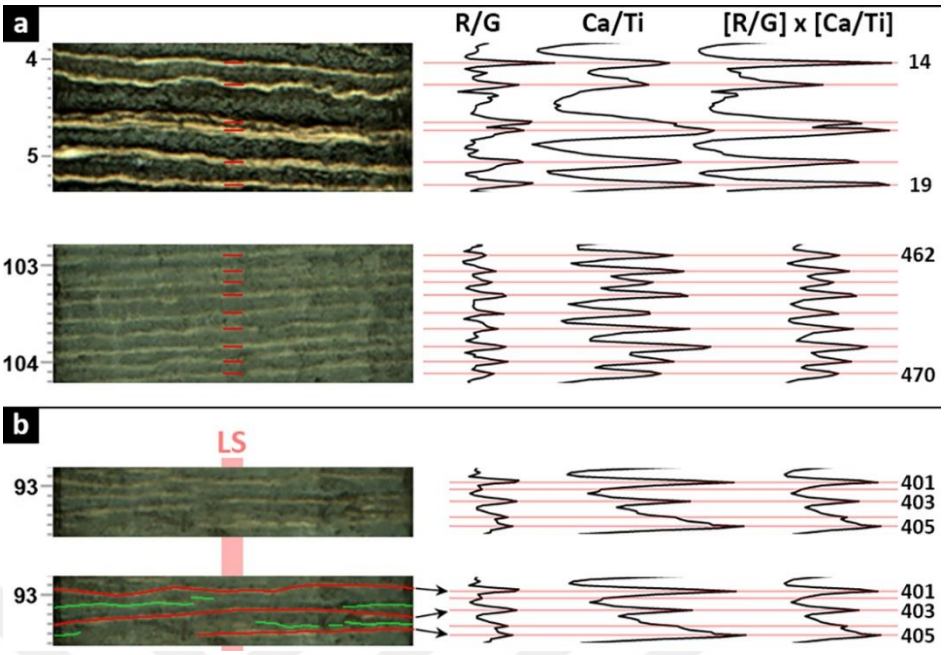

Figure 3.12. Close-up views of KYC-J, as examples of detection of distinct varves on the profiles and the full-width optical image (a) and missing varves along the LS (b).

The age-depth model (i.e., varve chronology) along the core is presented in Figure 3.13a. The sedimentation rate was calculated as 0.33 cm/year for the upper parts and 0.16 cm/year for the lower parts of the core. As it can be expected, sedimentation rate gets lower since the effect of compaction is higher on the deeper sediments. The core studied by Avşar et al. (2016) is approximately 300 meters to the west of KYC-J core also investigated in this study. For this reason, a stratigraphical correlation can be expected between these two cores. They present profiles of varve thickness and $[Cr/Ni]_{av}/[Ti,K,Fe]_{av}$ that can be compared with KYC-J core. Varve thickness profile was obtained by using peaks along the Ca/Ti profile. The difference between the depth corresponding to the peak point of the mentioned year and the depth corresponding to the peak point of the previous year was calculated as the varve thickness of the mentioned year. For example, the depth difference between 2016 and 2015 was taken as the varve thickness of 2016. In Figure 3.13b, comparison showed that although there seems to be a few years of discrepancy, varve thickness profiles of two studies correlate well.

On the other hand, the correlation between $[Cr/Ni]_{av}/[Ti,K,Fe]_{av}$ profiles is not obvious which is presented in Figure 3.13c. Avşar et al. (2016) reported anomalies along $[Cr/Ni]_{av}/[Ti,K,Fe]_{av}$ profile after earthquakes creating peak ground acceleration (PGA) values higher than 70 cm/s^2. They interpreted these anomalies as increased erosion rates in the catchment of the lake due to strong earthquakes, and hence increased sediment influx to the lake, i.e., Catchment Response (CR). Since the catchment of Köyceğiz Lake is dominated by peridotites, landslides caused by strong earthquakes remobilize sediments sourced from these ultramafic rocks. That results in Ni and Cr enriched sedimentation that lasted 5 to 10 years. It was observed that the CR due to 1959 earthquake is evident in KYC-J core (Figure 3.13c). However, the CRs related to 1852 and 1869 earthquakes are not seen in the core KYC-J. This is probably because the core studied by Avşar et al. (2016) is closer to the shoreline, which makes it more sensitive to sediment influx from catchment. Additionally, the CRs due to 1852 and 1869 earthquakes were probably weaker that the one after 1959 earthquake. Hence, their sediments could not reach the core location of KYC-J.

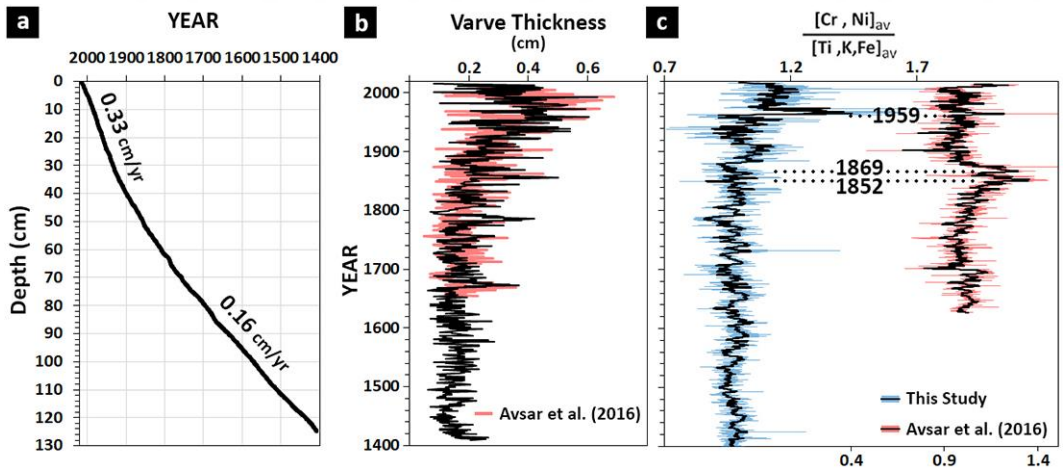

Figure 3.13. a) Age-depth model of KYC-J. b) Comparison of profiles of varve thickness. c) $[Cr/Ni]_{av}/[Ti,K,Fe]_{av}$ along KYC-J and the core studied by Avşar et al. (2016). Note that blue and red lines in the $[Cr/Ni]_{av}/[Ti,K,Fe]_{av}$ profiles represent the raw data where black lines that overlap them indicate 21-point moving average.

Full resolution (i.e., 0.2 mm increments) ITRAX data was plotted with respect to time in Figure 3.14. Profiles of individual elements and some of the most used paleoclimate proxy ratios in the literature, Sr/Ca, Ca/Ti and Sr/Ti were also plotted in the figure.

The elements Ca and Sr are indicators of calcium carbonate precipitation. Calcite usually precipitates from the water column either with increasing temperature in the lake waters or as a result of temperature-dependent increase in photosynthetic activity. They decrease the solubility of calcium carbonate and lead to its precipitation from the water column (Kelts and Hsü, 1978; Zolitschka et al., 2015). Sr following the pattern of Ca, indicate the Sr presence in calcite crystals (Dulski et al., 2015). Sr may also incorporate into aragonite. Sr/Ca ratio is used as a proxy for aragonite (Croudace and Rothwell, 2015). Increased evaporation with increasing temperatures rises the salinity of lake water. This promotes aragonite precipitation (Kelts and Hsü, 1978). The increase in Sr/Ca ratio is interpreted as aragonite precipitation during periods of intense evaporation in dry periods (Şimşek and Çağatay, 2018; Emmanouilidis et al., 2022). On the other hand, Ti is widely used indicator of the terrestrial clastic material since it is redox insensitive, and not affected by diagenetic and biologic processes. Ca/Ti and Sr/Ti ratio are used as a proxy for relative changes in carbonates versus clastic materials (Croudace and Rothwell, 2015). Geochemical carbonate precipitation during periods of increased temperatures increases these ratios (Avşar et al., 2016; Bonk et al., 2021).

In addition to profiles of individual elements and proxy ratios, Global Average Temperature Change (GATC) was also plotted in Figure 3.14. When GATC profile is carefully examined, there is a distinct cold period occurred at ca. 15th century. This period is marked with purple bar in the figure. However, traces of this cold period are not visible in any profile of individual element or proxy ratios. On the other hand, temperature starts to significantly increase around 1920 and 1980 in GATC profile. They are indicated by red bars in the figure. The increasing trend in temperature after 1920 in GATC profile is seen as a decrease in individual clastic elements (i.e., Si, S, K, Ti Cr, Mn, Fe, Ni, V and Zn). However, Rb profile does not seem to show any

change after 1920. There is also no significant change in individual element profiles of Sr, Ca, Br, Cl, Cu and Zr, and proxy ratios of Sr/Ca, Ca/Ti, and Sr/Ti. After 1980, the other significant increasing trend in temperature in GATC profile, clastic elements seem to continue to decrease with the same trend. While Cu and Zr profiles show slight increasing trend change, this significant trend in temperature is clearly seen in profiles of Sr, Ca, Br, Cl, and proxy ratios. However, it is seen that as with individual element profiles, proxy ratios do not show obvious correlation with GATC profile before 1980. For this reason, multivariate geochemical dataset should be investigated statistically in detail to reveal probable better proxies that could have recorded changes in temperature conditions.

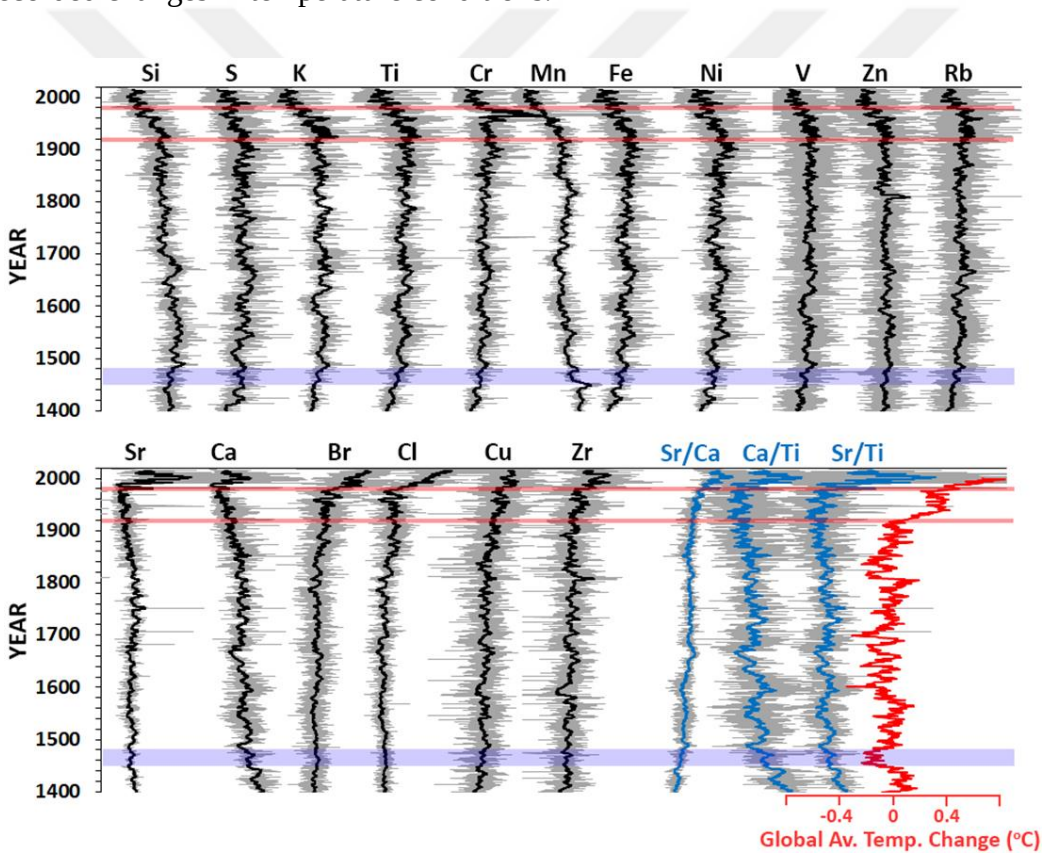

Figure 3.14. Profiles of individual elements and proxy ratios with respect to time. The profile of GATC was also plotted (PAGES2k Consortium, 2019). Note that grey lines on element profiles represent the raw data where black and blue lines overlapping them indicate 21-point moving average.

CHAPTER 4

DISCUSSION

Changes in temperatures are more comparable over extensive regions compared to precipitation patterns. Unlike temperature, precipitation is more complicated and shows more anisotropic spatial covariance, probably due to topographical properties in a region (Gómez-Navarro et al., 2015b). Hence, this study focuses on summer temperature reconstruction rather than precipitation reconstruction.

Visual and geochemical investigation of varved sediments of Köyceğiz Lake reveal that yellowish carbonaceous laminae were deposited in summer months (Avşar et al., 2016). A new ITRAX dataset (summer data) was created by selecting only the levels where Ca/Ti ratios reach peaks, i.e., approximately middle of each carbonaceous laminae.

4.1 Paleotemperature Record by Element-ratio Profiles

Profiles of commonly used proxy ratios in the literature (e.g., Sr/Ca, Ca/Ti and Sr/Ti) are plotted by using summer data (Figure 4.1). Since these element ratios stand for authigenic calcium carbonate precipitation with increasing temperatures during summer season, they would be related to long term temperature variations, and are expected to correlate with summer temperatures (average of June-July-August-September; JJAS) recorded at meteorological stations around Köyceğiz Lake; Muğla, Köyceğiz and Dalaman stations. The coefficient of determination (R^2) values obtained from the comparison of Sr/Ca and Ca/Ti profiles and meteorological station records are below 0.2. On the other hand, R^2 values between Sr/Ti profile and measured summer temperatures seem to be slightly higher. Even though there are positive correlations in the comparisons, obtained R^2 values indicate that proxy ratios weakly correlate with summer temperatures recorded at the meteorological stations.

Apart from these commonly used proxy ratios, a little bit inspection of ITRAX dataset revealed other possible proxy ratios that may represent summer temperatures (e.g., Cl/Ti). It is seen in Figure 4.1 that the R^2 value obtained from the comparison of Cl/Ti with Köyceğiz meteorological station reaches up to 0.45. This observation implies that the ITRAX dataset should be investigated for all other element ratios to obtain best possible proxies representing summer temperatures in the sediments of Köyceğiz Lake.

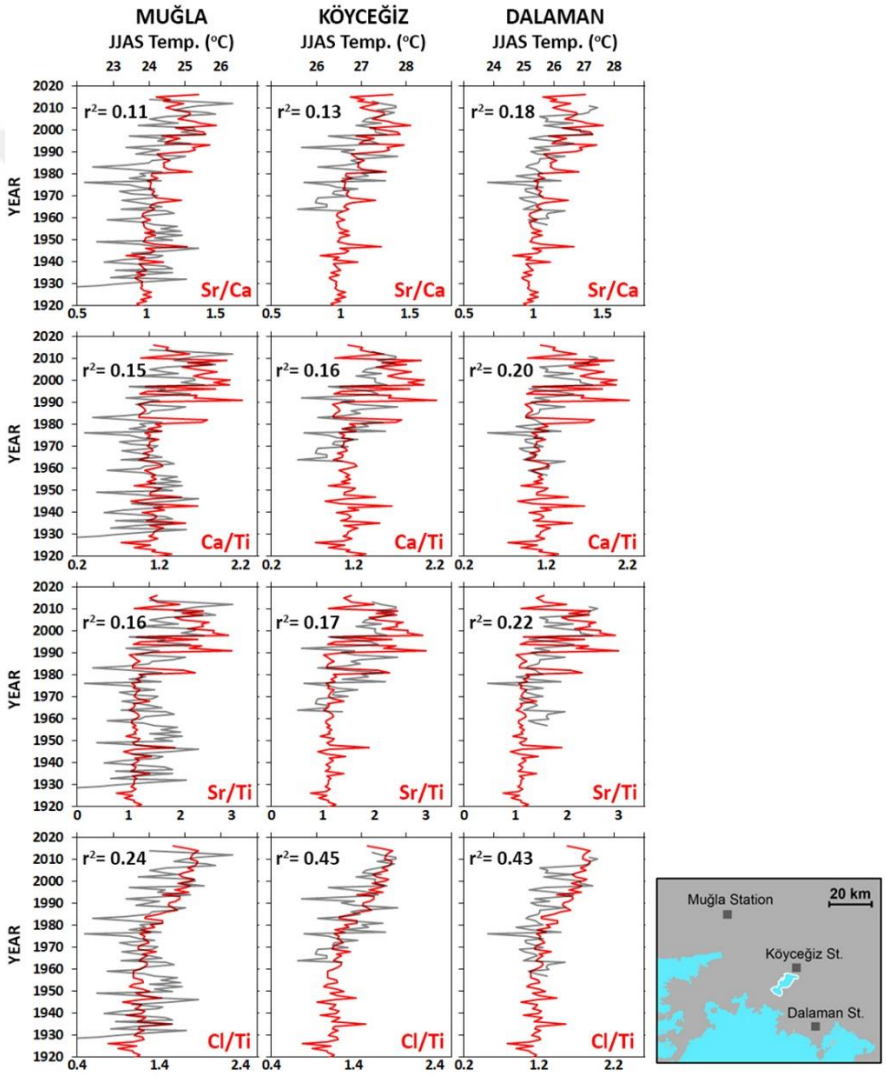

Figure 4.1. Comparison of proxy ratio profiles with average summer temperatures (JJAS) recorded at Muğla, Köyceğiz and Dalaman meteorological stations whose locations are shown in the lower right.

The R^2 values between all possible element ratios and the JJAS temperatures are presented in matrix form in Figure 4.2., where columns represent the elements in the numerator, while rows stand for the elements in the denominator. Hence, each intersection of columns and rows shows the R^2 value between corresponding element ratios and JJAS temperatures. For example, the intersection of the second column and the fifth row shows the correlation between S/Ca ratios and JJAS temperatures.

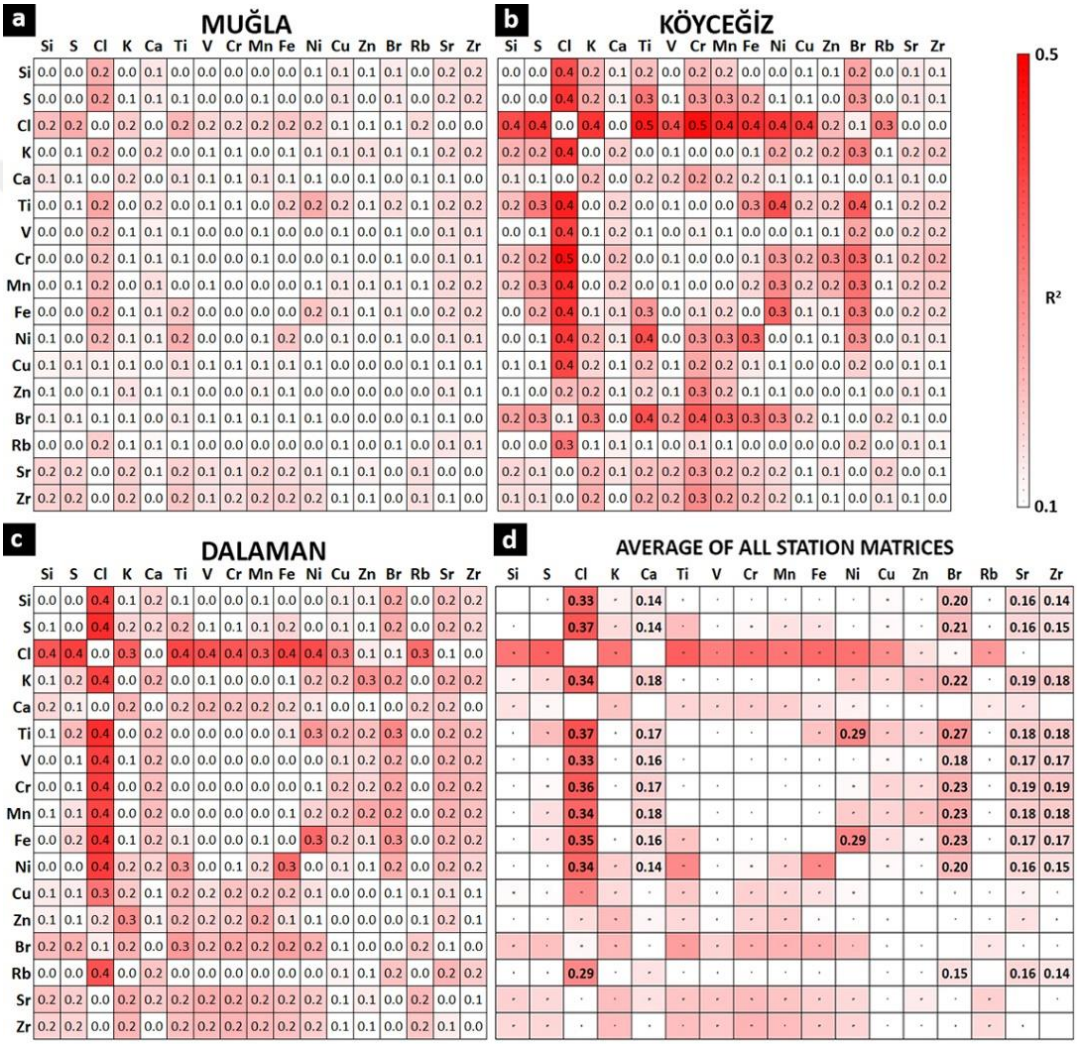

Figure 4.2. Matrices showing R^2 values of all possible element ratios with the JJAS temperatures recorded in Muğla (a), Köyceğiz (b) and Dalaman (c) meteorological stations. d) Average of matrices in a, b and c.

Even at the first glance, the ratio of Cl to elements representing clastic association (Si, S, K, Ti, V, Cr, Mn, Fe, Ni and Rb; CA) seem to have highest R^2 values, more reddish, in all matrices (Figure 4.2a, 4.2b and 4.2c). High correlation of sulfur with other clastic elements can be interpreted as influx of sulfur sourced from pyrite or chalcopyrite transported from the catchment into the lake. Among other element ratios, the ratios of Ca, Br, Sr and Zr to CA have relatively higher R^2 values. The matrix obtained by averaging the matrices for each station (Figure 4.2d) clearly illustrates that the ratios of Cl, Ca, Br, Sr and Zr to CA highly correlate with JJAS temperatures measured at the meteorological stations. In addition, Ni/Ti and Ni/Fe seem to have correlation with the temperatures.

Element ratio profiles detected in the light of matrix investigation are plotted and overlapped by the GATC reconstruction profile (Figure 4.3). Ca/CA and Sr/CA have low consistency with the GATC profile. Ni/Ti ratio, which seems to be consistent with the meteorological data, has almost no correlation ($R^2 = 0.07$) with the GATC profile. On the other hand, Cl/CA, Br/CA and Zr/CA profiles show considerably higher correlation with the GATC profile; 0.65, 0.63 and 0.46, respectively.

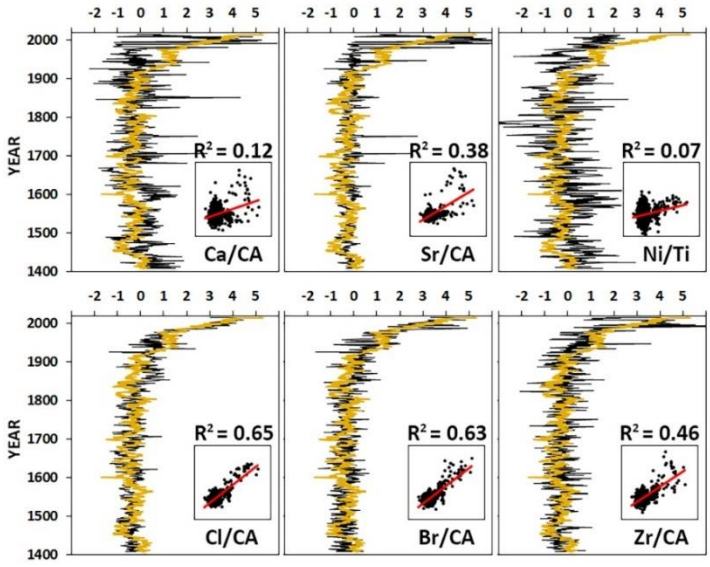

Figure 4.3. Comparison of Ca/CA, Sr/CA, Ni/Tİ, Cl/CA, Br/CA and Zr/CA profiles and GATC profile. Scatter plots and R^2 values are also shown. All data in the figure are standardized.

Cl/CA, Br/CA, and Zr/CA profiles that are consistent with the JJAS temperatures, as well as with the GATC profile, are overlapped and their average is plotted in Figure 4.4a. The correlation between these profiles with the meteorological data, and also the correlation between their average ($AVE_{[Br\text{-}Cl\text{-}Zr]}$ / CA) and the GATC ($R^2 = 0.67$, Figure 4.4b) imply that the $AVE_{[Br\text{-}Cl\text{-}Zr]}$ / CA profile can be accepted as a reasonable proxy in Köyceğiz sediments for summer temperature variations. The source of enriched Zr during high temperature periods, however, is not easy to understand since no related information could be found in the literature. On the other hand, probably, high temperature periods elevate evaporation in the lake and hence promote deposition of salts that are enriched in Cl and Br.

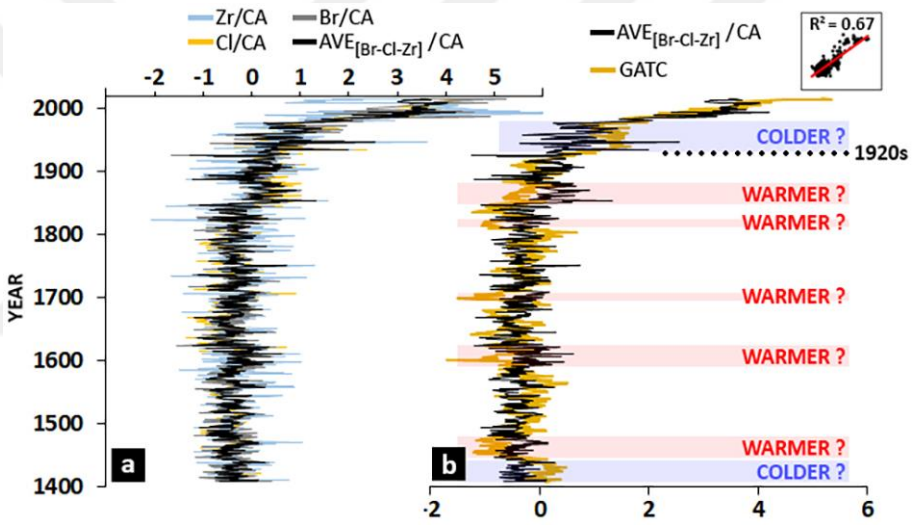

Figure 4.4. a) Overlapped profiles of Cl/CA, Br/CA, and Zr/CA, and their average. b) Comparison of the averaged profile and GATC profile. Colder and warmer periods relative to GATC are highlighted as blue and red bars, respectively.

Besides high correlation, there are some deviations between $AVE_{[Br\text{-}Cl\text{-}Zr]}$ / CA and GATC. $AVE_{[Br\text{-}Cl\text{-}Zr]}$ / CA profile implies two colder (ca. 1920-1980 and 1400-1460) and five warmer (ca. 1850-1880, 1820-1830, 1700's, 1600-1620 and 1520-1540) periods compared to the global average temperature change profile (GATC). Although the recent Global Warming seems evident in the $AVE_{[Br\text{-}Cl\text{-}Zr]}$ / CA profile, the significant increase around 1920 in GATC profile is not seen along it. This

observation raises doubt on the existence of above-mentioned colder/warmer periods, and the reliability of $AVE_{[Br\text{-}Cl\text{-}Zr]}$ / CA profile to evaluate paleoclimatic conditions. Therefore, a better reconstruction was targeted by using linear multiple regression analysis.

4.2 Paleotemperature Record by Multiple Regression Analysis

Multiple regression analysis is generally used to estimate a dependent variable by using several independent variables. In the scope of this study, the dependent variable is JJAS temperatures measured at meteorological stations, and the independent variables are element profiles measured by ITRAX micro-XRF scanner. An equation reasonably estimating JJAS values by ITRAX dataset could then be used for the estimation of pre-instrumental JJAS temperatures. Annual nature of carbonaceous laminae in Köyceğiz sediments allows year-by-year comparison between the meteorological and sediment geochemical datasets, and application of linear multiple regression analysis.

A common bias in multiple regression analysis is multicollinearity, when an independent variable highly correlates with one or more of other independent variables in the dataset. In such cases, regression equation obtained may result in totally arbitrary estimations (Davis, 2002). Multicollinearity problem can be avoided by applying Principle Component Analysis, which groups highly correlating independent variables and proposes new sets of uncorrelated variables called as Principle Components (PCs) (e.g., Avşar et al. 2014b). Principle Component Analysis was applied on the ITRAX summer data of KYC-J core by using SPSS software. Accordingly, SPSS extracted five PCs that compensate for 83% of the total variance in the dataset. The correlation coefficients (R) of each element profile with the extracted PCs are listed in Figure 4.5a. Basically, PC1 highly correlates with Fe, Ni, S, Ti, Cr, V, K, Si, Mn, hence stands for clastic element association in the sediments. PC2 positively correlates with Ca whereas negatively correlates with Cu, Br, and Cl. Zr and Sr in the dataset are represented by PC3. PC4 and PC5 stand for

Zn and Rb, respectively. In order to visualize the results of PCA, PCs are plotted together with corresponding elements with respect to time according to varve-based chronology (Figure 4.5b). Not surprisingly, it is seen that PC1 resembles the reverse of $AVE_{[Br\text{-}Cl\text{-}Zr]}$ / CA profile, where denominator is in fact represented by PC1.

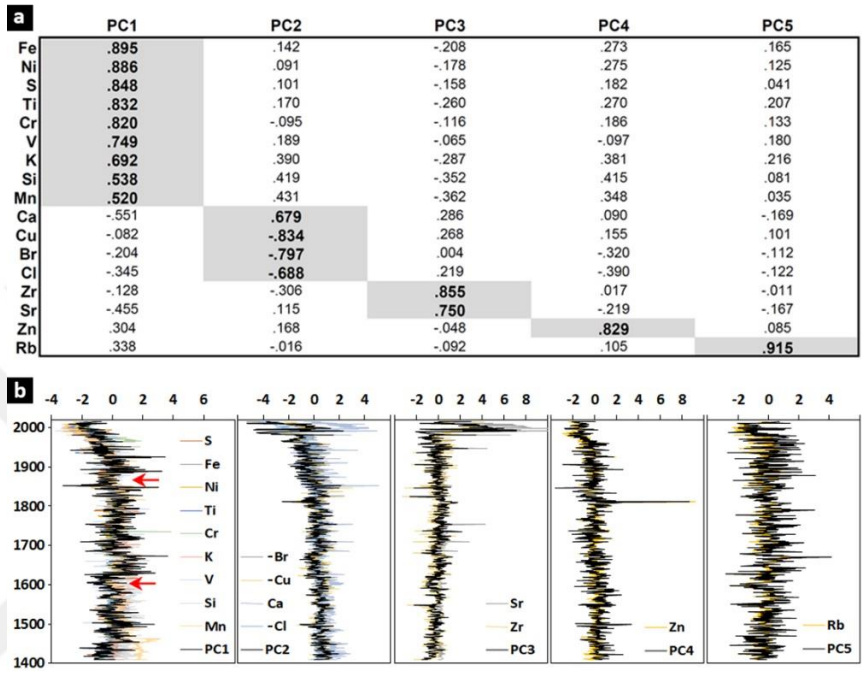

Figure 4.5. Results of Principle Component Analysis (PCA) on ITRAX summer data. a) Correlation coefficients of each element with five PCs. b) Plot of principle components and corresponding elements with respect to time. Note the red arrows showing warmer periods ca. 1850-1880 and 1600-1620 presented in Figure 4.4b.

Firstly, in order to illustrate multicollinearity problem, linear multiple regression analysis was applied by using all elements measured by ITRAX using summer JJAS temperatures recorded at each station. Elements were used as independent variables and temperature as the dependent variable. Constant values and multipliers of the obtained regression equation are presented in Table 4.1. R^2 values of 0.553, 0.759, 0.771 were obtained for the JJAS temperatures of Muğla, Köyceğiz and Dalaman meteorological stations, respectively. As the second step, the same process was applied by using PCs. Relatively lower R^2 values were obtained as 0.318, 0.578, 0.467 for Muğla, Köyceğiz and Dalaman meteorological stations, respectively.

Table 4.1 Results of multiple linear regression analysis using elements and PCs as independent variables. Constant values and multipliers for regression equations, and achieved R^2 values are presented.

	MUĞLA	KÖYCEĞİZ	DALAMAN		MUĞLA	KÖYCEĞİZ	DALAMAN
Constant	23.234	26.278	26.027	**Constant**	23.552	25.745	24.925
Si	-0.289	0.114	0.079	**PC1**	-0.152	-0.345	-0.333
S	-0.569	0.067	0.172	**PC2**	-0.212	-0.216	-0.213
Cl	0.285	0.153	0.351	**PC3**	0.155	0.086	0.130
K	0.346	-0.591	0.167	**PC4**	-0.042	-0.203	-0.005
Ca	-0.109	0.011	0.182	**PC5**	0.002	-0.060	-0.078
Ti	-0.602	-0.317	-0.043				
V	0.080	0.266	0.234				
Cr	0.113	-0.131	0.005				
Mn	0.199	0.014	0.318				
Fe	-1.239	0.065	-1.318				
Ni	1.776	0.460	0.990				
Cu	0.069	-0.052	0.066				
Zn	0.088	0.011	0.095				
Br	-0.015	0.006	0.076				
Rb	0.068	0.059	0.026				
Sr	0.088	0.032	0.070				
Zr	-0.054	-0.090	-0.055				
R^2	**0.553**	**0.759**	**0.771**		**0.318**	**0.578**	**0.467**

The formulas produced by the multiple linear regression analysis applied to both all elements and PCs can now be extrapolated down core to obtain summer temperature profiles for the last ca. 600 years. Element-based and PC-based reconstructed summer temperatures for each station are presented in Figure 4.6. Reconstructed temperatures were compared with GATC profile. In Figure 4.6a, the reconstructed temperatures obtained by using Muğla and Köyceğiz stations seem to be consistent with GATC profile. However, there is an obvious inconsistency with the reconstructed temperatures obtained by using Dalaman station, especially for the last and the 15th centuries. In Figure 4.6b, multicollinearity-free reconstructions (i.e., PC based) of each station and their comparison with GATC are shown. It is seen that reconstructed Dalaman temperature profile strongly correlates with GATC.

Long term reconstructed temperatures should correlate with each other since temperatures recorded by these stations are highly similar. When Figure 4.6c is inspected, reconstructed temperatures from different stations does not correlate well. For example, element-based reconstruction from Muğla and Dalaman stations has

R^2 value of 0.07. On the other hand, PC-based reconstruction from these two stations has R^2 value of 0.80. As it is expected, since PCA considerably minimizes multicollinearity problem, PC-based reconstructions from Muğla, Dalaman and Köyceğiz stations are consistent. Hence, the average of these stations is accepted as the "reconstructed summer temperature" (REC) obtained from multiple regression analysis. The R^2 value is 0.63 with GATC and their comparison is seen in the grey shaded area in Figure 4.6b.

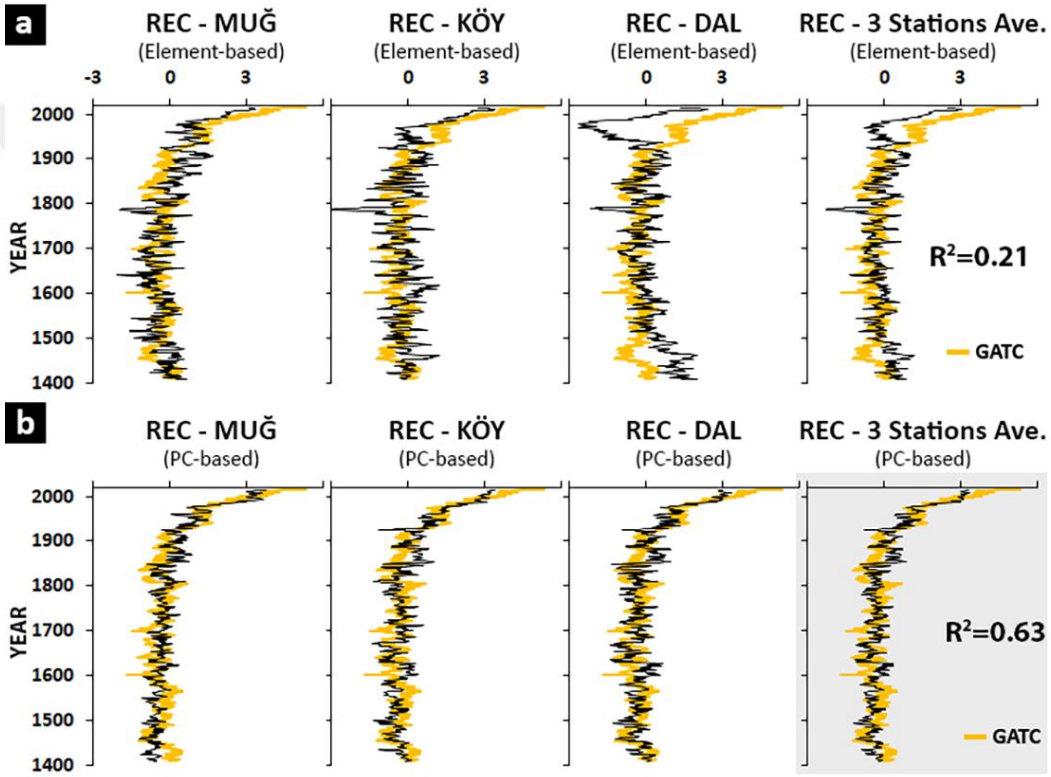

c

Element-based REC	Muğla	Köyceğiz	Dalaman
Muğla	1.00	0.30	0.07
Köyceğiz	0.30	1.00	0.15
Dalaman	0.07	0.15	1.00

PC-based REC	Muğla	Köyceğiz	Dalaman
Muğla	1.00	0.70	0.80
Köyceğiz	0.70	1.00	0.81
Dalaman	0.80	0.81	1.00

Figure 4.6. a) Overlapped plots of elements-based reconstructions from three stations and GATC profile. b) Overlapped plots of principle component-based reconstructions from three stations and GATC profile. c) correlation between reconstructed temperatures from different stations.

The comparison of $AVE_{[Br\text{-}Cl\text{-}Zr]}$ / CA proxy profile and the reconstructed summer (JJAS) temperature (REC) with the GATC profile are presented in Figure 4.7. The relatively longer and more significant deviations from GATC curve are highlighted as red and blue bars. Two warmer periods (ca. 1890-1860 and 1630-1600) and one colder period (ca. 1770-1800) that are common in both profiles are obvious. Although a colder period (ca. 1950-1980) appears in the $AVE_{[Br\text{-}Cl\text{-}Zr]}$ / CA profile relative to the GATC curve, it is not obvious in the REC profile.

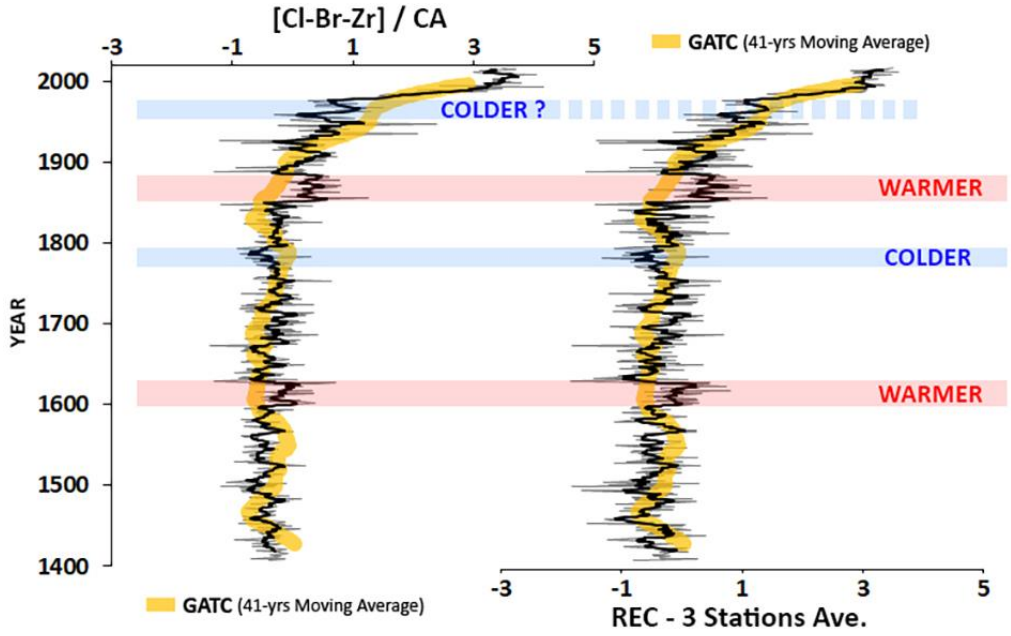

Figure 4.7. Overlapped plot of $AVE_{[Br\text{-}Cl\text{-}Zr]}$ / CA and GATC on the left, and REC and GATC on the right. Note that 41-years moving average was applied on GATC profile, where 5-years moving average was applied on $AVE_{[Br\text{-}Cl\text{-}Zr]}$ / CA and REC profiles (black lines).

Summer (JJAS) temperature reconstruction (REC) obtained from this study is compared with some other paleoclimate records obtained in Anatolia. Their comparison is presented in Figure 4.8. Although there are numerous records from Anatolia and its surrounding area, which are summarized in detail in "1.2. Previous Paleoclimatic Studies in Anatolia and the Neighboring Areas" section, for this comparison only the ones having precise chronology were selected; Jsibeli Forest

(tree-ring-based) and Nar Lake (varve-based). In addition to these two records, since Akçer-Ön, (2017) reports another record from Köyceğiz Lake, her study is also included in the comparison. GATC profile was overlapped with these records for a reference (Figure 4.8.).

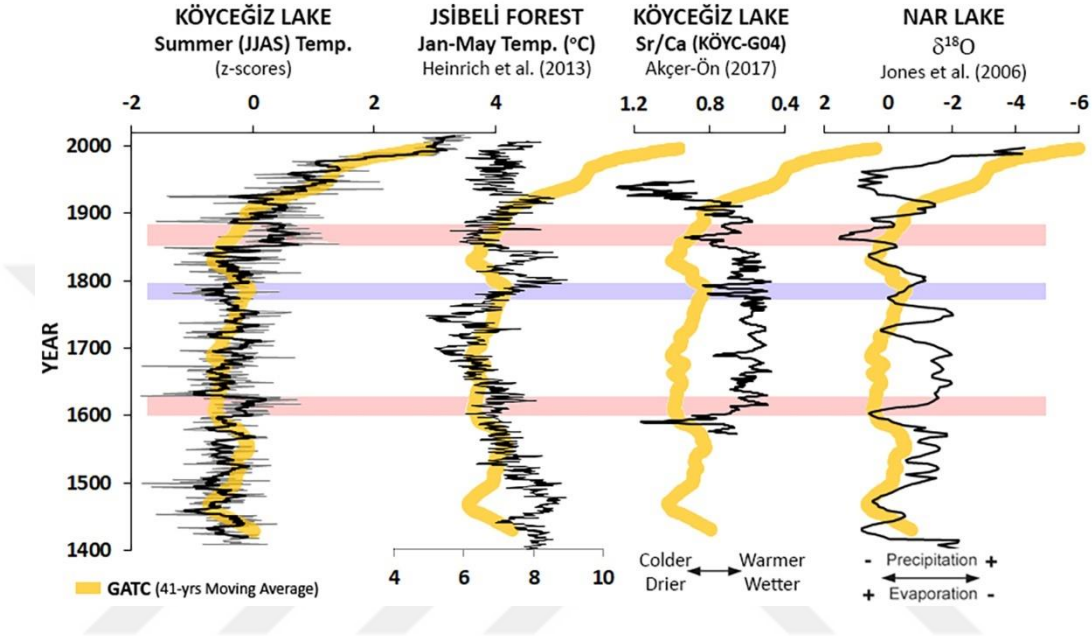

Figure 4.8. Comparison of reconstructed summer (JJAS) temperatures of this study with the other paleoclimate records obtained in Anatolia.

Heinrich et al. (2013) reconstructed January-May temperatures using tree rings from Jsibeli Forest, Antalya. The warmer period in the second half of 19th century and the colder period close to the end of 18th century detected in REC profile are not seen in Jsibeli record. On the other hand, Jsibeli record shows slight implication of warming in the first half of 17th century, which looks consistent with Köyceğiz record. This record does not show a distinct correlation with GATC curve. They fail to report recent "Global Warming" during the instrumental period. Akçer-Ön (2017) reported that Sr/Ca ratio, along a core ca. 2.5 km to the SE of KYC-J core of this study, recorded paleoclimatic conditions in Köyceğiz Lake. The warmer period in the second half of 19th century detected in REC profile is reported contrarily as a relatively colder/drier period. The colder period in REC profile is reported as slightly

colder/drier. The other warmer period at the beginning of 17th century in REC profile shows weak anomalies toward warmer/wetter conditions in Akçer-Ön (2017). The record by Akçer-Ön (2017) does not show correlation with GATC curve. The recent "Global Warming" during the instrumental period is reported as colder. Jones et al. (2006) reported $\delta^{18}O$ analysis of varved sediments of Nar Lake to record precipitation and evaporation changes. Two warmer periods detected in REC profile are reported as periods of increased evaporation in their record. In this context, there is slight consistency between Nar Lake and this study. The recent "Global Warming" during the instrumental period is not obvious in Nar Lake record. It should be noted that the REC obtained in this study and GATC profile are reconstructions of temperature. However, the records presented by Jones et al. (2006) and Akçer-Ön (2017) are proxy records inheriting not only temperature but also precipitation. The discrepancies discussed in Figure 4.8 may be due to the contribution of precipitation to the presented proxies in these studies. Although Jsibeli record is a temperature reconstruction, i.e., free of precipitation effect, it shows significant deviations from GATC. Heinrich et al. (2013), in their article, do not discuss possible reasons of this discrepancy.

CHAPTER 5

CONCLUSIONS AND RECOMMENDATIONS

The following conclusions and recommendations can be drawn from this study:

- Yellowish laminae in the sedimentary sequence of Köyceğiz Lake are carbonaceous sediments annually deposited during summer season.
- Counting these yellowish laminae with the help of visual inspection together with peaks along Ca/Ti ratio profile results in total of 609 years-long sedimentary record in 124.95 cm-long core, corresponding to a 0.205 cm/yr sedimentation rate in average.
- Since these carbonaceous laminae are deposited in summer season, which is the indication that their deposition can be related to temperature, their chemical content can be used to estimate past summer temperatures.
- Rather than the element ratios commonly used in the literature such as Sr/Ca, Ca/Ti and Sr/Ti, careful investigation of possible correlations between element-ratio profiles and the summer (JJAS) temperatures measured at Muğla, Köyceğiz and Dalaman meteorological stations revealed that the ratios of Br, Cl and Zr to clastic elements (CA; Si, S, K, Ti, V, Cr, Mn, Fe, Ni and Rb) have higher correlation to measured summer temperatures. The $AVE_{[Br\text{-}Cl\text{-}Zr]}$ / CA profile obtained from Köyceğiz sediments has strong correlation with the Global Average Temperature Change (GATC) reconstruction curve ($R^2 = 0.67$).
- Principle Component Analysis on the ITRAX data of summer laminae results in five PCs explaining 83% of the total variance in the raw data. Multiple regression analysis done by these PCs results in consistent temperature profiles obtained from different meteorological stations. The temperature reconstruction obtained in this study by multiple regression analysis has also

strong correlation with the Global Average Temperature Change (GATC) reconstruction curve ($R^2 = 0.63$).

- In addition to the recent significant "Global Warming" during the ca. 100 years, two warmer periods (ca. 1890-1860 and 1630-1600) and one colder period (ca. 1770-1800) compared to the GATC were detected in Köyceğiz varve-based paleotemperature record.
- Although the JJAS reconstructed temperatures in this study is in good agreement with the GATC, its comparison with the other paleoclimatic records from Anatolia does not show an obvious correlation.
- Linear multiple regression analysis applied to the ITRAX dataset indicates the importance of multicollinearity on the resulting regression equation. Application of Principle Component Analysis considerably rules multicollinearity problem out.
- The success of the approach followed in this study should also be tested by using winter/spring laminae to reconstruct precipitation.
- Studying one more core from the northern basin of Köyceğiz Lake, by also using data from more other meteorological stations in the region, could increase the reliability of the result achieved in this study.

REFERENCES

Akçer-Ön S. (2017). Küçük Buz Çağı'nda Güneş etkisine bağlı iklim değişimleri: Köyceğiz Gölü çökel kayıtları (GB Anadolu). Türkiye Jeoloji Bülteni 60 (4): 569-588 (in Turkish) doi:10.25288/tjb.370616.

Akkemik, Ü., & Aras, A. (2005). Reconstruction (1689–1994) of April-August precipitation in southwestern part of central Turkey. Int J Climatol 25:537–548.

Akkemik, Ü., Dağdeviren, N., Aras, A. (2005). A preliminary reconstruction (A.D. 1635–2000) of spring precipitation using oak tree rings in the western Black Sea region of Turkey. Int J Biometeorol 49:297–302. doi:10.1007/s00484-004-0249-8.

Akkemik, Ü, D'Arrigo, R., Cherubini, P., Köse, N., Jacoby, G.C., (2008). Tree-ring reconstructions of precipitation and streamflow for north-western Turkey. Int J Climatol 28:173–183.

Anderson, R.Y., Dean, W.E., Bradbury, J.P., Love, D. (1985). Meromictic lakes and varved lake sediments in North America. U.S. Geological Survey Bulletin 1607. Retrieved June 22, 2022, from https://pubs.usgs.gov/bul/1607/report.pdf.

Avsar, U. (2013). Lacustrine paleoseismic records from the North Anatolian Fault, Turkey, PhD thesis, Ghent University, Gent, Belgium.

Avşar, U., A. Hubert-Ferrari, M. De Batist, and N. Fagel. (2014a). A 3400-year lacustrine paleoseismic record from the North Anatolian Fault, Turkey: Implications for bimodal recurrence behavior, Geophys. Res. Lett., 41, 377–384, doi:10.1002/2013GL058221.

Avşar, U., Hubert-Ferrari, A., Batist, M. D., Lepoint, G., Schmidt, S., and Fagel, N. (2014b). Seismically-triggered organic-rich layers in recent sediments from Göllüköy Lake (North Anatolian Fault, Turkey). Quaternary Science Reviews, 103, 67-80.

Avşar, U., Jónsson, S., Avşar, Ö, and Schmidt, S. (2016). Earthquake-induced soft-sediment deformations and seismically amplified erosion rates recorded in varved sediments of Köyceğiz Lake (SW Turkey). Journal of Geophysical Research: Solid Earth, 121(6), 4767-4779. doi:10.1002/2016JB012820.

Avşar, Ö., & Kurtuluş, B. (2017). Distribution of water and bottom sediment temperature of Lake Köyceğiz. J. Geol. Eng. 41, 117–136.

Avşar, U., Akar, M., Pearson, C. (2019). Geoarchaeological investigations in the Amuq valley of Hatay: sediment coring project in the environs of Tell Atchana. in H. Sözbilir, Ç. Özkaymak, B. Uzel, Ö. Sümer, M. Softa, Ç. Tepe, S. Eski (eds), The Proceedings and Abstracts Book: 72nd Geological Congress of Turkey, January 28 – February 1, 2019. Ankara, TMMOB Jeoloji Mühendisleri Odası: 798–802.

Bar-Matthews, M., Ayalon, A., Gilmour, M., Matthews, A., and Hawkesworth, C. J. (2003). Sea-land Oxygen Isotopic Relationship from Planktonic Foraminifera and Speleothems in the Eastern Mediterranean Region and Their Implication for Paleorainfall during Interglacial Intervals. Geochim. Cosmochim. Ac., 67, 3181-3199.

Baykara M. O. (2014). Güneybatı Anadolu'da mağara çökellerinin incelenmesi ve paleoiklimsel değerlendirmeleri. (Doktora tezi, Pamukkale Universitesi). Retrieved April 20, 2022, from https://tez.yok.gov.tr/UlusalTezMerkezi/tezDetay.jsp?id=KYCK2PQfGhs53vVqZE1JQw&no=_ieB7rtQLZgG3p2bSXkHBQ.

Bayarı, C. S., Kazancı, N., Koyuncu, H., Çağlar, S.S. and Gökçe, D., (1995). Determination of the origin of the waters of Köyce¤iz Lake, Turkey, J. Hydrol.166: 171-191.

Björck, S., & Wohlfarth, B. (2002). 14C chronostratigraphic techniques in paleolimnology. In Tracking environmental change using lake sediments (pp. 205-245). Springer, Dordrecht.

Bonk, A., Müller, D., Ramisch, A., Kramkowski, M., Noryśkiewicz, A.M., Sekudewicz, I., Gąsiorowski, M., Luberda-Durnaś, K., Słowiński, M., Schwab, M., Tjallingii, R., Brauer, A., Błaszkiewicz, M. (2021). Varve microfacies and chronology from a new sediment record of Lake Gościąż (Poland). Quaternary Science Review 251, 106715. https://doi.org/10.1016/j.quascirev.2020.106715.

Böning, P., Bard, E., Rose, J., (2007). Toward direct, micron-scale XRF elemental maps and quantitative profiles of wet marine sediments. Geochemistry, Geophysics, Geosystems 8, Q05004. doi:10.1029/2006GC001480.

Bradley, R. S. (1999). Paleoclimatology: Reconstructing Climates of the Quaternary. New York: Harcourt.

Bradley, R.S. (2011). High-resolution paleoclimatology. In: M.K. Hughes, T.W. Swetnam and H.F. Diaz (eds). Dendroclimatology: Progress and Prospects. Developments in Paleoenvironmental Research 11, Springer, Berlin, 3-15.

Brewer, S., Guiot, J. & Barboni, D. (2007). Use of pollen as climate proxies. In Elias, S. A. (ed.): Encyclopedia of Quaternary Science 3, 2497–2508. Elsevier, Oxford. doi:10.1016/B0-444-52747-8/00177-0.

Bruckner, M. (2021). Paleoclimatology: How Can We Infer Past Climates? Retrieved April 8, 2022, from https://serc.carleton.edu/microbelife/topics/proxies/paleoclimate.html.

Brunelle-Daines, A. (2002): Holocene changes in fire, climate, and vegetation in the northern Rocky Mountains of Idaho and western Montana. (Ph.D. Dissertation, University of Oregon). Retrieved March 16, 2022, from https://www.proquest.com/pagepdf/305503997?accountid=13014.

Cheng, H., Sinha, A., Verheyden, S., Nader, F.H., Li, X.L., Zhang, P.Z., Yin, J.J., Yi, L., Peng, Y.B., Rao, Z.G., Ning, Y.F., Edwards, R.L. (2015). The Climate Variability in Northern Levant over the Past 20,000 years. Geophysical Research Letters, 42, 8641-8650.

Cohen, A. S. (2003). Paleolimnology: The History and Evolution of Lake Systems, Oxford Univ. Press, New York. doi:10.1093/oso/9780195133530.001.0001.

Croudace, I. W., Rindby, A., and Rothwell, R. G. (2006). ITRAX: description and evaluation of a new multi-function X-ray core scanner. Geological Society, London, Special Publications, 267(1), 51–63.

Croudace, I. W. and Rothwell, R. G. (Eds.). (2015). Micro-XRF studies of sediment cores: Applications of a non-destructive tool for the environmental sciences (Vol. 17). Dordrecht, Netherlands: Springer.

Cuven, S., Francus, P., Crémer, J. F., & Bérubé, F. (2015). Optimization of Itrax Core Scanner Protocols for the Micro X-Ray Fluorescence Analysis of Finely Laminated Sediment: A Case Study of Lacustrine Varved Sediment from the High Arctic. In book: Micro-XRF Studies of Sediment Cores (pp.279-303). doi:10.1007/978-94-017-9849-5_10.

Danladi, I. B., & Akçer-Ön, S. (2018). Solar forcing and climate variability during the past millennium as recorded in a high-altitude lake: Lake Salda (SW Anatolia). Quaternary International, 486, 185–198. doi: 10.1016/j.quaint.2017.08.068.

Danladi, I. B., Akcer-Ön, S., Z. B. Ön, Z.B, and Schmidt, S. (2021). High-resolution temperature and precipitation variability of southwest Anatolia since 1730 CE from Lake Gölcük sedimentary records, Turkish Journal of Earth Sciences, 30(5), 601-610, doi:10.3906/yer-2008-14.

Davis, J.C. (2002). Statistics and Data Analysis in Geology. John Wiley & Sons, New York.

Davies, S. J., Lamb, H. F., & Roberts, S. J. (2015). Micro-XRF Core Scanning in Paleolimnology: Recent Developments. Developments in Paleoenvironmental Research, 189–226. doi:10.1007/978-94-017-9849-5_7.

Dean, J.R., Jones, M.D., Leng, M.J., Noble, S.R., Metcalfe, S.E., Sloane, H.J., Sahy, D., Eastwood, W.J., and Roberts, N. (2015). Eastern Mediterranean Hydroclimate over the late Glacial and Holocene, reconstructed from the Sediments of Nar Lake, Central Turkey, Using Stable Isotopes and Carbonate Mineralogy. Quaternary Science Reviews, 124, 162–174.

Dulski, P., Brauer, A., Mangili, C. (2015). Combined μ-XRF and Microfacies Techniques for Lake Sediment Analyses. In: Croudace, I., Rothwell, R. (eds) Micro-XRF Studies of Sediment Cores. Developments in Paleoenvironmental Research, vol 17. Springer, Dordrecht. https://doi.org/10.1007/978-94-017-9849-5_12.

Fleitmann, D., Cheng, H., Badertscher, S., Edwards, R.L., Mudelsee, M., Gokturk, O.M., Fankhauser, A., Pickering, R., Raible, C.C., Matter, A., Kramers J., Tuysuz, O. (2009). Timing and Climatic impact of Greenland Interstadials Recorded in Stalagmites from Northern Turkey. Geophysical Research Letters, 36, L19707.

Eastwood, W.J., Leng, M.J., Roberts, N., Davis, B. (2007). Holocene climate change in the Eastern Mediterranean Region: A Comparison of Stable Isotope and Pollen Data from Lake Gölhisar, Southwest Turkey. Journal of Quaternary Science, 22(4), 327–341.

El Ouahabi, M., Hubert-Ferrari, A., & Fagel, N. (2017). Lacustrine clay mineral assemblages as a proxy for land-use and climate changes over the last 4 kyr: The Amik Lake case study, Southern Turkey. Quaternary International, 438, 15–29. doi: 10.1016/j.quaint.2016.11.032

El Ouahabi, M., Hubert-Ferrari, A., Lebeau, H., Karabacak, V., Vander Auwera, J., Lepoint, G., Dewitte, O., Schmidt, S. (2018). Soil erosion in relation to land-use changes in the sediments of Amik Lake near Antioch antique city during the last 4 kyr. The Holocene, 28(1), 104–118. doi :10.1177/0959683617715702.

Emmanouilidis, A., Katrantsiotis, C., Dotsika, E., Kokkalas, S., Unkel, I., Avramidis, P. (2022). Holocene paleoclimate variability in the eastern Mediterranean, inferred from the multi-proxy record of Lake Vouliagmeni, Greece, Palaeogeography, Palaeoclimatology, Palaeoecology, Volume 595. doi: 10.1016/j.palaeo.2022.110964.

Gillikin, D. P., Verheyden, A., & Goodwin, D. H. (2017). Paleoclimate Reconstruction from Oxygen Isotopes in a Coral Skeleton from East Africa: A DATA-ENHANCED LEARNING EXPERIENCE. Oceanography, 30(1), 104–107. http://www.jstor.org/stable/24897846.

Gómez-Navarro, J. J., Werner, J., Wagner, S., Luterbacher, J., and Zorita, E. (2015b). Establishing the skill of climate field reconstruction techniques for precipitation with pseudoproxy experiments, Clim. Dynam., 45, 1395–1413, https://doi.org/10.1007/s00382- 014-2388-x.

Gornitz, V. (2009). Mineral Indicators of Past Climates. Encyclopedia of Paleoclimatology and Ancient Environments, 573–583. doi:10.1007/978-1-4020-4411-3_143.

Göktürk, O. M. (2011). Climate in the Eastern Mediterranean through the Holocene inferred from Turkish stalagmites, Ph.D. Thesis, University of Bern.

Heinrich, I., Touchan, R., Dorado Liñán, I., Vos, H., & Helle, G. (2013). Winter-to-spring temperature dynamics in Turkey derived from tree rings since AD 1125. Climate Dynamics, 41(7-8), 1685–1701. doi:10.1007/s00382-013-1702-3.

Hulme, M., & Jones, P. D. (1994). Global climate change in the instrumental period. Environmental Pollution, 83(1-2), 23–36. doi:10.1016/0269-7491(94)90019-1.

IPCC, 2021: Climate Change 2021: The Physical Science Basis. Contribution of Working Group I to the Sixth Assessment Report of the Intergovernmental Panel on Climate Change (Masson-Delmotte, V., P. Zhai, A. Pirani, S.L. Connors, C.).

IPCC, 2022: Climate Change 2022: Impacts, Adaptation, and Vulnerability. Contribution of Working Group II to the Sixth Assessment Report of the Intergovernmental Panel on Climate Change [H.-O. Pörtner, D.C. Roberts, M. Tignor, E.S. Poloczanska, K. Mintenbeck, A. Alegría, M. Craig, S. Langsdorf, S. Löschke, V. Möller, A. Okem, B. Rama (eds.)]. Cambridge University Press. In Press.

Jacobson, M. J., Flohr, P., Gascoigne, A., Leng, M. J., Sadekov, A., Cheng, H., et al. (2021). Heterogenous late Holocene climate in the Eastern Mediterranean—The Kocain Cave record from SW Turkey. Geophysical Research Letters, 48, e2021GL094733. https://doi.org/10.1029/2021GL094733.

Jex, C. N., Baker, A., Eden, J. M., Eastwood, W. J., Fairchild, I. J., Leng, M. J., … Sloane, H. J. (2011). A 500 yr speleothem-derived reconstruction of late autumn–winter precipitation, northeast Turkey. Quaternary Research, 75(03), 399–405. doi: 10.1016/j.yqres.2011.01.005

Jones, M.D., (2004). High-resolution Records of Climate Change from Lacustrine Stable Isotopes Through the Last Two Millennia in Western Turkey. Ph.D thesis, Plymouth University.

Jones, M.D., Leng, M.J., Roberts, C.N., Türkeş, M., and Moyeed, R. (2005). A coupled calibration and modelling approach to the understanding of dry-land lake oxygen isotope records: Journal of Paleolimnology, v. 34, p. 391–411, doi: 10.1007/s10933-005-6743-0.

Jones, M.D., Roberts, N.C., Leng, M.J., Türkes, M. (2006). A high-resolution late Holocene Lake isotope record from Turkey and links to North Atlantic and monsoon climate. Geology 34, 361e364.

Kaniewski, D., Van Campo, E., Guiot, J., Le Burel, S., Otto, T., & Baeteman, C. (2013). Environmental Roots of the Late Bronze Age Crisis. PLoS ONE, 8(8), e71004. doi: 10.1371/journal.pone.0071004.

Kazancı, N., Plasa, R.-H., Neubert, E., & İzbirak, A. (1992). On the limnology of Lake Köyceğiz (SW Anatolia). Zoology in the Middle East, 6(1), 109–126. doi:10.1080/09397140.1992.10637619.

Kazancı, N., Muzaffer D., Sonmez, G. (2008). The physico-chemical and biological characteristics of Köyceğiz Lake in southwestern Turkey between 1991 and 1993 and future management proposals. Rev Hydrobiol 2:165–205.

Kelts, K., & Hsü, KJ. (1978). Freshwater carbonate sedimentation. In: Lerman A (ed.) Lakes. New York: Springer, pp. 295–323.

Köse, N., Akkemik, Ü., Dalfes, HN, Özeren, M.S. (2011) Tree-ring reconstructions of May–June precipitation of western Anatolia. Quat. Res 75:438–450. doi: 10.1016/j.yqres.2010.12.005.

Köse, N., Akkemik, Ü., Güner, H. T., Dalfes, H. N., Grissino-Mayer, H. D., Özeren, M. S., & Kındap, T. (2013). An improved reconstruction of May–June precipitation using tree-ring data from western Turkey and its links to volcanic eruptions. International Journal of Biometeorology, 57(5), 691–701. doi:10.1007/s00484-012-0595-x.

Köse, N., Güner, H. T., Harley, G. L., & Guiot, J. (2017). Spring temperature variability over Turkey since 1800 CE reconstructed from a broad network of tree-ring data. Climate of the Past, 13(1), 1–15. doi:10.5194/cp-13-1-2017.

Kurtuluş, T., Kurtuluş, B., Avşar, Ö., & Avşar, U. (2019). Evaluating the thermal stratification of Köyceğiz Lake (SW Turkey) using in-situ and remote sensing observations. Journal of African Earth Sciences, 103559. doi: 10.1016/j.jafrearsci.2019.103559.

Leng, M. J., & Marshall, J. D. (2004). Palaeoclimate interpretation of stable isotope data from lake sediment archives. Quaternary Science Reviews, 23(7-8), 811–831. doi: 10.1016/j.quascirev.2003.06.0

Litt, T., Ohlwein, C., Neumann, F. H., Hense, A., & Stein, M. (2012). Holocene climate variability in the Levant from the Dead Sea pollen record. Quaternary Science Reviews, 49, 95–105. doi: 10.1016/j.quascirev.2012.06.012.

Löwemark, L., Chen, H. F., Yang, T. N., Kylander, M. E., Yu, E. F. & Hsu, Y. W. (2011): Normalizing XRF-scanner data: a cautionary note on the interpretation of high-resolution records from organic rich lakes. Journal of Asian Earth Sciences 40, 1250–1256.

McKillup, S., & Dyar, M. D. (2010). Geostatistics Explained: An Introductory Guide for Earth Scientists (1st ed.). Cambridge University Press.

Meyers, P.A., & Teranes, J.L. (2001). Sediment organic matter. In: Last, W.M., Smol, J.P. (Eds.), Tracking Environmental Change Using Lake Sediments. Volume 2: Physical and Geochemical Methods. Kluwer Academic Publishers, Dordrecht, the Netherlands, pp. 239– 269.

Munroe, T., & Taylor, R. (2020). 4 Things to Know About Australia's Wildfires and Their Impacts on Forests. Global Forest Watch. Retrieved June 2, 2022, from https://www.globalforestwatch.org/blog/fires/4-things-to-know-about-australias-wildfires-and-their-impacts-on-forests/.

Naidoo, D. (2022). KwaZulu-Natal floods sound the alarm on climate adaptation. Retrieved June 3, 2022, from https://issafrica.org/iss-today/kwazulu-natal-floods-sound-the-alarm-on-climate-adaptation.

NASA Earth Observatory. (2022). World of Change: Global Temperatures. Retrieved May 26, 2022, from https://earthobservatory.nasa.gov/world-of-change/global-temperatures.

NASA Global Climate Change. (2022). Why does the temperature record shown on your "Vital Signs" page begin at 1880? Retrieved June 6, 2022, from https://climate.nasa.gov/faq/21/why-does-the-temperature-record-shown-on-your-vital-signs-page-begin-at-1880/.

National Geographic. (n.d.) Paleoclimatology. Retrieved May 28, 2022, from https://education.nationalgeographic.org/resource/paleoclimatology-RL.

National Centers for Environmental Information, NOAA. (2016). How Can Corals Teach Us About Climate? Retrieved May 8, 2022, from https://www.ncei.noaa.gov/news/how-can-corals-teach-us-about-climate.

Ocakoğlu, F., Dönmez, E. O., Akbulut, A., Tunoğlu, C., Kır, O., Açıkalın, S., … Leroy, S. A. (2015). A 2800-year multi-proxy sedimentary record of climate change from Lake Çubuk (Göynük, Bolu, NW Anatolia). The Holocene, 26(2), 205–221. doi :10.1177/0959683615596818.

Ojala, A. E. K., Francus, P., Zolitschka, B., Besonen, M., & Lamoureux, S. F. (2012). Characteristics of sedimentary varve chronologies – A review. Quaternary Science Reviews, 43, 45–60. doi: 10.1016/j.quascirev.2012.04.006.

Olsson, I. (1991). Accuracy and Precision in Sediment Chronology. Hydrobiologia 214, 25-34.

O'Sullivan, P. E. (1983). Annually laminated lake sediments and the study of Quaternary environmental changes – a review. Quaternary Science Reviews 1:245 – 313.

Ön, Z.B., Akçer-Ön, S., Özeren, M.S., Eriş, K.K., Greaves, A.M., Çağatay, M.N. (2018). Climate Proxies for the Last 17.3 ka from Lake Hazar (Eastern Anatolia), Extracted by Independent Component Analysis of m-XRF data, Quaternary International, 486, 17-28.

PAGES 2k Consortium. (2019). Consistent multidecadal variability in global temperature reconstructions and simulations over the Common Era. Nat. Geosci. 12, 643–649. https://doi.org/10.1038/s41561-019-0400-0.

Riebeek, H. (2005). Paleoclimatology: The Oxygen Balance. The Nasa Earth Observatory. Retrieved May 15, 2022, from https://earthobservatory.nasa.gov/features/Paleoclimatology_OxygenBalance

Riebeek, H. (2005). Paleoclimatology: The Ice Core Record. The Nasa Earth Observatory. Retrieved May 10, 2022, from https://earthobservatory.nasa.gov/features/Paleoclimatology_IceCores

Riebeek, H. (2005). Paleoclimatology: Written in the Earth. The Nasa Earth Observatory. Retrieved May 14, 2022, from https://earthobservatory.nasa.gov/features/Paleoclimatology_Speleothems

Riebeek, H. (2010). Global Warming. The Nasa Earth Observatory. Retrieved June 3, 2022, from https://earthobservatory.nasa.gov/features/GlobalWarming.

Roberts, N., Allcock, S. L., Barnett, H., Mather, A., Eastwood W. J., Jones, M., Primmer, N., Yiğitbaşıoğlu, H., Vannière, B. (2018). Cause-and-effect in Mediterranean erosion: The role of humans and climate upon Holocene sediment flux into a central Anatolian Lake catchment. Geomor. https://doi.org/10.1016/j.geomorph.2018.11.016

Schlachter, Kyle James. (2005). "Macroscopic Sedimentary Charcoal as a Proxy for Past Fire in Northwestern Costa Rica. " Master's Thesis, University of Tennessee. Retrieved April 12, 2022, from https://trace.tennessee.edu/utk_gradthes/4574.

Sharifi, A., Pourmand, A., Canuel, E. A., Ferer-Tyler, E., Peterson, L. C., Aichner, B., Feakins, S. J., Daryaee, T., Djamali, M., Naderi, A., Lahijani, H. A. K., and Swart, P. K. (2015). Abrupt Climate Variability since the Last Deglaciation Based on a High-resolution, Multi-proxy Peat Record from NW Iran: the Hand that rocked the Cradle of Civilization? Quaternary Science Reviews, 123, 215-230.

Stoller- Conrad, J. (2017). Tree rings provide snapshots of Earth's past climate. The NASA Global Climate Change. Retrieved June 5, 2022, from https://climate.nasa.gov/news/2540/tree-rings-provide-snapshots-of-earths-past-climate/.

Şenel, M., 1997. Geological Map Series of Turkey 1:100 000 Scale. No. 1, Geologic Map of Fethiye L7 Quadrangle. General Directorate of Mineral Research and Exploration, Geological Research Department, Ankara (in Turkish).

Şenel, M., 1997. Geological Map Series of Turkey 1:100 000 Scale. No. 2, Geologic Map of Fethiye L8 Quadrangle. General Directorate of Mineral Research and Exploration Geological Research Department, Ankara (in Turkish).

Şimşek, F. B., & Çağatay, M.N. (2018). Late Holocene high resolution multi-proxy climate and environmental records from Lake Van, eastern Turkey. Quaternary International. doi: 10.1016/j.quaint.2017.12.043.

Tandon, A. (2022). Climate change made extreme rains in 2022 South Africa floods 'twice as likely'. Retrieved June 2, 2022, from https://www.carbonbrief.org/climate-change-made-extreme-rains-in-2022-south-africa-floods-twice-as-likely/.

Tjallingii, R., Röhl, U., Kölling, M., Bickert, T. (2007). Influence of the water content on X-ray fluorescence corescanning measurements in soft marine sediments. Geochemistry, Geophysics, Geosystems 8 (2), Q02004. doi:10.1029/2006GC001393

Touchan, R., Garfin, G.M., Meko, D.M., Funkhouser, G., Erkan, N., Hughes, M.K., Wallin, B.S. (2003). Preliminary reconstructions of spring precipitation in southwestern Turkey from tree-ring width. Int J Climatol 23:157–171.

Touchan, R., Akkemik, Ü., Hughes, MK., Erkan, N. (2007). May–June precipitation reconstruction of southwestern Anatolia, Turkey during the last 900 years from tree-rings. Quat Res 68:196–202.

Tylmann, W., Enters, D., Kinder, M., Moska, P., Ohlendorf, C., Poręba, G., & Zolitschka, B. (2013). Multiple dating of varved sediments from Lake Łazduny, northern Poland: Toward an improved chronology for the last 150 years. Quaternary Geochronology, 15, 98–107. doi: 10.1016/j.quageo.2012.10.001.

UNICEF. (2022). Water and the global climate crisis: 10 things you should know. Retrieved June 8, 2022, from https://www.unicef.org/stories/water-and-climate-change-10-things-you-should-know.

U.S. Environmental Protection Agency. (2021). Climate Change Indicators: Wildfires. Retrieved June 4, 2022, from https://www.epa.gov/climate-indicators/climate-change-indicators-wildfires.

Ülgen, U. B., Franz, S. O., Biltekin, D., Çagatay, M. N., Roeser, P. A., Doner, L., & Thein, J. (2012). Climatic and environmental evolution of Lake Iznik (NW Turkey) over the last ~4700 years. Quaternary International, 274, 88–101. doi: 10.1016/j.quaint.2012.06.016.

Zanchetta, G., Van Welden, A., Baneschi, İ., Drysdale, R., Sadori, L., Roberts, N., Giardini, M., Beck, C., Pascucci, V., Sulpizio, R. (2012). Multiproxy Record for the Last 4500 Years from Lake Shkodra (Albania/Montenegro). Journal of Quaternary Science, 27(8), 780–789.

Zolitschka, B. (1991). Absolute dating of late Quaternary Lacustrine sediments by high resolution varve chronology. Hydrobiologia, 214(1), 59–61. doi:10.1007/bf00050932.

Zolitschka, B. (2003). Dating based on freshwater and marine laminated sediments. In: Mackay, A., Battarbee, R., Birks, J., Oldfield, F. (Eds.), Global Change in the Holocene. Edward Arnold Publishers, London, pp. 92-106.

Zolitschka, B., & Enters, D. (2009). Lacustrine sediments. In: Gornitz, V. (Ed.), Encyclopedia of Paleoclimatology and Ancient Environments. Springer, Dordrecht, pp. 485-488.

Zolitschka, B., Francus, P., Ojala, A. E. K., and Schimmelmann, A. (2015). Varves in lake sediments- A review, Quat. Sci. Rev., 117, 1–41. doi: 10.1016/j.quascirev.2015.03.019.

Walker, M. (2005). Quaternary Dating Methods. John Wiley, Chichester, and New York.

Weinheimer, A., & Biondi, F. (2003). PALEOCLIMATOLOGY | Varves. Encyclopedia of Atmospheric Sciences, 1680–1685. doi:10.1016/b0-12-227090-8/00305-5.

Wick, L., Lemcke, G., Sturm, M. (2003). Evidence of Late glacial and Holocene climatic change and human impact in eastern Anatolia: high-resolution pollen, charcoal, isotopic and geochemical records from the laminated sediments of Lake Van, Turkey. The Holocene, 13, 665-675.

World Health Organization. (n.d.). Heatwaves. Retrieved June 10, 2022, from https://www.who.int/health-topics/heatwaves#tab=tab_1.

World Meteorological Organization. (2022). 2021 one of the seven warmest years on record, WMO consolidated data shows. Retrieved June 4, 2022, from https://public.wmo.int/en/media/press-release/2021-one-of-seven-warmest-years-record-wmo-consolidated-data-show.